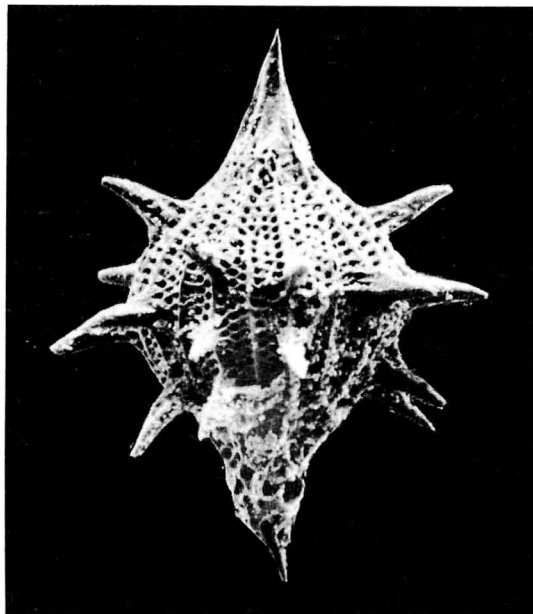


日本古生物学会
報告・紀事

Transactions and Proceedings
of the
Palaeontological Society of Japan

New Series No. 141



日本古生物学会

Palaeontological Society of Japan

April 30, 1986

Co-Editors

Hisayoshi IGO and Takashi HAMADA

Officers for 1985–1986

President: Toshimasa TANAI

Honorary President: Teiichi KOBAYASHI

Councillors: Kiyotaka CHINZEI, Takashi HAMADA, Tetsuro HANAI, Yoshikazu HASEGAWA, Itaru HAYAMI, Hisayoshi IGO, Junji ITOIGAWA, Tadao KAMEI, Tatsuaki KIMURA, Tamio KOTAKA, Kei MORI, Ikuwo OBATA, Tsunemasa SAITO, Yokichi TAKAYANAGI, Toshimasa TANAI

Members of Standing Committee: Kiyotaka CHINZEI (Membership), Takashi HAMADA (Co-Editor of Transactions), Yoshikazu HASEGAWA (Foreign Affairs), Itaru HAYAMI (Planning), Hisayoshi IGO (Co-Editor of Transactions), Tatsuaki KIMURA (Finance), Ikuwo OBATA (General Affairs), Yokichi TAKAYANAGI (Editor of "Fossils"), Juichi YANAGIDA (Editor of Special Papers)

Secretary: Hiroshi NODA (Editor of Transactions)

Auditor: Yoshiaki MATSUSHIMA

The fossil on the cover is *Unuma (Spinunuma) echinatus* ICHIKAWA and YAO, a Middle Jurassic multisegmented radiolaria from Unuma, Gifu Prefecture, central Japan (photo by A. YAO, × 260).

All communication relating to this journal should be addressed to the
PALAEONTOLOGICAL SOCIETY OF JAPAN

c/o Business Center for Academic Societies,
Yayoi 2-4-16, Bunkyo-ku, Tokyo 113, Japan

807. EARLY INTERNAL SHELL MICROSTRUCTURE OF SOME MESOZOIC AMMONOIDEA: IMPLICATIONS FOR HIGHER TAXONOMY*

YASUO OHTSUKA

Department of Geology, Kyushu University, Fukuoka 812, Japan

Abstract. Characteristics of early internal shell structure in four early Jurassic and twenty-three late Cretaceous ammonoid species are described and their taxonomic implications are also discussed. Early whorls of all species examined are distinctly divided into the ammonitella and post-ammonitella stages, which are bounded by a primary constriction; and only two stages of irregular subprismatic or prismatic structure are distinguished in the protoconch and the whorl of the ammonitella. Although the early shells of the species examined consist of common structural elements, the form and growth of several early structural elements appear to be stable within a given suborder of the Mesozoic Ammonoidea.

Introduction

Submicroscopic studies of ammonoid shell structure have hitherto been made by many authors (*e.g.*, Branco, 1879–80; Grandjean, 1910; Shimizu, 1929; Spath, 1933; Böhmers, 1936; Erben *et al.*, 1969). Recent microstructural observations on various Mesozoic taxa by Drushchits and Khiami (1969, 1970), Drushchits and Doguzhayeva (1974), Zakharov (1974, 1977), Drushchits *et al.* (1976) and Tanabe *et al.* (1979) have further demonstrated the significance of early internal shell structure at higher taxonomic levels. Most previous taxonomic studies of ammonoid early ontogeny are, however, based on optical microscopic observations, and detailed microstructural relations of early morphologic features have little examined.

In the present study scanning electron microscope (SEM) observations were on the early

whorls of four Jurassic and twenty-three Cretaceous ammonoid species, to evaluate the taxonomic significance of early internal structure. Morphological variation and growth of early internal shell characters of the species examined and their bearing on early life history are summarized in another paper (Tanabe and Ohtsuka, 1985).

This paper is a part of Master's thesis submitted to Ehime University in 1983. The author is grateful to Dr. K. Tanabe of Ehime University for his guidance throughout this study and for critical reading of the manuscript, Dr. W. J. Kennedy of the University of Oxford for reviewing an early draft of the manuscript, and Profs. Emeritus T. Matsumoto and T. Shuto of Kyushu University for fruitful suggestions. Thanks are extended to Prof. H. Matsuo and Dr. M. Matsukawa of Ehime University for helpful discussions, Prof. U. Lehmann of Hamburg Universität for providing him with specimens of *Eleganticeras*, and Dr. Y. Fukuda of Chiba Prefectural Institute of Public Health for his kind advice on SEM preparation.

*Received December 10, 1984: Read October 17, 1982 at the Meeting of the Society at Mie University.

Table 1. List of ammonite species studied.
 Registered numbers of the specimens examined are shown in parentheses.
 Major taxonomic positions of the species follow Arkell *et al.* (1957),
 Donovan *et al.* (1981), and Wright (1981).

Cretaceous Ammonoidea

Suborder Lytoceratina

Superfamily Tetragonitaceae

Family Tetragonitidae

Tetragonites glabrus (Jimbo) 7 specimens (EE.S 01-07)

Family Gaudryceratidae

Gaudryceras denseplicatum (Jimbo) 2 specimens (EE.S 08,12)

G. tenuiliratum Yabe 1 specimen (EE.S 13)

G. striatum (Jimbo) 4 specimens (EE.S 09-11,17)

Anagaudryceras yokoyamai (Yabe) 1 specimen (EE.S 14)

Suborder Phylloceratina

Superfamily Phyllocerataceae

Family Phylloceratidae

Hypophylloceras subramosum (Spath) 5 specimens (EE.S 16,18-21)

Phyllopachyceras ezoense Yokoyama 2 specimens (EE.S 15,22)

Suborder Ammonitina

Superfamily Desmocerataceae

Family Desmoceratidae

Mesopuzosia yubarensis (Jimbo) 4 specimens (EE.S 52,57-59)

Kitchinites japonicus Spath 5 specimens (EE.S 33-35,45,46)

Desmoceras japonicum (Yabe) 3 specimens (EE.S 39-41)

Tragodesmoceroides subcostatus Matsumoto 3 specimens (EE.S 53-55)

Damesites damesi (Jimbo) 2 specimens (EE.S 25,26)

D. semicostatus Matsumoto 2 specimens (EE.S 23,24)

D. sugata (Forbes) 5 specimens (EE.S 27-31)

Desmophyllites diphylloides (Forbes) 3 specimens (EE.S 42-44)

Desmophyllites sp. 2 specimens (EE.S 37,38)

Family Pachydiscidae

Pachydiscus sp. 1 specimen (EE.S 32)

Pachydiscinae gen. et sp. indet. 1 specimen (EE.S 47)

Menuites pusillus Matsumoto 1 specimen (EE.S 56)

M. sp. 1 specimen (EE.S 36)

Superfamily Acanthocerataceae

Family Acanthoceratidae

Obiraceras ornatum Matsumoto 1 specimen (EE.S 51)

Family Collignoniceratidae

Collignoniceras woollgari (Mantell) 3 specimens (EE.S 48-50)

Reesidites minimus (Hayasaka et Fukada) 3 specimens (EE.S 90-92)

Jurassic Ammonoidea

Suborder Ammonitina

Superfamily Eoderocerataceae

Family Dactylioceratidae

Dactylioceras sp. 4 specimens (EE.S 61-64)

Peronoceras fibulatum (J. C. Sowerby) 2 specimens (EE.S 65,66)

Superfamily Hildocerataceae

Family Hildoceratidae

Eleganticeras elegantulum (Young et Bird) 2 specimens (EE.S 80,81)

Grammoceras sp. 1 specimen (EE.S 60)

Material and methods

Material.—Table 1 lists the ammonoid species examined in this paper. The author follows Arkell *et al.* (1957), Donovan *et al.* (1981) and Wright (1981) for their major taxonomic positions. The Cretaceous material utilized was collected from the Upper Cenomanian to Upper Campanian deposits in the central axial zone of Hokkaido (Abeshinai, Obira, Manji and Urakawa areas; see Text-fig. 1 for index map) by Tanabe and the author. Their locations are shown in Text-fig. 2. The author further examined nine specimens of four early Jurassic species in this study; they were collected from the shales of the northern Holzmaden area, South Germany (for EE.S 60) and the Whitby area on the Yorkshire Coast, England (for EE.S 61–66) by Tanabe, and from a derived nodule in a late Quarternary glacial deposit near Hamburg, North Germany (for EE.S 80, 81) by Lehmann. All of the specimens examined were preserved in calcareous nodules. They are stored at Ehime University with registered numbers beginning EE.S.

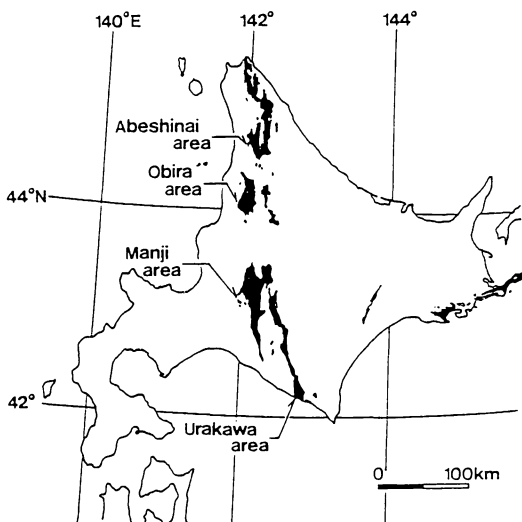
Methods.—Every specimen examined was prepared in the following manner for SEM obser-

vation. Firstly, early whorls of less than 15 mm in diameter were removed from each specimen. Subsequently, they were cut and polished precisely along or perpendicular to the median plane. These sections were etched with 4% hydrochloric acid for several minutes and washed in distilled water. The etched surface was coated with gold or platinum using an ion coater (Eiko Engineering Co., IB-3 or IB-5). Observations on early internal shell structure were made on a JEOL, JXA-733 SEM. Measurements of several characters were performed by means of a profile projector (NIKON, V-12) attached to a digital micrometer (accuracy, 1 μ m).

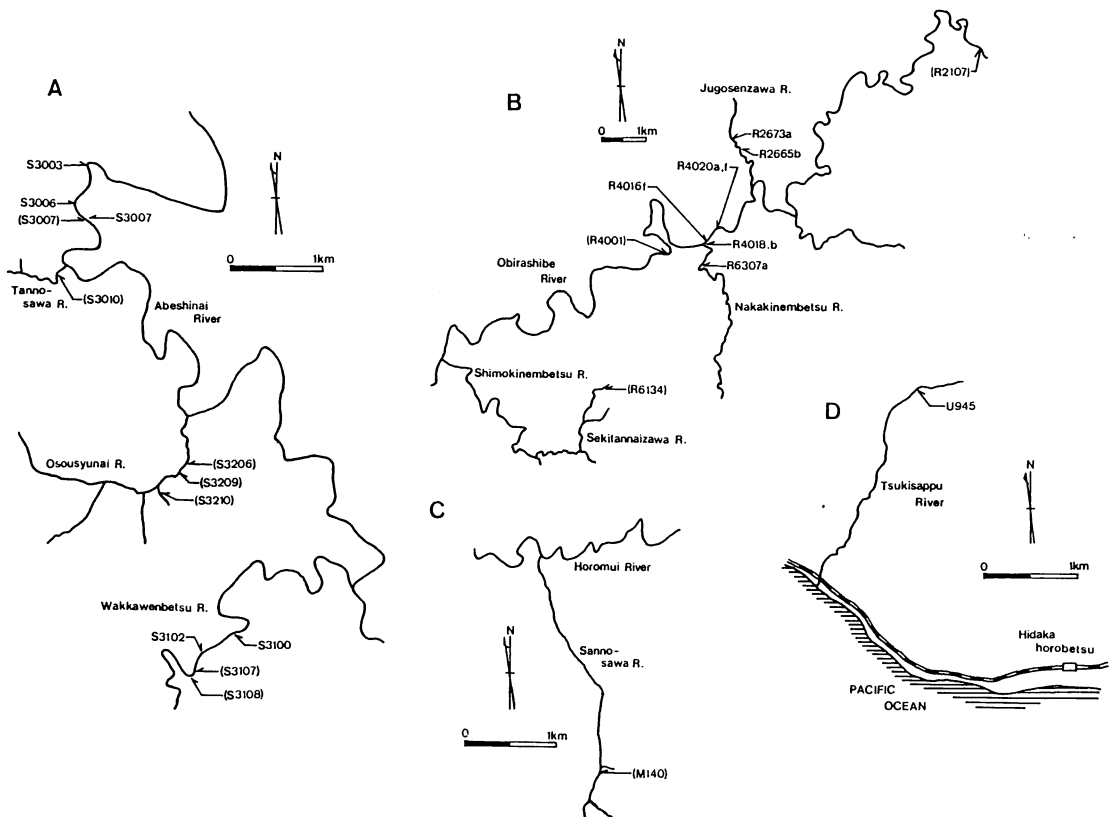
General characteristics of early shell structure

The description given below summarizes the characteristics of early internal shell structure, which were commonly observed in the species examined. Basic morphology and terminology of the ammonoid early internal shell structure in median and cross sections in the *Lytocerotina*, *Phyllocerotina* and *Ammonitina* are diagrammatically shown in Text-fig. 3. Descriptive terminology used in this paper mostly follows Branco (1879–80), Granjean (1910), and Drushchits and Khiami (1969). Measurements of several early internal structural elements in median section are diagrammatically shown in Text-fig. 4. All species examined possess a clear constriction (primary constriction; Drushchits *et al.*, 1977; = nepionic constriction; Birkelund, 1981) near the end of the first whorl (Text-fig. 3; Pl. 45; Pl. 46, Fig. 2; Pl. 48, Figs. 1–4). Drushchits and Khiami (1969) named the conch terminating at the primary constriction the ammonitella. The early shell growth of ammonoids, thus, can be divided into the ammonitella and post-ammonitella stages. Early whorls consist of such common structural elements as protoconch and outer shell walls, prosiphon and its accessory ones, caecum, proseptra, septa and siphuncular tube (Text-fig. 3).

Protoconch.—The protoconch is elliptical or semi-circular in median section (Pls. 45–47). It is distinctly separated from the succeeding



Text-fig. 1. Index map of Hokkaido showing the distribution of Upper Cretaceous deposits (shaded) and areas of ammonite samples studied.



Text-fig. 2. A: Campanian fossil localities in the Abeshinai area, northern central Hokkaido. B: The Middle Turonian to Lower Santonian fossil localities in the Obira area, north-western Hokkaido. Detailed horizons are shown in Tanabe *et al.* (1977, figs. 6 and 9). C: The Upper Turonian fossil locality in the Manji area, central Hokkaido. Detailed horizon is shown in Tanabe *et al.* (1978, fig. 1). D: The Upper Turonian fossil locality in the Urakawa area, southern central Hokkaido. (): calcareous nodule in the river gravels.

Abbreviations: The following abbreviations are used for internal shell structural features in SEM photographs. c: caecum, dp: dorsal prismatic layer, f: flange, ip: inner prismatic layer, n: nacreous layer, op: outer prismatic layer, p: prismatic layer, pc: primary constriction, ps: prosepium, psh: prosiphon, s: septum, sn: septal neck, sp: secondary prosiphon, sph: siphuncle.

Explanation of Plate 45

Figs. 1–6. Scanning electron micrographs showing the early internal shell structure of selected Cretaceous Lytoceratina (1, 2), Phylloceratina (3) and Ammonitina (4–6).

Fig. 1. *Gaudryceras striatum* (Jimbo). EE.S 11.

Fig. 2. *Anagaudryceras yokoyamai* (Yabe). EE.S 14.

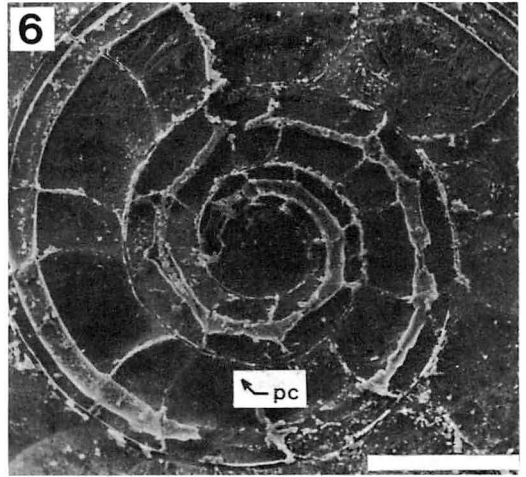
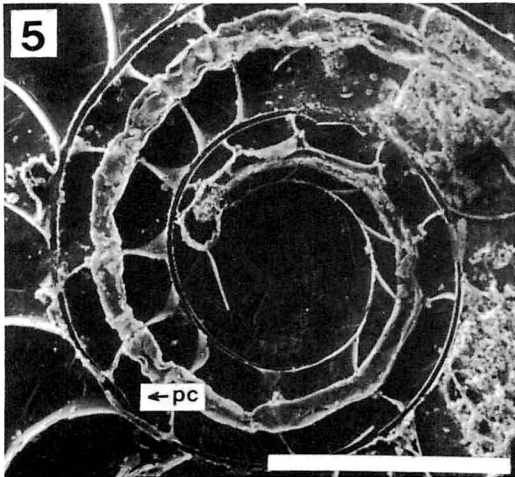
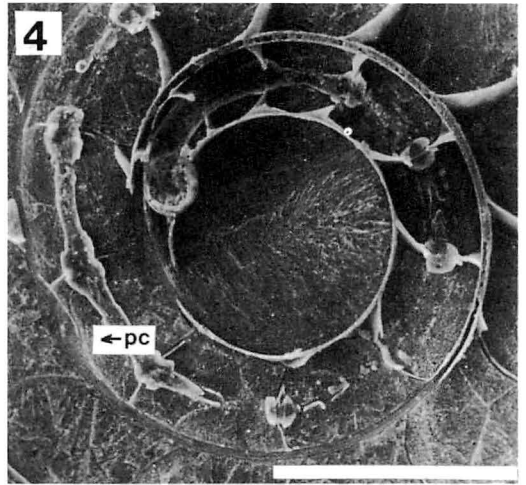
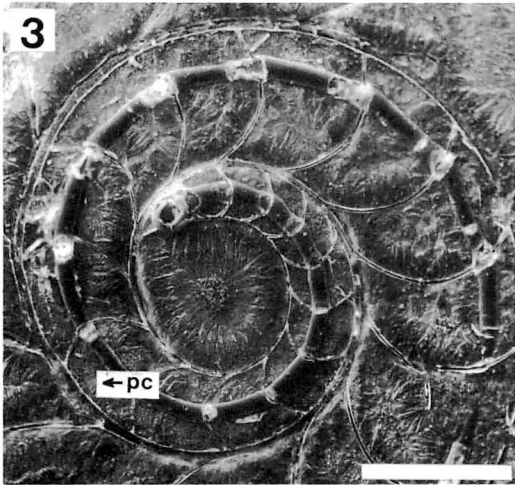
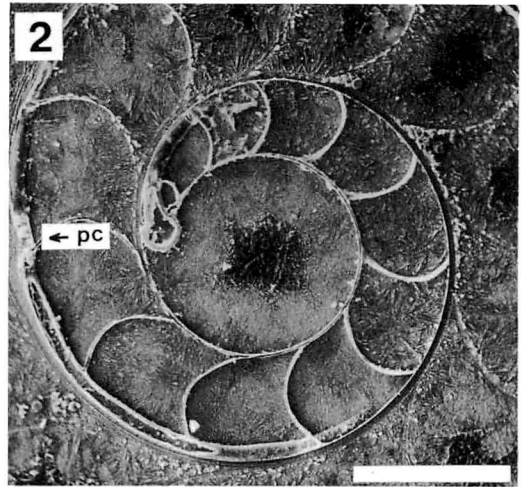
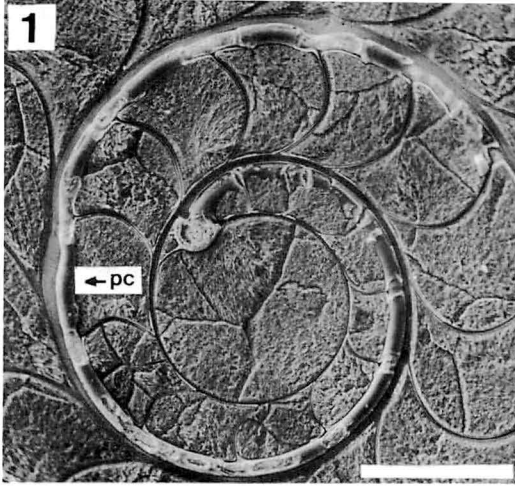
Fig. 3. *Hypophylloceras subramosum* (Spath). EE.S 19.

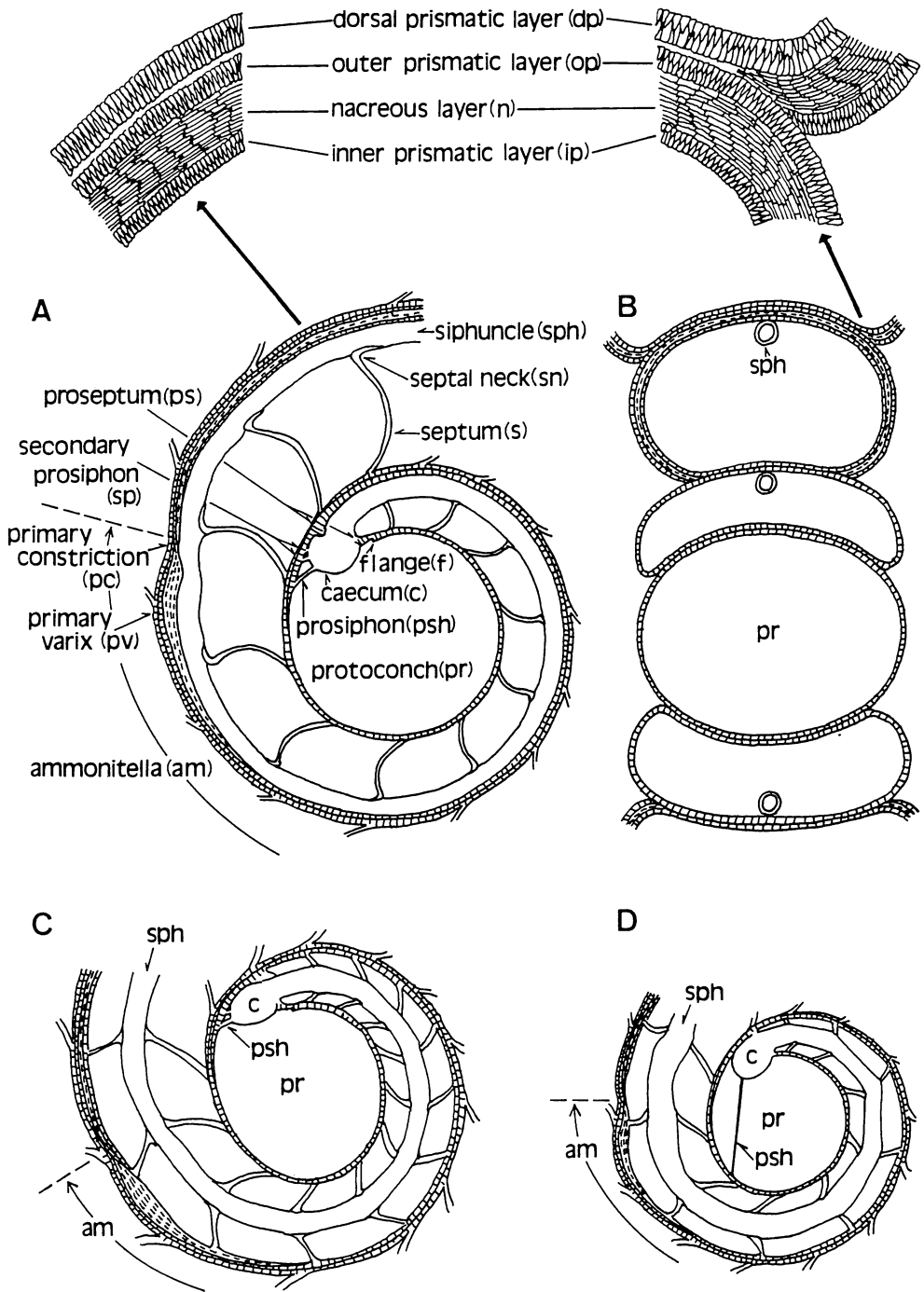
Fig. 4. *Menuites* sp. EE.S 36.

Fig. 5. *Damesites damesi* (Jimbo). EE.S 25.

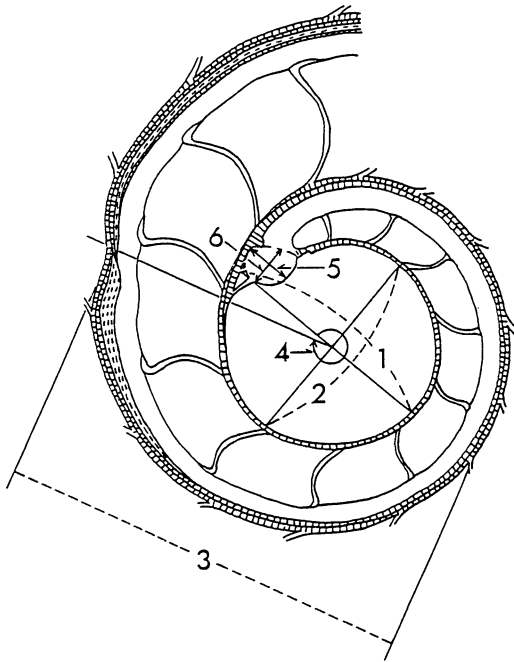
Fig. 6. *Reesidites minimus* (Hayasaka et Fukada). EE.S 90.

Scale bar: 500 μ m.





Text-fig. 3. Diagram of ammonoid early internal shell structures in median (A, C and D) and cross (B) sections. A and B: Lytoceratina, C: Phylloceratina, D: Ammonitina. Terminologies from Branco (1879–80), Grandjean (1910), Shimizu (1929), Drushchits & Khiami (1969), Tanabe *et al.* (1979) and Lominadze (1981).



Text-fig. 4. Measurements of the ammonoid early internal structural elements in median section. 1, 2: maximum and minimum diameters of protoconch, 3, 4: ammonitella size and length, 5, 6: dimensions of caecum (D1, D2).

septate whorls by a caecum wall. The wall of protoconch is made up of a single subprismatic layer about $5\ \mu\text{m}$ thick. Enlarged SEM photographs (Pl. 46, Figs. 3, 5) show that the subprismatic layer is further divided into the inner sublayer of longer and wider crystallites and the outer sublayer of shorter and narrower

crystallites, although the boundary between the two sublayers is partly unclear. This observation is almost identical with those of Birkelund (1967) and Birkelund and Hansen (1974) on the well-preserved specimens of Cretaceous *Saghalinites* from West Greenland. The primary protoconch wall disappears in the initial part of the first whorl (e.g., Pl. 46, Fig. 3).

Outer shell wall of ammonitella.—Near the ventral side of caecum a new prismatic layer begins to appear beneath the preceding subprismatic layer of protoconch wall. It gradually thickens with growth to form the main shell wall of the ammonitella (e.g., Pl. 46, Fig. 3; Pl. 47, Fig. 1a). Like the protoconch wall, the prismatic layer is divided into the inner and outer sublayers on the basis of crystallite size (Pl. 46, Fig. 4).

Prosiphon.—The prosiphon is a narrow circular or tabular horny tube, which extends from the adapical part of the caecum to the inner side of protoconch (Pl. 46, Fig. 3; Pl. 47). In the species referred to the *Lytoceratina* and the *Phylloceratina*, one or two fine tubes are present in the ventral side of caecum. They were previously named the partial septa by Shimizu (1929). Based on optical microscope observations on many late Cretaceous ammonoid specimens, Tanabe *et al.* (1979) have pointed out that the “partial septa” are easily distinguished from the prosepta because of their restriction to the ventral side of caecum. This fact has also been confirmed by the present author in

Explanation of Plate 46

Figs. 1, 2. Scanning electron micrographs showing the early internal shell structure of selected Jurassic Ammonitina.

Fig. 1. *Peronoceras fibulatum* (J. C. Sowerby). EE.S 66.

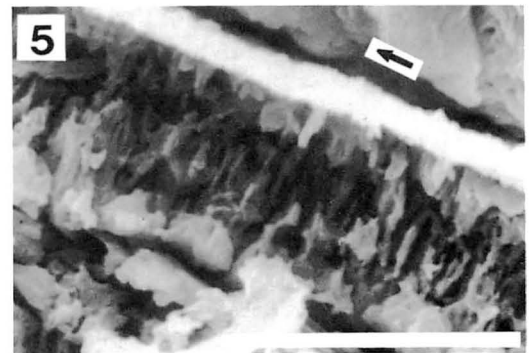
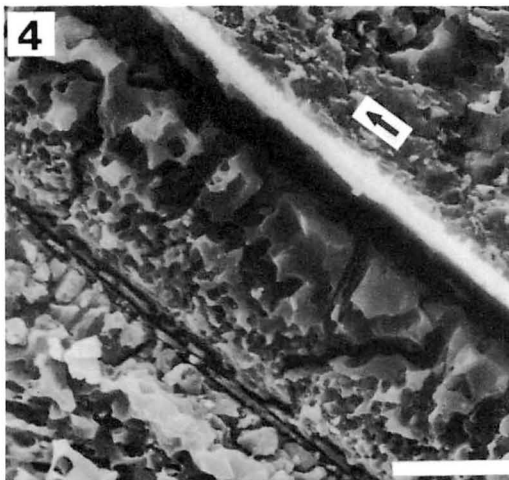
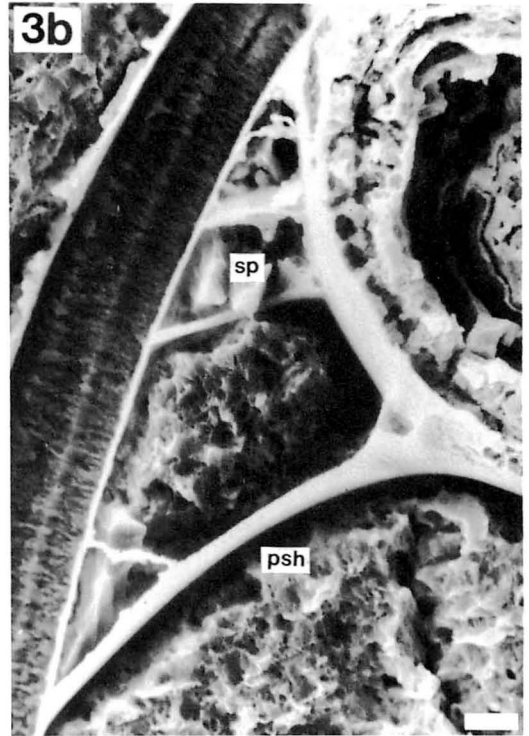
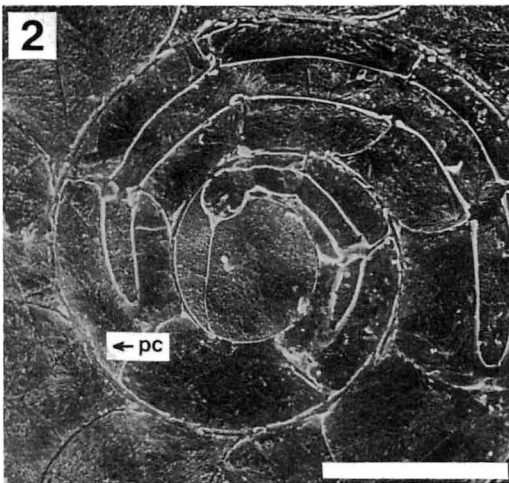
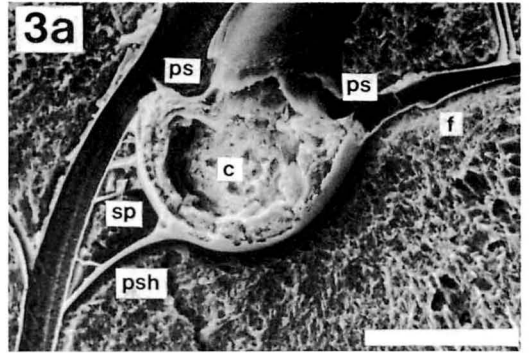
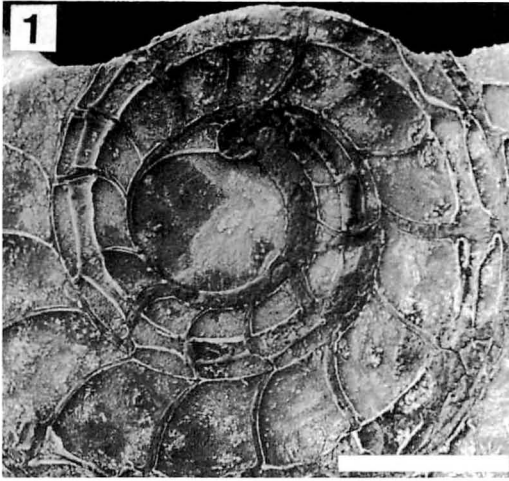
Fig. 2. *Eleganticeras elegantulum* (Young et Bird). EE.S 80.

Figs. 3a–b. Scanning electron micrographs showing the early internal shell structure near caecum in *Gaudryceras striatum* (Jimbo). EE.S 11.

Fig. 4. Scanning electron micrograph of prismatic ammonitella wall in *Anagaudryceras yokoyamai* (Yabe). EE.S 02.

Fig. 5. Scanning electron micrograph of subprismatic protoconch wall in *Tetragonites glabrus* (Jimbo). EE.S 14.

Scale bar: $500\ \mu\text{m}$ (1, 2), $100\ \mu\text{m}$ (3a) and $10\ \mu\text{m}$ (3b, 4, 5). Arrow indicates the adoral direction.



the specimen examined. Under the optical microscope, the "partial septa" are dark-colored, like the prosiphon, without any trace of mineralized structure. Thus, they are more similar to the prosiphon than septa. For these reasons, the author proposes the new term secondary prosiphons for them. The secondary prosiphon is absent in the species of Ammonitina examined in the present study.

Caecum.—This corresponds to the initial part of siphuncle which is in part linked with the prosiphon, and in the case of the Lytoceratina and the Phylloceratina, with both prosiphon and secondary prosiphons. It is projected adapically showing a gentle bowl-shaped curvature. The wall of the caecum is much thicker than the siphuncular wall, but both consist of multi-layered conchiolinic membranes (Pl. 50, Fig. 2). A thin outer calcareous caecum wall described in three Cretaceous ammonite specimens by Tanabe *et al.* (1980) appears to be based on a misinterpretation of several exfoliated conchiolinic membranes.

Prosepta.—One or two septum-like structures, named proseptum or prosepta by Branco (1879–80) are recognized in the adoral end of caecum of every specimen examined. The prosepta are adapically convex, and are made of a single prismatic layer (typically observed in *Gaudryceras striatum*: EE.S 11; Pl. 46, Fig. 3a). Thus, they are easily distinguished from the succeeding nacreous septa in the different microstructure and convexity.

Flange.—The protoconch wall is connected with prosepta near the dorsal side of the caecum. In such species as *Gaudryceras striatum*; EE.S 11, a flange, a short adapical extension of the protoconch wall, can be seen at the connected portion with prosepta (Pl. 46, Fig. 3a; Pl. 47, Fig. 2a), but is absent in other species examined.

Primary constriction.—As stated before, the primary constriction is marked by abrupt changes in shell structure and whorl growth, and is present at the end of the first whorl. Near the end of the first whorl a thin nacreous layer first appears on the dorsal side of the preceding subprismatic layer. Just before the

constriction the nacreous layer abruptly thickens forming a primary varix (Pl. 48, Figs. 1–4). At the end of the constriction, the nacreous layer as well as the prismatic layer of the ammonitella suddenly disappears and is replaced by a new outer shell wall in the post-ammonitella stage. The ventral shell wall in the post-ammonitella stage is composed of three layers: inner prismatic, middle nacreous and outer prismatic layers (Pl. 49, Figs. 4–6; Pl. 50, Fig. 4).

Siphuncle.—The siphuncle is initially located in the central or subcentral part of the chamber, but gradually or rapidly shifts its position toward the ventral side during the growth of the first whorl (Pl. 45; Pl. 46, Figs. 1, 2). It is a long horny tube which runs through each chamber. The ratios of siphuncle diameter to whorl size are relatively large in the first two or three whorls (typically in the Ammonitina), but they gradually decrease with growth. The siphuncular wall is constructed of multi-layered concentric membranes of conchiolin (Pl. 50, Fig. 3). The outermost conchiolin membrane (pellicle) covers not only the main siphuncular membranes but also the inner surface of the chamber. Tanabe *et al.* (1982, pl. 67, figs. 2, 3) showed clear SEM photomicrographs of an exceptionally well-preserved specimen of *Reesidites minimus*, in which unorientated conchiolinic microfibrils of the pellicle cover the main siphuncular wall which consists of orientated, coarse conchiolinic fibrils. Such fine structure of the pellicle was not observed in any specimen examined during the present study. The horny siphuncular wall is not continuous between two contiguous chambers. A thin calcareous layer is intercalated within the septal neck region, where the horny layer is partly absent (Pl. 48, Figs. 1, 5; Pl. 49, Fig. 3). The specimen of *Gaudryceras striatum* (EE.S 9; Pl. 50, Fig. 1) retains the fine structure of the calcareous layer, which is characterized by loosely packed, unorientated aragonitic needles. Such a porous calcareous layer within the septal neck region has already been found in well-preserved specimens of Jurassic *Quenstedtoceras* (Bandel, 1982) and *Eleganticeras* (Tanabe *et al.*, 1982). As Bandel and Boletzky (1979) and

Tanabe *et al.* (1982) have already emphasized, the porous calcareous layer is apparently homologous with the pillar zone (chalky layer) within the septal neck region of other modern and fossil chambered cephalopods.

Septa and septal necks.—The septa are composed of a nacreous layer, and their adapical and adoral sides are covered by a pellicle. The septal neck is a tube-shaped projection of the septal layer, which is extended adorally (prochoanitic), adapically (retrochoanitic) and/or both adorally and adapically (amphichoanitic) (Pl. 49, Figs. 1–3).

Shell wall of the post-ammonitella stage.—As already mentioned, the ventral shell wall in the post-ammonitella stage consists of inner prismatic, middle nacreous and outer prismatic layers (Pl. 49, Figs. 4–6). The relative thickness of these three layers, however, varies at different growth-stages even in a single species. The dorsal wall is made of a single prismatic layer (dorsal prismatic layer) only, which is continuous with the inner prismatic layer of the ventral wall (see Text-fig. 3). Thus, the outer prismatic and middle nacreous layers disappear at the umbilical shoulder (Pl. 50, Fig. 4).

Systematic descriptions

Suborder Lytoceratina Hyatt, 1889

Superfamily Tetragonitaceae Hyatt, 1900

Diagnosis.—Protoconch large in size, nearly spherical; prosiphon short, narrow and circular in cross section; slightly convex ventrally (*e.g.*, Pl. 46, Fig. 3a), with one or two more short

secondary prosiphonal tubes near the ventral side of caecum; caecum large, semi-circular in median section with a distinct constricted base at the connection with siphuncle (Pl. 45, Figs. 1, 2; Pl. 46, Fig. 3a); flange well developed; ammonitella extremely large in size with a whorl longer than 320° ; siphuncle initially located in a sub-central position, but immediately shifts toward the venter in second or third chamber, thereafter maintaining a ventral position (Pl. 45, Figs. 1, 2) throughout almost all stages of ontogeny; siphuncle diameter generally narrower than the Ammonitina and the Phylloceratina at the same growth stage; near the primary constriction it tends to decrease; septal necks short and retrochoanitic in the first whorl and prochoanitic after the second whorl. As the shell grows, the septal necks are conspicuously projected adorally to occupy about a half of a chamber (Pl. 45, Fig. 1; Pl. 49, Fig. 1).

Family Gaudryceratidae Spath, 1927

Observations.—Both protoconch and ammonitella sizes are the largest among the species examined at family level. The number of secondary prosiphons is one in *Anagaudryceras yokoyamai* (EE.S 14; Pl. 45, Fig. 2) and two in *Gaudryceras striatum* (EE.S 11; Pl. 46, Fig. 3a). Flange well-developed, especially in *Gaudryceras* species (*e.g.*, *G. striatum*, EE.S 11; Pl. 46, Fig. 3a). Spiral length of the ammonitella (ammonitella angle) is rather long ranging from 340° to 360° in the specimens examined. Primary constriction is well marked by an abrupt thickening of the primary varix. The gap of whorl growth followed

Explanation of Plate 47

Figs. 1–4. Scanning electron micrographs showing the early internal shell structure near the caecum of selected Cretaceous Phylloceratina (1), Ammonitina (2) and Jurassic Ammonitina (3, 4).

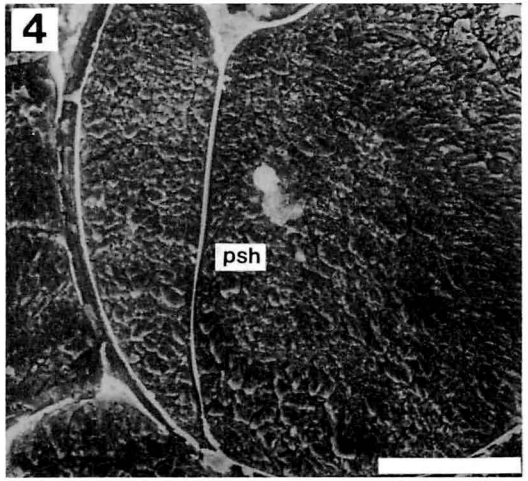
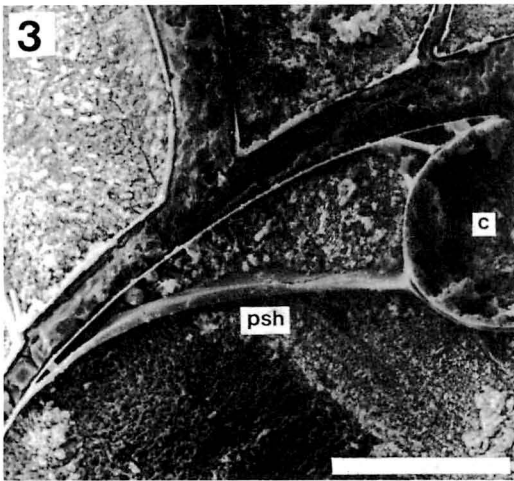
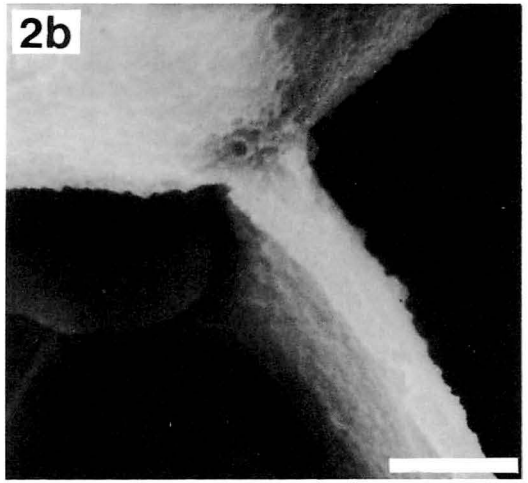
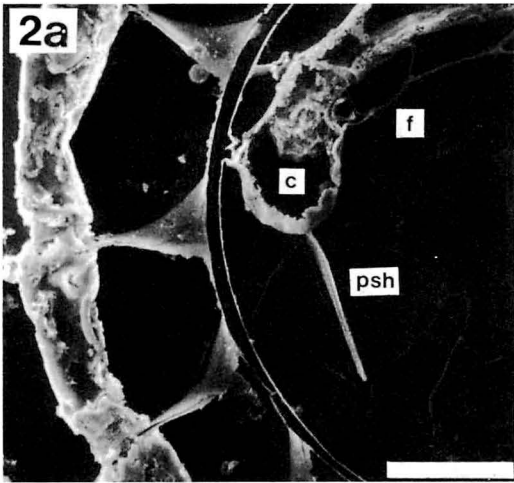
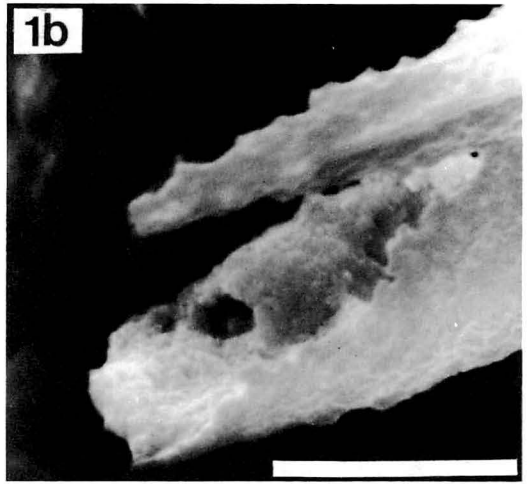
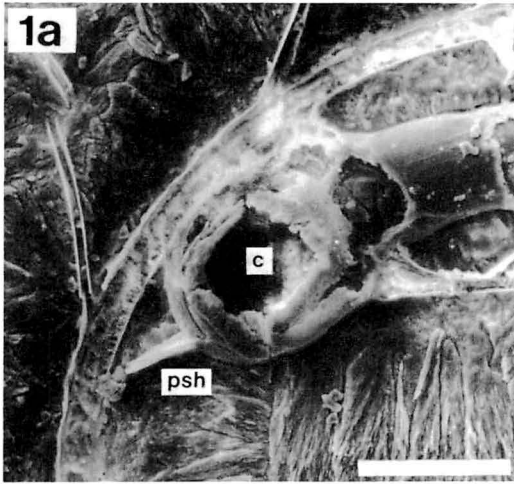
Figs. 1a–b. *Hypophylloceras subramosum* (Spath). EE.S 19.

Figs. 2a–b. *Damesites damesi* (Jimbo). EE.S 25.

Fig. 3. *Peronoceras fibulatum* (J. C. Sowerby). EE.S 66.

Fig. 4. *Eleganticeras elegantulum* (Young et Bird). EE.S 80.

Scale bar: 100 μm (1a, 2a, 3, 4) and 10 μm (1b, 2b).



by the constriction is especially conspicuous in *G. striatum* (EE.S 11; Pl. 48, Fig. 5). Siphuncular tube narrow in diameter, running through the ventral side of the whorls in parallel with the growth of spiral.

Family Tetragonitidae Hyatt, 1900

Observations.—The early internal shell structural features of *Tetragonites glabrus* belonging to the Tetragonitidae are essentially similar to those of the species of the Gaudryceratidae. Although the author examined only seven specimens of *T. glabrus*, this species has a smaller protoconch, caecum and ammonitella, and shorter ammonitella length than those of the *Gaudryceras* species.

Suborder Phylloceratina Arkell, 1950

Superfamily Phyllocerataceae Zittel, 1884

Family Phylloceratidae Zittel, 1884

Diagnosis.—Protoconch medium-sized, nearly spherical; prosiphon short, narrow and circular in cross section as in the Lytoceratina, but slightly convex ventrally; caecum elliptical in median section without a conspicuously constricted base (Pl. 47, Fig. 1a); ammonitella medium-sized, spiral length (ca. 270°–290°) shorter than those of the species referable to the Lytoceratina and the Ammonitina; siphuncular tube almost straight within each of the first three chambers, and thereafter convex ventrally in parallel with the curvature of the outer shell wall; thus in the earliest growth stage siphuncular tube bends sharply at the septal neck region forming an obtuse angle; siphuncle position central or slightly approximated to the dorsal side within the first several chambers, thereafter shifted toward the venter, but the marginal approximation is prolonged at some stages of the third whorl (Pl. 45, Fig. 3); septal neck of short amphichoanitic type (projected both adapically and adorally) within the first whorl, but after the second whorl its adapical extension is strongly projected than the adoral one (Pl. 49, Fig. 2).

Remarks.—According to Shimizu (1929, pl. 2, fig. 2) and Tanabe *et al.* (1979, fig. 4–1) two or three secondary prosiphons are present in the ventral side of the caecum of *Hypophylloceras subramosum*, but they are absent in *Phyllopachyceras ezoense*.

Suborder Ammonitina Hyatt, 1889

Diagnosis.—Protoconch small in size, nearly spherical (Pl. 45, Figs. 4–6; Pl. 46, Figs. 1, 2); prosiphon long, almost straight and spatula-shaped, being quite different from those of the Lytoceratina and the Phylloceratina; caecum elliptical in median section without any conspicuous constriction at its base (Pl. 47, Fig. 2a); ammonitella small in size as compared with those of the Lytoceratina and the Phylloceratina; siphuncle initially located in a subcentral position within a chamber, gradually shifts its position toward the venter during the growth of the second to third whorls; nearly straight in each chamber within the first whorl, but thereafter gently curved ventrally; septal neck of retrochoanitic type in the first whorl and of long prochoanitic type after the second whorl (Pl. 49, Fig. 3a).

Superfamily Desmocerataceae Zittel, 1895

Observations.—Protoconch small in size ranging from 0.4 mm to 0.5 mm in median section. Ammonitella rather small (0.8–0.9 mm diameter). Of the species examined, protoconch, caecum and ammonitella are largest among the Ammonitina at superfamily level. At family level, there is no great difference in the early internal structural features between the Desmoceratidae and the Pachydiscidae. However, the specimen of *Damesites damesi* (EE.S 25; Pl. 47, Fig. 2a) of the former family possesses a remarkable flange, while it is apparently absent in the specimen of *Menuites* sp. (EE.S 36; Pl. 45, Fig. 4) of the latter family. Owing to insufficient data, it is unclear whether or not the two families can be distinguished from each other on the basis of the presence or absence of this flange.

Superfamily Acanthocerataceae Grossouvre,
1894

Family Collignoniceratidae Wright and Wright,
1955

Observations.—Although the author examined only two species belonging to the Collignoniceratidae, it can be pointed out that the protoconch, ammonitella and caecum are the smallest in size among the species examined at superfamily level. The most characteristic feature in the early stage of the Collignoniceratidae is a regular approximation of two contiguous septa within the second to third whorls (Pl. 45, Fig. 6).

Superfamily Eoderocerataceae Spath, 1929

Family Dactylioceratidae Hyatt, 1867

Observations.—Although the author examined only an oblique section of *Peronoceras fibulatum*, it shows characteristic features such as, small protoconch, elliptical caecum, long spatula-shaped prosiphon and centrally located siphuncle in the early stage, as in Cretaceous Ammonitina (Pl. 46, Fig. 1). The prosiphon of the former is slightly convex ventrally as compared with the nearly straight one of the latter (Pl. 47, Fig. 3).

Superfamily Hildocerataceae Hyatt, 1867

Family Hildoceratidae Hyatt, 1867

Observations.—One specimen of *Eleganticeras elegantulum* examined has an extremely long prosiphon (Pl. 46, Fig. 2). As the prosiphon approximates to the protoconch, it is gently

curved externally to cover the inner surface of the protoconch wall (Pl. 47, Fig. 4). The other early internal structural features are essentially similar to those of the Cretaceous Ammonitina.

Concluding remarks

As a result of this study, it was realized that the early internal shell structure is essentially similar among the various taxonomic groups of the Mesozoic Ammonoidea, and that each of the Lytoceratina, Phylloceratina and Ammonitina have their own characteristic features of prosiphon shape, caecum and septal necks, and position of siphuncle. This result has already confirmed in many ammonoid species by Drushchits and Khiami (1969), Drushchits and Doguzhayeva (1974, 1982), Zakharov (1974) and Tanabe *et al.* (1979). The resemblance of early internal structure between the Jurassic and Cretaceous Ammonitina also strongly suggests that these features were stable through time within a given suborder. Although the relative thickness of the ventral and dorsal shell layers in the post-ammonitella stage changes with growth even in a single species, it can be shown that in the Lytoceratina the middle nacreous layer is the thickest developed. In the Phylloceratina the three ventral layers have nearly the same thickness, being thinner than the dorsal prismatic layer. In the Ammonitina the ventral and dorsal layers are almost equal in thickness. Below suborder level, there is no significant difference among the species examined in terms of shape and growth of early qualitative characters. The variation of

Explanation of Plate 48

Figs. 1–4. Scanning electron micrographs of the primary constriction in selected Cretaceous Lytoceratina (1, 4), Phylloceratina (2) and Ammonitina (3).

Fig. 1. *Gaudryceras striatum* (Jimbo). EE.S 11.

Fig. 2. *Hypophylloceras subramosum* (Spath). EE.S 20.

Fig. 3. *Damesites sugata* (Forbes). EE.S 27.

Figs. 4a–b. *Tetragonites glabrus* (Jimbo). EE.S 2.

Fig. 5. Scanning electron micrographs of constriction showing the gap of whorl growth in *Gaudryceras striatum* (Jimbo). EE.S 11.

Scale bar: 100 μ m (1–3, 4a, 5) and 10 μ m (4b). Arrow indicates the adoral direction.

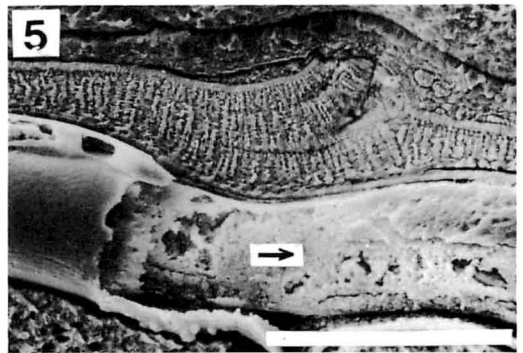
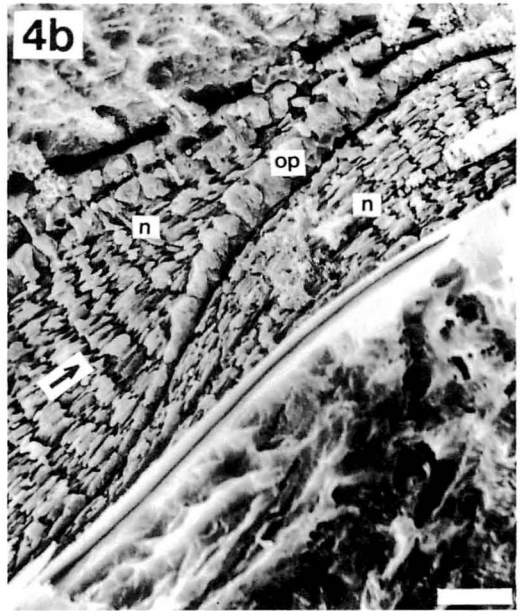
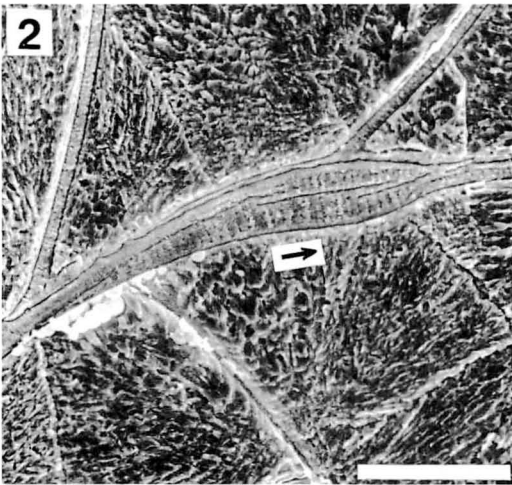
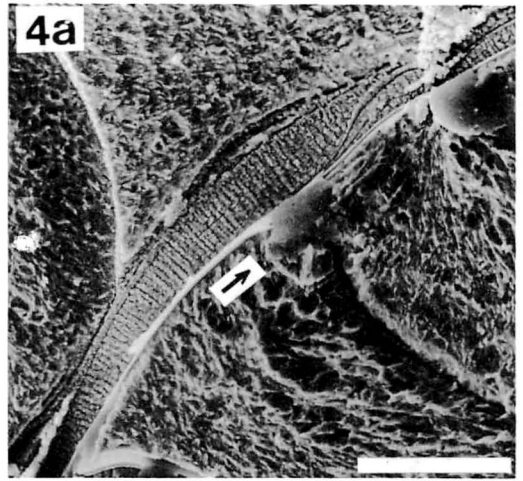
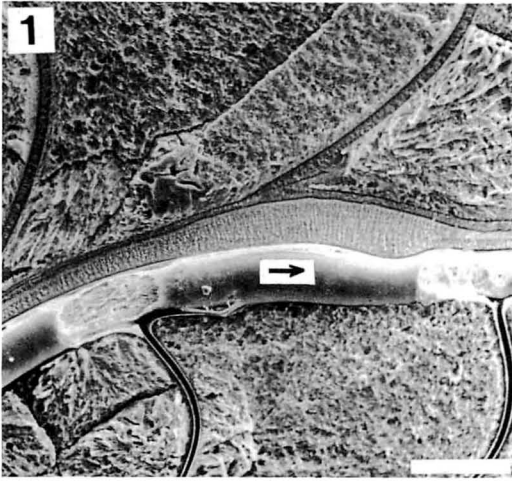


Table 2. Measurements of selected early internal shell structural elements in the specimens examined.

Age	Sub-order	Species	E.E.S.	Protoconch size		Ammonitella		Caecum size		
				Max. (mm)	Min. (mm)	Size (mm)	Length (π)	D1 (mm)	D2 (mm)	
Cretaceous	Lytoceratina	<i>T. glabrus</i>	1	.55	.51	1.09	1.84	.07	.07	
		<i>T. glabrus</i>	3	.59	.53	1.10	1.83	.08	.10	
		<i>T. glabrus</i>	4	.58	.52	1.13	1.91	.12	.10	
		<i>T. glabrus</i>	7	.53	.48	1.01	1.78	.08	.07	
		<i>G. denseplicatum</i>	8	.56	.53	1.12	1.93	.13	.12	
		<i>G. denseplicatum</i>	12	.67	.63	1.37	1.94	.12	.14	
		<i>G. tenuiliratum</i>	13	.63	.59	1.26	1.93	.14	.15	
		<i>G. striatum</i>	9	.67	.62	1.39	1.96	.13	.13	
		<i>G. striatum</i>	11	.66	.61	1.21	1.90	.12	.14	
		<i>A. yokoyamai</i>	14	.69	.63	1.41	2.03	.12	.13	
		Phyllo.	<i>N. subramosum</i>	18	.55	.46	.95	1.56	.13	.12
			<i>N. subramosum</i>	19	.57	.47	1.03	1.62	.11	.10
			<i>N. subramosum</i>	20	.50	.43	.98	1.59	.12	.08
			<i>P. ezoense</i>	22	.47	.38	.85	1.58	.11	.10
	Ammonitina		<i>K. japonicus</i>	35	.45	.44	.87	1.91	.12	.13
			<i>D. japonicum</i>	39	.47	.43	.95	1.87	.11	.12
			<i>D. japonicum</i>	40	.48	.43	.95	1.87	.11	.12
			<i>D. damesi</i>	25	.41	.38	.78	1.74	.09	.09
		<i>D. sugata</i>	27	.42	.39	.85	1.89	.12	.08	
		<i>D. sugata</i>	30	.39	.37	.79	1.78	.11	.10	
		<i>D. sugata</i>	31	.39	.37	.82	1.77	.11	.10	
		<i>D. diphylloides</i>	42	.44	.41	.83	1.78	.09	.08	
<i>D. diphylloides</i>		44	.47	.42	.89	1.79	.09	.10		
<i>D. sp.</i>		37	.43	.41	.84	1.76	.12	.11		
Pachydiscinae	47	.48	.53	.88	1.95	.10	.10			
<i>M. pusillus</i>	56	.50	.46	.87	1.82	.11	.10			
<i>M. sp.</i>	36	.49	.48	.91	1.89	.12	.11			
<i>C. woollgari</i>	49	.36	.31	.65	1.63	.08	.07			
<i>C. woollgari</i>	50	.36	.30	.65	1.56	.08	.07			
<i>R. minimus</i>	90	.35	.30	.66	1.61	.09	.08			
Ju.	<i>E. elegantulum</i>	80	.42	.37	.88	1.62	.12	.12		
	<i>E. elegantulum</i>	81	.40	.34	.80	1.54	.10	.08		

quantitative characters in the early stage may be stable within a given superfamily or family, but the range partly overlaps with that of the other taxa.

The results of this work are concisely summarized in Tables 2—3.

References

- Arkell, W. J., Kummel, B. and Wright, C. W. (1957): Mesozoic Ammonoidea. In R. C. Moore (ed.): *Treatise on Invertebrate Paleontology, Part L*: L80—L456. Geol. Soc. Amer. & Univ. Kansas Press.
- Bandel, K. (1982): Morphologie und Bildung der frühontogenetischen Gehäuse bei conchiferen Mollusken. *Facies*, 7: 1—198.
- and Boletzky, S. V. (1979): A comparative study of the structure, development and morphological relationships of chambered cephalopod shells. *The Veliger*, 21: 313—354.
- Birkelund, T. (1967): Submicroscopic structures in early growth-stages of Maastrichtian ammonites (*Saghalinites* and *Scaphites*). *Medd. fra Dansk Geol. Forening København*, 17: 95—101.
- (1981): Ammonoid shell structure. In House, M. R. & Senior, J. R. (eds.): *The Ammonoidea*, 177—214. Academic Press. London & New York.
- and Hansen, H. J. (1974): Shell ultrastructures of some Maastrichtian Ammonoidea and Coleoidea and their taxonomic implications. *Kong. Dansk. Vidensk. Sel. Biol. Skrift*, 20: 1—34.

Table 3. List showing the major internal shell structural features in the early growth stage of the Ammonoidea at superfamily level.

Suborder	Superfamily	Caecum	Prosiphon	Secondary prosiphon	Protoconch size	Position of siphuncle	Septal neck
Lytoceratina	Tetragonitaceae	Semi-circular	Short, curved, horny	Present (1-2)	Large (0.53-0.69 mm)	Ventral	Prochoanitic
Phylloceratina	Phyllocerataceae	Elliptical	Short, curved, horny	Present (2-3)	Medium (0.47-0.57 mm)	Subcentral → ventral	Amphichoanitic
Ammonitina	Desmocerataceae	Elliptical	Extremely long, straight, spatulate	Absent	Small (0.39-0.50 mm)	Subcentral → ventral	Prochoanitic
	Acanthocerataceae	Elliptical	Long, straight, spatulate	Absent	Very small (0.35-0.36 mm)	Subcentral → ventral	Prochoanitic
	Eoderocerataceae	Elliptical	Long, gently curved, spatulate	Absent	Small (0.49 mm ?)	Subcentral → ventral	Prochoanitic
	Hildocerataceae	Elliptical	Extremely long, straight, spatulate	Absent	Small (0.40-0.42 mm)	Subcentral → ventral	Prochoanitic

Böhmers, J. C. A. (1936): *Bau und Struktur von Schale und Siphon bei Permischen Ammonoidea*. 125 p. Drukkerij Univ. Apeldoorn.

Branco, W. (1879-80): Beiträge zur Entwicklungsgeschichte der fossilen Cephalopoden. *Palaeontographica* (Stuttgart), 26(1879): 15-50, 27(1880): 17-81.

Donovan, D. T., Callomon, J. H. and Howarth, M. K. (1981): Classification of the Jurassic Ammonitina. In House, M. R. & Senior, J. R. (eds.): *The Ammonoidea*, 101-155. Academic Press, London & New York.

Drushchits, V. V., Bogoslovskaya, M. F. and Doguzhayeva, L. A. (1976): Evolution of septal necks in the Ammonoidea. *Paleont. Jour.*, 1976(1): 37-50.

— and Doguzhayeva, L. A. (1974): Some morphogeneric characteristics of phylloceratids and lytoceratids (Ammonoidea). *Ibid.*, 1974(1): 37-48.

— and — (1982): *Ammonites under the Electron Microscope*. 240 p. (in Russian). Moscow Univ. Press, Moscow.

—, — and Mikhaylova, I. A. (1977): The structure of the ammonitella and the direct development of ammonites. *Paleont. Jour.*, 1977(2): 188-199.

— and Khiami, N. (1969): Characteristics of early stages of ontogeny in some early Cretaceous ammonites. *Moskov Obschch. Ispytateley Prirody Byull., Otdel. Geol.*, 44: 156-157 (in Russian).

Explanation of Plate 49

Figs. 1-3. Scanning electron micrographs of median-sections of septum and septal neck in selected Cretaceous Lytoceratina, Phylloceratina and Ammonitina. In Fig. 3 septum and septal neck show thin intercalated prismatic layer.

Fig. 1. *Tetragonites glabrus* (Jimbo). EE.S 03. 5 π stage.

Fig. 2. *Hypophylloceras subramosum* (Spath). EE.S 20. 5.5 π stage.

Figs. 3a-b. *Desmoceras japonicum* (Yabe). EE.S 40. 6 π stage.

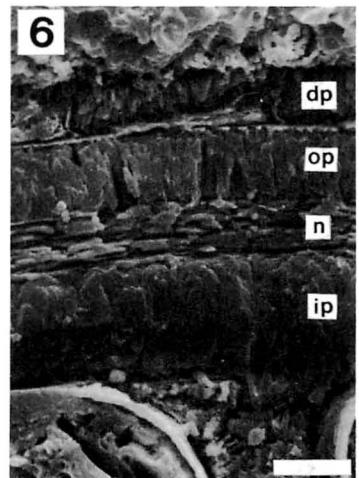
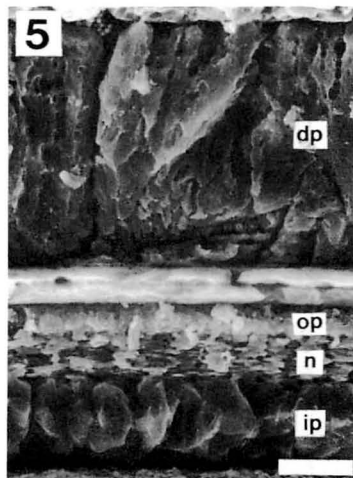
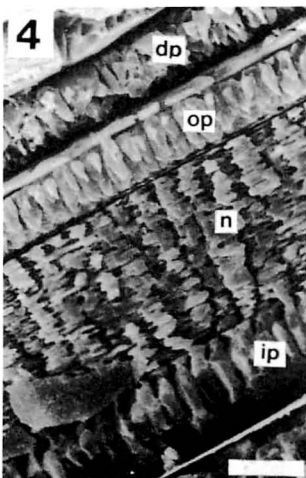
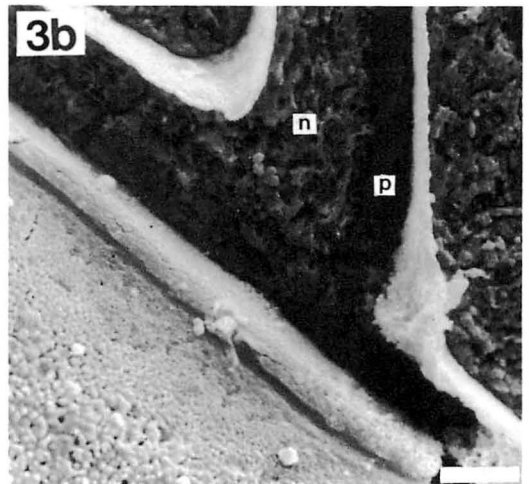
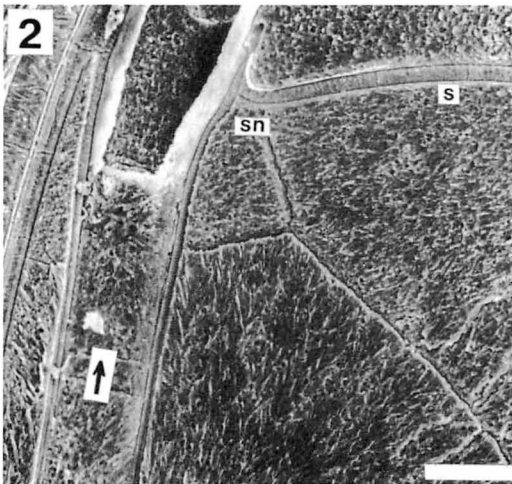
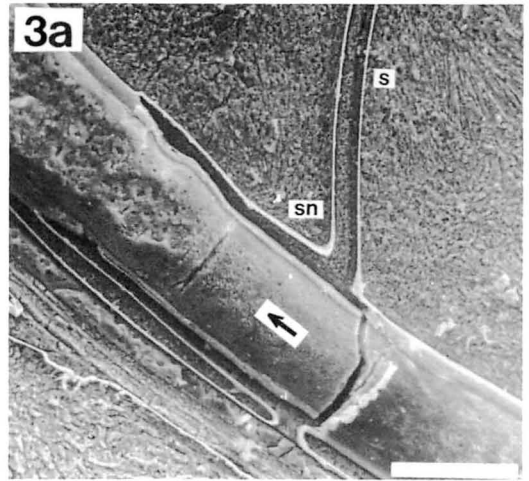
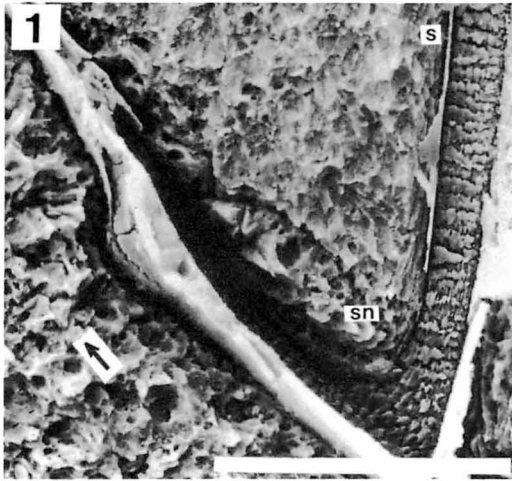
Figs. 4-6. Scanning electron micrographs of the shell wall in selected Cretaceous Lytoceratina, Phylloceratina and Ammonitina.

Fig. 4. *Tetragonites glabrus* (Jimbo). EE.S 02. 4 π stage.

Fig. 5. *Hypophylloceras subramosum* (Spath). EE.S 20. 5 π stage.

Fig. 6. *Kitchinites japonicus* Spath. EE.S 45. 4.5 π stage.

Scale bar: 100 μ m (1, 2, 3a) and 10 μ m (3b, 4-6). Arrow indicates the adoral direction.



- and — (1970): Structure of the septa, protoconch walls and initial whorls in early Cretaceous ammonites. *Paleont. Jour.*, 1970(1): 26—38.
- Erben, H. K., Flajs, G. and Siehl, A. (1969): Die frühontogenetische Entwicklung der Schalenstruktur ectocochlearer Cephalopoden. *Palaeontographica*, 132A: 1—54.
- Grandjean, F. (1910): Le siphon des ammonites et des bélemnites. *Soc. géol. France, Bull., Ser. 4*, 10: 496—519.
- Lominadze, T. A. (1981): The taxonomic significance of various features of the internal structure of Callovian ammonitids. *Plaeont. Jour.*, 1981(4): 119—123.
- Shimizu, S. (1929): On siphuncle in some Upper Cretaceous ammonites. *Saito Ho-on Kai Publ.* 1929(4): 91—116 (in Japanese).
- Spath, L. F. (1933): The evolution of the Cephalopoda. *Biol. Rev.* 8: 418—462.
- Tanabe, K., Fukuda, Y. and Obata, I. (1980): Ontogenetic development and functional morphology in the early growth-stages of three Cretaceous ammonites. *Bull. Natn. Sci. Mus., Tokyo*, C6: 9—26.
- , — and — (1982): Formation and function of the siphuncle-septal neck structures in two Mesozoic ammonites. *Trans. Proc., Palaeont. Soc. Japan, N.S.*, no. 128: 433—443.
- , Hirano, H., Matsumoto, T. and Miyata, Y. (1977): Stratigraphy of the Upper Cretaceous deposits in the Obira area, north-western Hokkaido. *Sci. Repts., Dept. Geol., Kyushu Univ., D*, 12(3): 181—202 (in Japanese with English abstract).
- , Obata, I., Fukuda, Y. and Futakami, M. (1979): Early shell growth in some Upper Cretaceous ammonites and its implications to major taxonomy. *Bull. Natn. Sci. Mus., Tokyo*, C5: 153—176.
- , — and Futakami, M. (1978): Analysis of ammonoid assemblages in the Upper Turonian of the Manji area, central Hokkaido. *Ibid.*, C4: 37—62.
- and Ohtsuka, Y. (1985): Ammonoid early internal shell structure: its bearing on early life history. *Paleobiology*, 11(3): 310—322.
- Wright, C. W. (1981): Cretaceous Ammonoidea. In M. R. House & J. R. Senior (eds.): *The Ammonoidea*, 157—174. Academic Press: London and New York.
- Zakharov, Y. D. (1974): New data on internal shell structure in Carboniferous, Triassic and Cretaceous ammonoids. *Paleont. Jour.*, 1974(1): 25—36.
- (1977): Ontogeny of Ceratites of the genus *Pinacoceras* and developmental features of the suborder Pinacoceratina. *Ibid.*, 1977(4): 445—452.

Abeshinai アベシナイ, Manji 万字, Obira 小平, Urakawa 浦河

中生代アンモナイト類の初期殻体内部構造—高次分類との関係: 北海道上部白亜系産の保存の良いアンモナイト 23 種と 英国及び西ドイツの下部ジュラ系産アンモナイト 4 種を走査型電子顕微鏡を用いて観察し, その初期殻体内部構造の特徴を記載するとともに高次分類との関係を検討した。

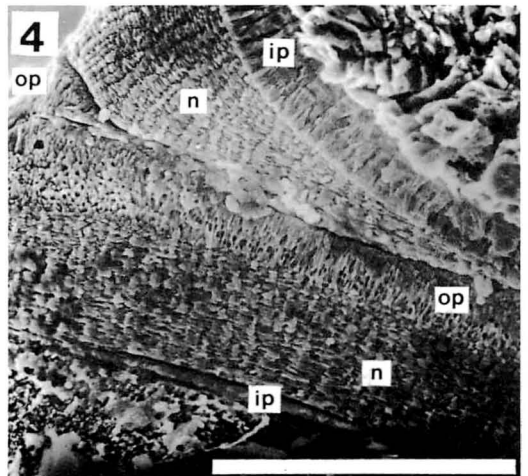
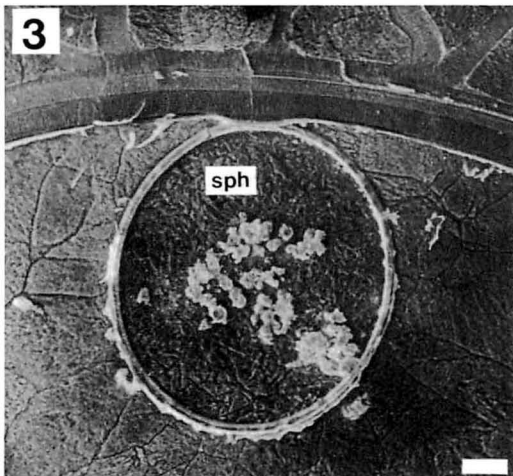
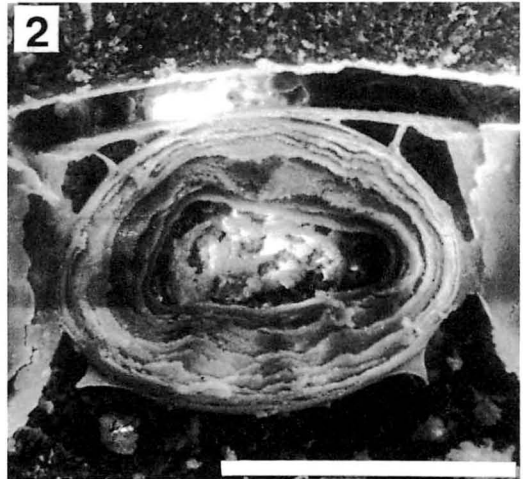
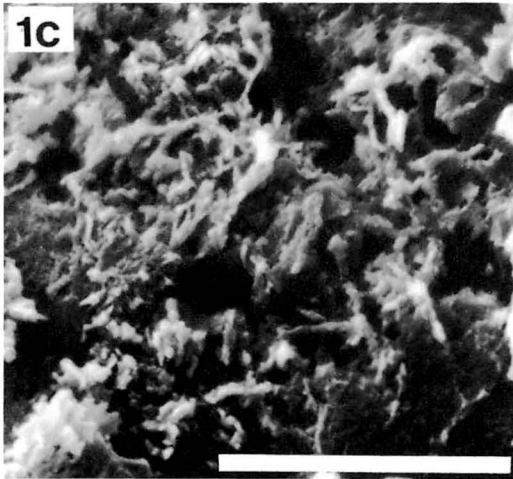
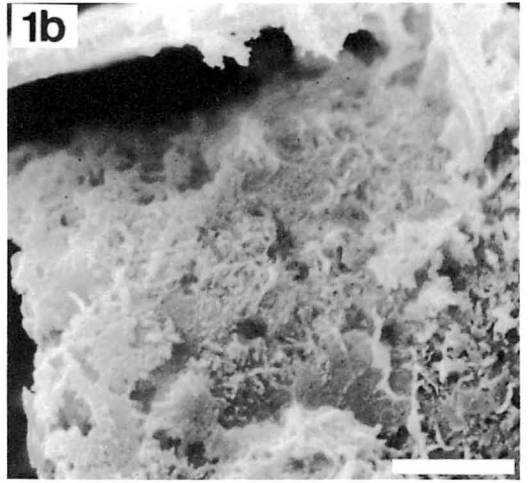
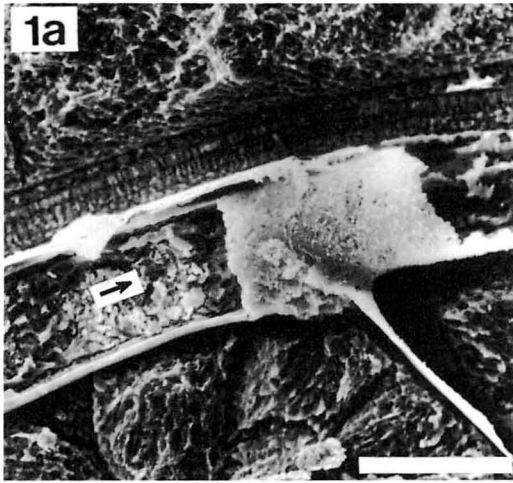
検討したすべての個体の初期螺環は最初のくびれ (primary constriction) を境にして, 稜柱層一層よりなるアンモニテラ (ammonitella) と二つの稜柱層が真珠層を挟む三層構造よりなるそれ以降の段階の 2 つに分けられる。不規則な稜柱層 (亜稜柱層) よりなる胚殻 (protoconch) からアンモニテラにかけての殻構造も, 盲管 (caecum) 付近を境に 2 つの段階に分けられる。

初期殻の構成要素は検討したすべての個体で共通するが, その形態及び成長にともなう変化は, 中生代アンモナイトの亜目レベルで安定している。

大塚康雄

Explanation of Plate 50

- Figs. 1a–c. Scanning electron micrographs of the highly porous calcareous layer within the septal neck region of *Gaudryceras striatum* (Jimbo), EE.S 09, consisting of unorientated aragonitic prisms.
- Fig. 2. Scanning electron micrograph of cross-section of caecum in *Damesites semicostatus* (Yabe), EE.S 24, consisting of multi-layered conchiolin membranes.
- Fig. 3. Scanning electron micrograph of cross-section of siphuncle and shell wall in *Kitchinites japonicus* Spath. EE.S 34.
- Fig. 4. Scanning electron micrograph of umbilical shoulder in *Gaudryceras striatum* (Jimbo). EE.S 17.
- Scale bar: 100 μm (1a, 2–4) and 10 μm (1b, c). Arrow indicates the adoral direction.



808. MICROSTRUCTURE OF GROWTH INCREMENTS IN THE SHELL OF *MERCENARIA MERCENARIA* (LINNE)*

HIROKO KOIKE

Department of Biology, College of Liberal Arts,
Saitama University, Urawa, Saitama 338, Japan

Abstract. Periodical growth increments in molluscan shells have been interpreted by anaerobiosis hypothesis which states that growth lines in growth increments are formed by organic deposits left after decalcification of the shell during valve closure. Growth lines detected as transparent zones in thin section, however, are not stained with bromphenol-blue solution, suggesting that they are not organic-rich deposits. A complete decalcification of the *Mercenaria mercenaria* shell with the EDTA, CPC and formaldehyde solution showed the presence of two types of organic membranes: "the interprismatic membrane" surrounding the calcified prisms, and "organic membrane of the growth increment" intersecting the interprismatic membrane at a right angle. Comparisons between images of completely-decalcified sections and that of etched surfaces in the same individuals indicated that these organic membranes did not correspond to the etch-resistant zone produced by the organic-free etching, and the depressions seen in the organic-free etching, and stained striations in the thin sections. The etch-resistant zone itself was evidenced by lace-like row of the interprismatic membranes. The highly calcified zones frequently appeared immediately following after the organic membranes of the growth increment.

Introduction

Periodic growth increments are a striking feature of molluscan shell. Clark (1974) and Pannella (1975) in their reviews noted that these increments could reflect solar days maintaining internal circadian oscillations (Barker, 1964; Pannella and MacClintock, 1968; House and Farrow, 1968), or lunar-day periodicity created in direct response to environmental fluctuations, including the tides (Evans, 1972; Richardson *et al.*, 1979; Ohno and Takenouchi, 1984).

Growth lines have been described as organic-rich zones in the growth increments (Pannella, 1975; Carter, 1980) whose origin has been explained by the anaerobiosis hypothesis (Lutz and Rhoads, 1977, 1980). According to this hypothesis, growth lines are produced from organic deposits left after the decalcification of the shell which took place in an acidic circumstance during anaerobiosis (Crenshaw and Neff, 1969; deZwaan and Wijsman, 1976). The anaerobiosis is induced by valve closure, especially during tidal exposure (Gordon and Carriker, 1978). Growth lines, however, can be observed in many bivalves even among molluscs living below the tidal zone. Moreover, anaerobic decalcification evidently takes place only inside the

*Received December 21, 1984; revised manuscript received June 18, 1985.

pallial line (Dugal, 1939; Wilkes and Crenshaw, 1979).

The purpose of the present paper is to describe the microstructure of the organic and mineral components of growth increments in the clam, *Mercenaria mercenaria* (Linne), and to discuss their periodic formation.

Materials and methods

The clam, *Mercenaria mercenaria* was collected at middle Marsh near Beaufort, North Carolina during May to September in 1979.

The calcified prisms of the clam was observed on fractured and growing surfaces of the shell edges. Shells used for the observation of the growing surface were fixed for 24 hours in filtered sea water containing 3% paraformaldehyde and 0.5% CPC (cetylpyridinium chloride). To observe the growth increment in cross-section, growth margin of the shells were embedded in SPURR embedding media and polished with carborundum sheets (#240 and #400) and diamond paste. Simple etching: Polished surfaces were then etched with 0.1 M Na-EDTA for 3 minutes, or 0.1 N HCl for 2 minutes. Organic etching: The samples of the adjacent portion were polished and immersed in Clorox (5.25% sodium hypochlorite) for 2 hours to remove the organic matrix before the etching, and then etched by the same technique as the simple etching.

The distribution of the organic membrane in the shell was examined using thin sections (40–60 μm thickness) stained with bromphenol-blue solution (1% alcoholic bromphenol blue-saturated with HgCl_2) for about 30 minutes. To observe organic membranes in the shell, thin sections of the shell (about 500 μm in the thickness) were decalcified in a solution containing 0.1 M Na-EDTA, 0.5% CPC and 4% formaldehyde for about 2 weeks. After dehydration with an ethanol series and substitution in Freon 13, the decalcified sections were dried in a critical point apparatus (SAMDR1 PVT-3) with Freon 13. The sections for SEM observations were examined mainly with a JEOL TSMT20 scanning electron

microscope under 20 KV current.

Calcified prisms and growth increments

The shell of *Mercenaria mercenaria* has a composite prismatic structure in the outer layer, and outer part of the middle layer is composed of crossed lamellar structure which becomes homogeneous structure inwards the inner layer (Taylor *et al.*, 1973). The prism of the outer layer appears as an elongate cylindrical shape aligned normal to the growth direction when viewed on fractured sections (Pl. 51, Fig. 1). When viewed at growing surface of the outer layer (Pl. 51, Fig. 2), the prisms exhibit a polygonal pattern and are about 10–15 μm in diameter. The surface of the prism seems to be coated by thin organic materials. The calcified part of the prism is composed of fine rods aligned normal to the growth direction (Pl. 51, Fig. 3).

As seen in radial thin sections through an optical microscope, growth increments intersect the prisms at a right angle. A growth increment is made up of a transparent zone and an opaque area. Pannella and MacClintock (1968) recognized the transparent zone as a growth line. Marking experiments using tetracycline indicated that rhythmically-formed growth increments of the present species indicated a daily periodicity, with an variation in daily growth induced by lunar cycle.

Etching of the polished surface of the shell with EDTA solution and Clorox treatment after etching (Pl. 51, Fig. 4) produced clear images of a growth increment composed of a set of a narrow etch-resistant zone and an etch-sensitive part. At higher magnification (Pl. 51, Fig. 5), the prism is seen to be composed of fine rods, or "the second order of prisms" (Taylor *et al.*, 1973; Nakahara *et al.*, 1980) of under 0.2 μm in breadth. Etch-resistant zones have a greater density of fine rods and are composed of slightly larger rods than those in etch-sensitive parts of growth increments. Comparing the growth-increment patterns on SEM photographs of EDTA-etched surfaces with those of the thin sections, the etch-resistant zones correspond to the trans-

parent zones in the thin sections.

Organic membranes

Bromphenol-blue staining is useful to detect the organic membrane in the shell by the optical microscope. Growth line has been interpreted as an organic-rich portion. However, the transparent zones in the thin section, or so-called growth lines, were not stained (Pl. 51, Fig. 6), indicating that they are not organic-rich deposits. On the other hand, well-stained, fine striations appeared frequently in the dark opaque parts, especially immediately adjacent to the transparent zones. Outer surfaces of the prisms also seem to be covered with organic membrane, as indicated by stained striations between prisms.

A complete decalcification of the shell with the EDTA, CPC and formaldehyde solution showed the presence of two types of organic membranes (Pl. 51, Figs. 7 and 8). One was "the interprismatic membrane" surrounding the calcified prisms, which appeared as fibrous sheets oriented in the growth direction. The interprismatic membrane corresponds to the blue-stained outer surface of the prisms.

The other organic membrane is very thin and intersects the interprismatic membrane at a right angle (Pl. 51, Fig. 8). This membrane is called "organic membrane of growth increment" in this paper. This membrane is about 0.2 μm in thickness and seems to correspond to the fine striation in the bromphenol-blue-stained section.

Interprismatic membrane was not homogeneous in thickness, becoming thin and lace-like in the zones immediately following the organic membrane of the growth increment. The width of the lace-like zone is about 1–3 μm .

Complete decalcification of thin-sectioned shells showed two types of organic membrane: the interprismatic membrane and the organic membrane of the growth increment. Organic membranes similar to the interprismatic membrane of the present species are reported in the outer layer of shell composed of the prismatic structure (Bevelander and Nakahara, 1980; Nakahara *et al.*, 1980) and of the crossed la-

mellar structure (Uozumi and Suzuki, 1979; Nakahara *et al.*, 1981) and the nacreous layer (Erben, 1974; Mutvei, 1980) of molluscan shells.

Organic-free etching

Although the transparent zones in growth increments was not stained by the bromphenol-blue solution, indicating that the so-called growth line itself is not an organic-rich deposition, the organic membrane of growth increments was detected by the complete decalcification. Otherwise, the stained fine striations detected in the dark opaque zone, frequently located adjacent to the transparent zone. There might be a possibility that the organic membrane of the growth increment would obstruct the etching efficiency. Then, organic-free etching of the polished surface by immersion in Clorox was carried out to remove the organic matrix before the etching. If the organic membrane of growth increments would affect on the etching, organic-free etching could not produce clear etch-resistant zone. However, etch-resistant zones were still observed after the organic-free etching, indicating that the etch-resistancy were not produced by the influence of the organic membrane.

Fine depressions in the growth increments close to the etch-resistant zones were produced after removal of the organic matrix by Clorox. In addition, depressions which correspond to the interprismatic membrane were seen between the prisms.

Relationship between growth line and organic membrane of growth increments

In order to clarify the relationship between the etch-resistant zone and the organic membrane of growth increment, SEM micrographs of the organic-free-etched surfaces were compared with the simple EDTA-etched surfaces and the completely decalcified sections of the same individual (sample No. Mm 2003). A growth increment observed after simple etching appeared to consist of an etch-resistant zone

and an etch-sensitive part (Pl. 52, Fig. 1). Organic-free etching showed that an etch-resistant zone is accompanied by a fine depression (D in Pl. 52, Fig. 2) adjacent to, *i.e.*, the place where was precipitated just before the zone. A decalcified section at the same position (Pl. 52, Fig. 3) suggests that the depression corresponds to the organic membrane of growth increment.

The etch-resistant zone itself cannot be observed in the decalcified section, but its past presence is evidenced by the remnant thin and lace-like zone seen in the row of the interprismatic membranes, since the race-like zone appears immediately after the organic membrane and thus corresponds to the etch-resistant zone.

Discussion

Growth lines, detected as transparent zones in thin section and as etch-resistant zones formed by acid etching, have been interpreted as organic-rich portions. Surfaces etched with EDTA or HCl solution is frequently covered with organic matrix which remained after decalcification, and such a mistreatment make the etch-resistant zone to look like a "convex stripe of organic

line" (Pannella, 1975). The etch-resistant zone, or transparent zone, however, is organic-poor as shown in the organic-free etching and bromphenol-blue staining experiments. Its etch-resistance may be not due to organic membrane or matrix, but rather to a difference in density of calcified rods. Their highly calcified features are also suggested by the lace-like pattern in the completely-decalcified sections.

Periodic formation of growth increments in molluscan shells has been explained by the anaerobiosis hypothesis which states that growth lines are formed by organic matrix left after the decalcification of the shell during valve closure (Gordon and Carriker, 1978; Lutz and Rhoads, 1980). However, SEM observations of growth increments on several etchings showed that the growth line itself is an organic-poor deposit. Growth lines seen in an EDTA etching appeared as rows of especially dense rods (Koike, 1980). This indicates that the formation of growth increments cannot be explained by the anaerobiosis theory. According to Wilkes and Crenshaw (1979), the dissolution layer caused by anaerobic decalcification was observed only inside the pallial line of bivalve shells.

Explanation of Plate 51

Shell structure and growth increments of *Mercenaria mercenaria*. Scale bars indicate length in μm and arrows indicate the growth direction.

Fig. 1. Fractured section showing an elongate cylindrical prism (P).

Fig. 2. Growing surface in shell edge fixed with 4% formaldehyde, showing polygonal pattern of prisms (P) of complex prismatic structure.

Fig. 3. Growing surface rinsed with Clorox to dissolve organic matrix covering the surface of prisms (P).

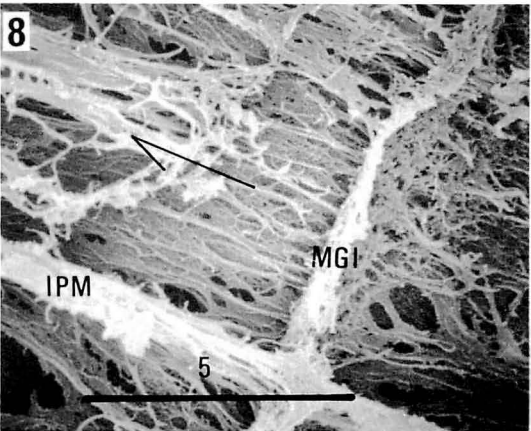
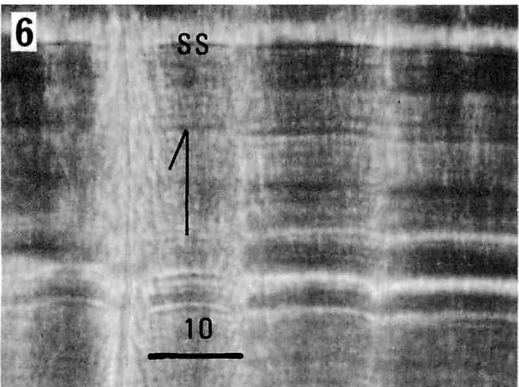
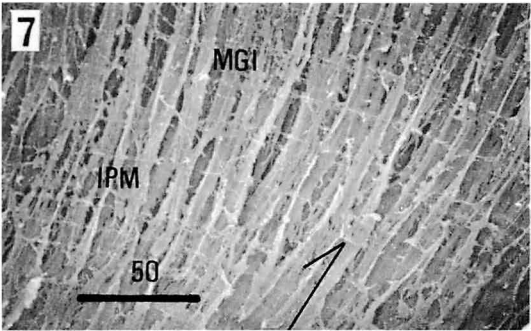
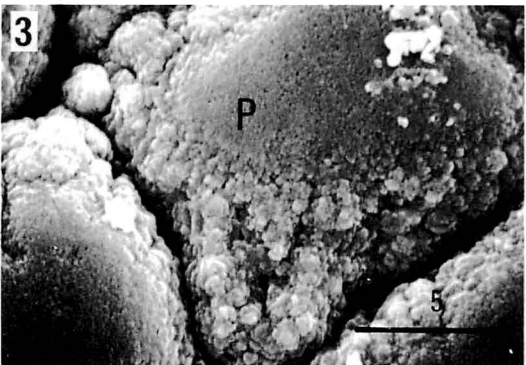
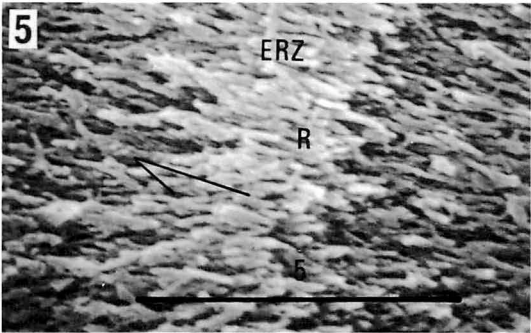
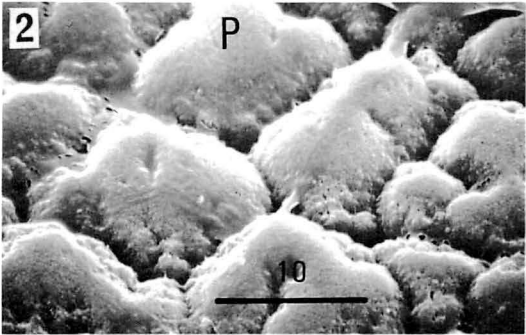
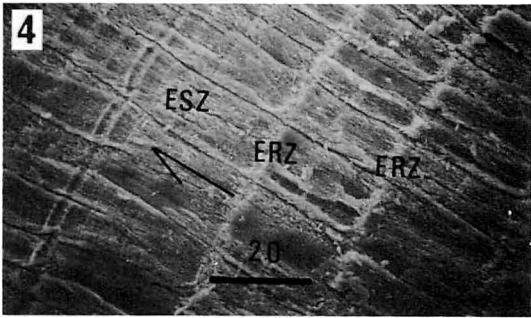
Fig. 4. Growth increments in radial section showing etch-resistant zone (ERZ) and etch-sensitive zone (ESZ) produced by EDTA etching.

Fig. 5. Higher magnification of an etch-resistant zone (ERZ) consisting of slightly larger rods (R) than in the etch-sensitive zone.

Fig. 6. Fine striations stained by bromphenol-blue staining (SS) detected through the optical microscope.

Fig. 7. Organic membrane retained after 2 weeks of decalcification with EDTA, CPC and formaldehyde solution. Interprismatic membrane (IPM) appeared to be fibrous sheets oriented in the growth direction. The organic membrane of the growth increment (MGI) intersecting the interprismatic membrane.

Fig. 8. Higher magnification of the organic membrane of the growth increment (MGI) intersecting the interprismatic membrane (IPM).



In Plate 52, the etch-resistant zone is located immediately following the organic membrane of the growth increment in the growth direction. This pattern is most typical, more than 60% of the growth increments which formed during 2 weeks of marking experiment. It is difficult, however, to determine the sequence of appearance of the etch-resistant zone and the organic membrane, and to infer their function in shell formation. As shown in Pl. 52, Fig. 4, the growth increments had variable patterns: the etch-resistant zone sometimes was not accompanied by an organic membrane, or some organic membranes appeared even after the etch-resistant zone.

According to Nakahara *et al.* (1980), the prismatic structure contained two types of organic components: the interprismatic wall separating the calcified prisms and the intraprismatic portions surrounding each crystallite. The latter was recognized as the "envelope" at the growing surface of the prism. The "envelope" surrounding growing mineral crystals was commonly found among molluscan shells (Bevelander and Nakahara, 1980) and considered to be involved in the initiation and acceleration of crystal growth. The "envelope" is very thin (3–5 nm thick) and cannot be the same organic membrane in the growth increment described in this paper.

In a study of shell regeneration using mussel, Uozumi and Suzuki (1979) described an initial mineralization of "organic membrane-shell" which is composed of three layers: laminated, brown (homologous to the periostracum) and "conchiolin" membranous layers. The first deposition of the particles (nucleus of mineralization) takes place within the conchiolin membranous layer, and the conchiolin sheet was recognized to be closely associated with the initiation of the shell regeneration. The organic membrane in the growth increment may have a function similar to that of the conchiolin sheet in shell regeneration.

It is interesting that the organic membranes of the growth increment were frequently formed just before highly-calcified zones. Further investigation on microstructural differences of

growing surfaces are needed to elucidate the function of this membrane in shell growth.

Acknowledgments

The author wishes to express her deepest gratitude to Professor Miles A. Crenshaw of the University of North Carolina in Chapel Hill for his valuable instructions in the present research. The author is indebted to Professor Karl M. Wilbur of Duke University for his kind arrangements for field experiments and for the use of scanning electron microscope in the Department of Zoology, Duke University.

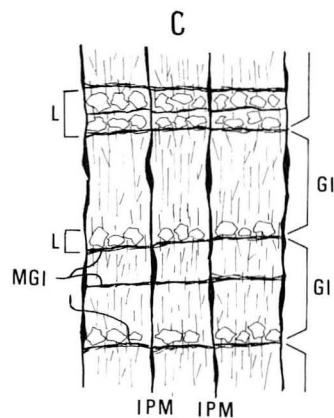
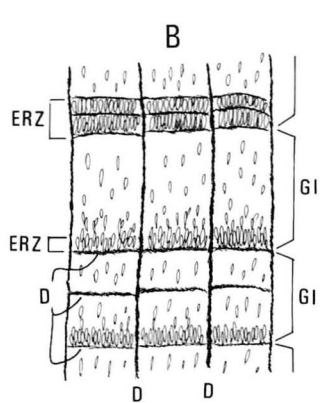
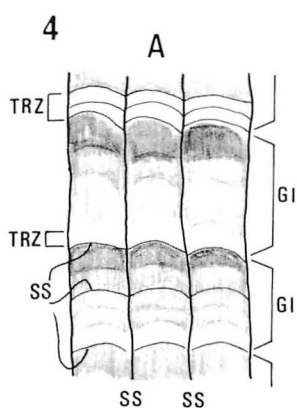
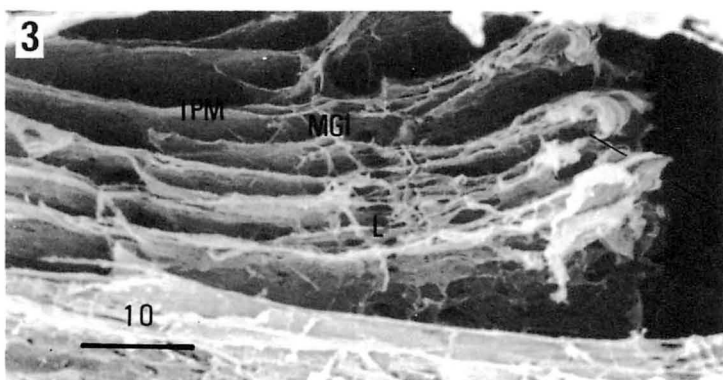
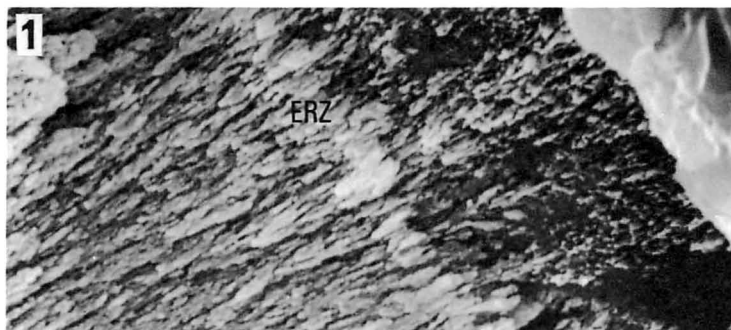
References

- Barker, R. M. (1964): Microstructural variation in pelecypod shells. *Malacologia*, 2(1): 69–86.
- Bevelander, G. and Nakahara, H. (1980): Compartment and envelop formation in the process of biological mineralization. In, Omori, M. and Watabe, N. (eds.) *The mechanisms of biomineralization in animals and plants*, 19–27. Tokai University Press, Tokyo.
- Carter, J. G. (1980): Guide to bivalve shell microstructures. In, Rhoads, D. C. and Lutz, R. A. (eds.) *Skeletal growth of aquatic organisms*, 645–673. Plenum Publishing Corporation.
- Clark II, G. R. (1974): Growth lines in invertebrate skeletons. *Annu. Rev. Earth and Planet. Sci.*, 2: 77–99.
- Crenshaw, M. A. and Neff, J. M. (1969): Decalcification at the mantle-shell interface in molluscs. *Am. Zoologist*, 9: 881–885.
- Dugal, L. P. (1939): The use of calcareous shell to buffer the product of anaerobic glycolysis in *Venus mercenaria*. *Jour. Cell. Comp. Physiol.*, 13: 235–251.
- Erben, H. K. (1974): On the structure and growth of the nacreous tablets in gastropods. *Biomaterialization*, 7: 14–27.
- Evans, J. W. (1972): Tidal growth increments in the cockle, *Clinocardium nuttalli*. *Science*, 176: 416–417.
- Gordon, J. and Carriker, M. C. (1978): Growth

- lines in a bivalve mollusk: Subdaily patterns and dissolution of the shell. *Ibid.*, 202: 519–521.
- House, M. R. and Farrow, C. E. (1968): Daily growth banding in the shell of the cockle, *Cardium edule*. *Nature*, 219: 1384–1386.
- Koike, H. (1980): Microstructure of the growth increment in the shell of *Meretrix lusoria*. In, Omori, M. and Watanabe, N. (eds.) *The mechanisms of biomineralization in animals and plants*, 93–98. Tokai University Press, Tokyo.
- Lutz, R. A. and Rhoads, D. C. (1977): Anaerobiosis and a theory of growth line formation. *Science*, 198: 1222–1227.
- and — (1980): Growth patterns within the molluscan shell: An overview. In, Rhoads, D. C. and Lutz, R. A. (eds.) *Skeletal growth of aquatic organisms*, 203–254. Plenum Publishing Corporation.
- Mutvei, H. (1980): The nacreous layer in molluscan shells. In, Omori, M. and Watabe, N. (eds.) *The mechanisms of biomineralization in animals and plants*, 49–56. Tokai University Press, Tokyo.
- Nakahara, H., Kakei, M. and Bevelander, G. (1980): Fine structure and amino acid composition of the organic “envelop” in the prismatic layer of some bivalve shells. *Venus (The Japan. Jour. Malac.)*, 39(3): 167–177.
- , — and — (1981): Studies on the formation of the crossed lamellar structure in the shell of *Strombus gigas*. *The Veliger*, 23: 207–211.
- Ohno, T. and Takenouchi, K. (1984): Tidal growth patterns in recent *Monodonta labio* (Linnaeus, 1758) (Gastropoda, Trochidae). *NOM*, no. 12, 51–55.
- Pannella, G. (1975): Paleontological clocks and the history of the Earth’s rotation. In, Rosenberg, G. D. and Runcorn, S. K. (eds.) *Growth rhythms and the history of the Earth’s rotation*, 253–284. John Wiley & Sons.
- and MacClintock, C. (1968): Biological and environmental rhythms reflected in molluscan shell growth. *Jour. Paleont.*, 42: 64–80.
- Richardson, C. A., Crisp, D. J. and Runham, N. W. (1979): Tidally deposited growth bands in the shell of the common cockle, *Cerastoderma edule* (L.). *Malacologia*, 18: 277–290.
- Taylor, J. D., Kennedy, W. J. and Hall, A. (1973): The shell structure and mineralogy of the bivalvia. *Bull. British Mus. (Nat. Hist.) Zool.*, 22(9): 255–294.
- Uozumi, S. and Suzuki, S. (1979): “Organic membrane-shell” and initial calcification in shell regeneration. *Jour. Fac. Sci., Hokkaido Univ., Ser. 4*, 19(1/2): 37–74.
- Wilkes, D. A. and Crenshaw, M. A. (1979): Formation of a dissolution layer in molluscan

Explanation of Plate 52

- Fig. 1. Feature of a growth line appeared as an etch-resistant zone (ERZ) when produced by normal etching with EDTA at the shell edge of specimen Mm 2003.
- Fig. 2. Feature of the growth increment with organic-free etching at the adjacent portion in Fig. 1. The etch-resistant zone (ERZ) was accompanied by a depression (D) after dissolution of the organic matrix.
- Fig. 3. Organic membranes in completely-decalcified section of the adjacent portion in Figs. 1 and 2. Interprismatic membrane (IPM) becomes thin and lace-like (L) immediately following after the organic membrane of the growth increment (MGI) in the growth direction.
- Figs. 4A–C. Schematic representation of the growth increment (GI) seen in a thin section stained by bromphenol-blue solution (A), on an organic-free etched surface (B), and in a completely-decalcified section (C). Based on comparisons of these images, the transparent zones (TRZ), or so-called growth lines correspond to the etch-resistant zones (ERZ) in Fig. B and to the lace-like portions (L) in the interprismatic membrane in Fig. C. On the other hand, stained, fine striations (SS) in Fig. A correspond to the fine depressions (D) in Fig. B and the organic membrane of the growth increment (MGI) and interprismatic membrane (IPM) in Fig. C.



shells, *SEM* 1979, 2: 457—465.
 deZwaan, A. and Wijsman, T. C. M. (1976):
 Anaerobic metabolism in bivalvia (Mol-

lusca): Characteristics of anaerobic metabolism. *Comp. Biochem. Physiol.*, 54B: 313—324.

Mercenaria mercenaria の殻の成長線の微細構造：嫌氣的呼吸説によると、貝殻成長線の周期的形成は、閉殻時の嫌氣的呼吸下では貝殻表面の脱灰がおこり、あとに残された有機物が成長線として見えると説明されている。しかしながら貝殻の外層の薄片をブノールフェノールで染色すると、成長線部分は染まらず、いわゆる成長線は富有機物層ではないという疑問もあった。*Mercenaria mercenaria* (Linne) を用い、貝殻中の炭酸カルシウムを完全に除去し、有機物層の微細構造をみると、プリズムをつつむ“interprismatic membrane”と、それと直交する“organic membrane of the growth increment”の二種類の有機物層が認められた。同一個体の標本を用いて完全脱灰標本の電顕像とエッチング像を比較すると、この二種類の有機物層は、いわゆる成長線部分とは対応せず、ブノールフェノール染色法の濃染層および有機物除去脱灰法の凹みによく対応した。一方成長線部分は、完全脱灰標本では interprismatic membrane の薄く粗になった部分に対応し、organic membrane of the growth increment はその成長線部分の直前に多く出現する傾向を示した。

小池裕子

809. *DUSISIREN DEWANA*, N. SP. (MAMMALIA: SIRENIA),
A NEW ANCESTOR OF STELLER'S SEA COW FROM THE UPPER
MIOCENE OF YAMAGATA PREFECTURE, NORTHEASTERN JAPAN*

SHIZUO TAKAHASHI

Yamagata Prefectural Museum, 1-8, Kajo-machi, Yamagata 990, Japan

DARYL P. DOMNING

Laboratory of Paleobiology, Department of Anatomy, Howard University,
Washington, D.C. 20059

and

TSUNEMASA SAITO

Department of Earth Sciences, Yamagata University, Yamagata 990, Japan

Abstract. *Dusisiren dewana*, n. sp. (Sirenia: Hydrodamalinae) is described on the basis of a skull and partial skeleton from the Hashigami Sandstone Member of the Hongo Formation (Upper Miocene, 9.0–10.4 Ma) in Yamagata Prefecture, Honshu, Japan. It is morphologically, chronologically, and phyletically intermediate between *Dusisiren jordani* (Kellogg) and *Hydrodamalis cuestae* Domning, and therefore directly ancestral to the recently exterminated Steller's sea cow, *Hydrodamalis gigas* (Zimmermann). The new species exhibits reduced but still functional teeth in the adult, together with extremely reduced metacarpals and phalanges and a clawlike flipper structure. This combination of characters corresponds to that predicted by Domning (1977, 1978) for "Dusisiren Species D", which the new species represents. The structure of the flipper provides the first unquestionable corroboration of Steller's 18th-century description of the peculiar forelimbs of *Hydrodamalis*. Other recent reports of fossil sirenians from Japan are also reviewed; in addition to *Dusisiren dewana*, *Hydrodamalis gigas* and possibly *H. cuestae* now appear to have lived in Japan contemporaneously with their occurrences in North America.

Introduction

In the summer of 1978, a large fossil mammal was discovered by two elementary school children in the bed of the Mogami River. Owing to a

severe drought that affected a large part of north-eastern Japan in that year, the normally water-covered river bed became emergent, revealing partially exposed vertebrae and ribs on the rock surface. The specimen was brought to the Yamagata Prefectural Museum under the direction of S. Takahashi, who undertook initial preparation

*Received January 10, 1985; revised manuscript received June 24, 1985.

of the skeleton. During the course of preparation, three teeth were discovered, one still attached to the lower jaw. One of the teeth and photographs of the entire skeleton were then sent to D. Domning in Washington, D.C., who identified the specimen as a fossil sea cow. He subsequently visited Japan at the invitation of the Yamagata Prefectural Museum and studied the skeleton while preparation was still in progress.

The Yamagata sea cow specimen is unusually complete and comprises the entire front half of the skeleton, including the head and limb bones. It is very significant in that it forms a "missing link" between two previously known evolutionary stages and fills a gap in our knowledge of the evolution of this particular lineage of sirenians (the hydrodamaline dugongids).

In its age and stage of evolution, the Yamagata sea cow is intermediate between two fossil forms known from California. The earlier of these, *Dusisiren jordani* (Kellogg, 1925), is about 10 to 12 million years old and is directly ancestral to the Yamagata sea cow, which is a new species of *Dusisiren*. The latter in turn is older than and directly ancestral to another species described from California, *Hydrodamalis cuestae* Domning, 1978. This in turn is the direct ancestor of Steller's sea cow, *Hydrodamalis gigas* (Zimmermann, 1780), which lived in the North Pacific until the 18th century.

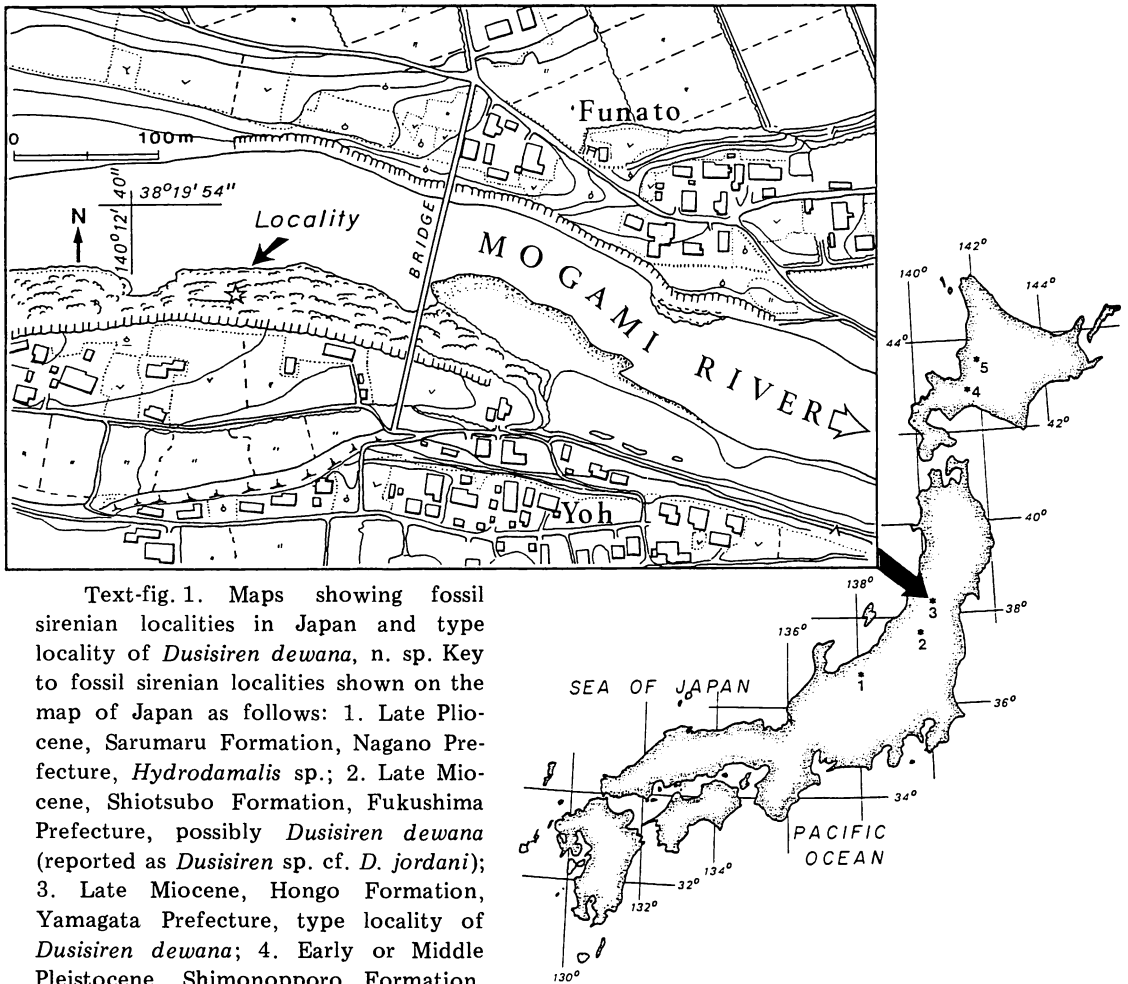
In the course of evolution leading to Steller's sea cow, two notable anatomical changes occurred: the teeth were completely lost and the bones of the fingers were almost or completely lost. Domning (1977, 1978) predicted the existence of an intermediate stage in which functional teeth were still present but the flipper had already taken on a *Hydrodamalis*-like form. Documentation of this intermediate stage was previously lacking, but the Yamagata skeleton now fulfills this prediction precisely. The Yamagata sea cow possesses a fully developed set of teeth which are, however, somewhat smaller and simpler than those of its immediate ancestor, *Dusisiren jordani*. Of course, its dentition is far better developed than anything in its descendants

H. cuestae and *H. gigas*, where the teeth are completely absent, at least in the adult. On the other hand, the Yamagata specimen has already reduced the flipper to a form resembling that of Steller's sea cow, which is to say that it is clawlike and almost entirely lacks finger bones. This is in contrast to the earlier, more primitive sea cows where the flipper still had a well-developed paddle-like form similar to that of the modern manatee and dugong. The phalanges and metacarpals are greatly reduced in the Yamagata specimen and, as we know from the description made by Steller himself on Bering Island almost 250 years ago, the phalanges were even more reduced, and possibly even completely lost, in Steller's sea cow. The flipper's clawlike form was useful for pulling the animal along the bottom in shallow water and scaping algae off the rocks. However, no complete flipper skeleton of *Hydrodamalis* has ever been found, so the Yamagata specimen is additionally important in that it provides our first adequate look at the type of flipper structure Steller described.

Abbreviation: UCMP = University of California Museum of Paleontology, Berkeley.

Geologic setting

The new sea cow specimen comes from the bed of the Mogami River in the hamlet of Yoh, Ohe Town, Nishimurayama County, Yamagata Prefecture (Text-fig. 1). Several authors have described the geology of this area (Ichimura, 1958; Funayama, 1961; Itoh *et al.*, 1979). According to them, the fossil site lies in the Hashigami Sandstone Member of the Hongo Formation. Sediments of the Hongo Formation consist largely of pyroclastic materials, and differences in lithologic characters enable further subdivision of the formation into four members. These are, in upward sequence, the Jyuhassai Pyroclastic Debris Flow, Hashigami Sandstone, Kuzusawa Siltstone, and Ohya Tuffaceous Sandstone Members. The Hongo Formation rests conformably upon the Mizusawa Formation, which consists largely of dark gray siltstone, and is in turn unconformably overlain by the nonmarine Ate-

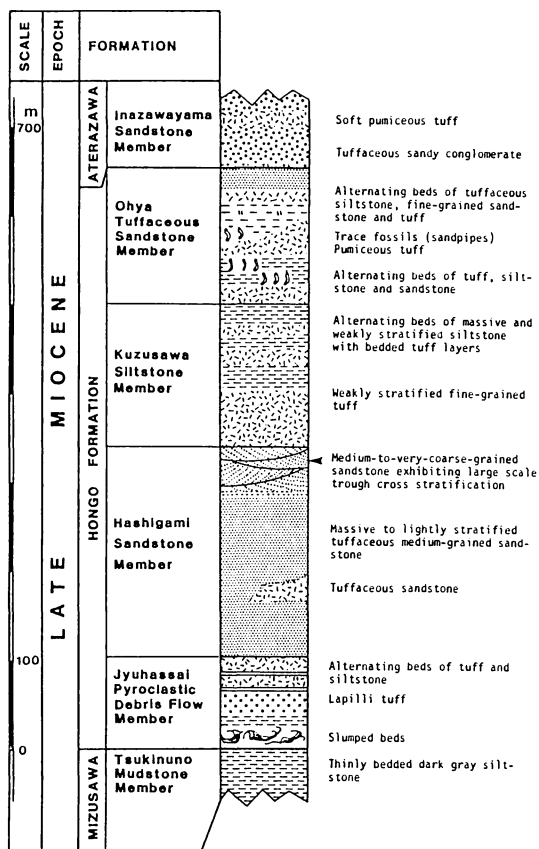


Text-fig. 1. Maps showing fossil sirenian localities in Japan and type locality of *Dusisiren dewana*, n. sp. Key to fossil sirenian localities shown on the map of Japan as follows: 1. Late Pliocene, Sarumaru Formation, Nagano Prefecture, *Hydrodamalis* sp.; 2. Late Miocene, Shiotsubo Formation, Fukushima Prefecture, possibly *Dusisiren dewana* (reported as *Dusisiren* sp. cf. *D. jordani*); 3. Late Miocene, Hongo Formation, Yamagata Prefecture, type locality of *Dusisiren dewana*; 4. Early or Middle Pleistocene, Shimonoppo Formation, Hokkaido, *Hydrodamalis gigas*; 5. Early Pliocene, Takikawa Formation, Hokkaido, possibly *Hydrodamalis cuetae* (reported as *Hydrodamalis* n. sp.).

razawa Formation (Text-fig. 2).

The Hashigami Sandstone Member consists predominantly of tuffaceous, cross-bedded, medium- to very-coarse-grained sandstone containing small pebbles of older rocks such as rhyolite, andesite, prophyllite, and green tuff. The most characteristic feature of this sandstone member is the prevalence of large-scale cross-bedding assignable to trough cross-stratification (Harms et al., 1975). The fossil sea cow was found in this cross-stratified facies. Trough sets of the trough cross-stratification have a width of up

to three meters and a maximum length of more than 15 m. From their size and appearance, these cross-strata are interpreted to have been formed by migrating sand dunes. Local flow directions ranging from northward to north-northwestward were deduced from the orientation of scoop-shaped laminae present in the trough-shaped sets. Ichimura (1958) showed that the Hashigami Sandstone bearing the large-scale trough cross-stratification occurs in a somewhat elliptical geographical area about 7.5 km wide meridionally and about 13 km long latitudinally. Geological data on the surrounding area indicate that the Hashigami Sandstone was deposited in a marine embayment which was open to the northwest (Suzuki, 1979). The



Text-fig. 2. Geologic section in area of type locality of *Dusisiren dewana*, n. sp. Arrow indicates horizon of the fossil sirenian.

trough cross-stratification is therefore attributed to strong tidal currents, which are known to form dune and sand-wave bed forms in many partially enclosed seas and blind gulfs (Reading, 1978).

With the exception of displaced freshwater diatoms, only marine fossils occur in the Hashigami Sandstone. A shell bed about 70 cm thick, composed only of one pectinid mollusk (*Mizuhopecten paraplebejus murataensis* Masuda and Takegawa), crops out in a roadside cliff near the hamlet of Taira, about 6.2 km southeast of the sea cow site (Ogasawara, 1983). *Chlamys cosibensis* (Yokoyama), another pectinid, also occurs at a few localities. In addition, this sandstone member yields several forms of calcareous microplankton: calcareous nannoplankton, *Coc-*

colithus pelagicus (Wallich) Schiller, *C. neohelis* McIntyre and Bé, *Reticulofenestra pseudoumbilica* (Gartner) Gartner, and *Sphenolithus neoabies* Bukry and Bramlette; and planktonic foraminifera, *Globigerina bulloides* d'Orbigny, *Globigerinoides immaturus* LeRoy, *G. ruber* (d'Orbigny), *G. trilobus* (Reuss), and *Sphaeroidinellopsis seminulina grimsdalei* (Keijzer). Diatoms, which will be discussed later in more detail, also occur in the basal part of this member. The sea cow fossil was found in direct association with teeth of the large extinct white shark, *Carcharodon megalodon* Agassiz (Ueno, 1983), and part of the skeleton of an unidentified whale has been found in the bed of the Mogami River near the sea cow locality. Remains of these large vertebrates show that whales and sharks frequented the embayment together with the sea cow; the sharks no doubt preyed on the marine mammals and scavenged their carcasses.

Ogasawara (1983) considers the two pectinids occurring in the Hashigami Sandstone Member to be characteristic elements of a late Miocene molluscan assemblage of northeastern Japan called the Shiobara Fauna, and he estimates the depth of deposition of the sandstone to be shallower than 30–40 m. Chinzei (1978) discussed in detail the distribution and species composition of the Shiobara Fauna and interpreted it to be a coastal assemblage living in cold waters of the temperate region. However, *Globigerinoides* (all species), *Sphaeroidinellopsis seminulina grimsdalei*, and *Sphenolithus neoabies* are all plankton inhabiting warm surface currents. Thus these species suggest that some warm currents were washing the Sea of Japan side of northern Japan during Late Miocene time, in much the same way as the warm Tsushima Current flows up the present Sea of Japan coast.

Geologic age of the sea cow

Geologic age of the fossil sea cow is determined on the basis of diatom floras occurring in the Hashigami Sandstone. Only diatoms occur in sufficient numbers to include age-diagnostic species. According to Akiba (1983a), three age-

diagnostic species are present in the Hashigami diatom flora. These are common occurrences of *Denticulopsis katayamae* Maruyama and *Actinocyclus ingens* Rattray, and somewhat less abundant *Thalassionema nitzschioides* Grunow. This floral association suggests a correlation with the *Denticulopsis katayamae* Zone of Maruyama (1984). Since the formal description of the species *D. katayamae* Maruyama did not appear until the spring of 1984, the zonal interval corresponding to the *D. katayamae* Zone was previously called the *Denticulopsis hustedtii* a Zone by Barron (1981) or alternatively Subzone A of the *D. hustedtii* Zone by Akiba *et al.* (1982). Barron and Keller (1983) calibrated the North Pacific diatom zonation with the geomagnetic reversal sequence and gave a date of from 8.4 to 10.2 Ma to the *D. hustedtii* a Zone. By reexamining stratigraphic ranges of diatoms in DSDP holes 438A and 584, Akiba (1983b) established the age of the *D. katayamae* Zone as from 9.0 to 10.4 Ma. On this basis, a middle Late Miocene age of the sea cow is indicated. Two calcareous nannoplankton species also provide broadly supportive evidence for a minimum date for the sea cow, as *Reticulofenestra pseudoumbilica* and *Sphenolithus neobabies* are known to have become extinct nearly simultaneously at about 3.5 Ma (Haq, 1984).

Systematics

Class MAMMALIA Linnaeus, 1758

Order SIRENIA Illiger, 1811

Family DUGONGIDAE Gray, 1821

Subfamily HYDRODAMALINAE
(Palmer, 1895 [1833]) Simpson, 1932

Genus *Dusisiren* Domning, 1978

Dusisiren dewana, new species

Dusisiren Species D, Domning, 1978, *Univ. Calif. Publ. Geol. Sci.*, 118: 72.

Etymology:—From *Dewa*, the ancient name of the present-day Yamagata Prefecture. The name first appears in Japanese history in A.D. 712.

It was abolished in 1868 during the Meiji Restoration, and survives only in the name of the Dewa Hills, within which the type locality lies.

Holotype:—Anterior half of skeleton of a young adult individual, housed at the Yamagata Prefectural Museum, Yamagata, Japan. Collected by Yamagata Prefectural Museum party, August 1978. (Casts of upper teeth and bones of manus deposited in Department of Paleobiology, United States National Museum of Natural History, Washington, D.C.).

Type locality:—Bed of Mogami River near its east bank, about 100 m upstream of the Yoh Iron Bridge over the river, in hamlet of Yoh, Ohe Town, Nishimurayama County, Yamagata Prefecture, Honshu, Japan.

Formation:—Hashigami Sandstone Member of Hongo Formation.

Age:—Late Miocene (*Denticulopsis katayamae* Diatom Zone), 9.0 to 10.4 Ma.

Diagnosis:—Hydrodamaline dugongids more derived than *Dusisiren jordani* in reduction of size and complexity of molars, reduction of rostral deflection to about 40°, development of narrower and more rectangular mandibular masticating surface, extension of a vertical ridge onto anteromedial side of coronoid process, broadening of anterior process of manubrium, incipient development of median keel on xiphisternum, narrowing of suprascapular fossa of scapula, increased circularity of humeral head, reduction of deltoid crest, medial bowing of radius-ulna, extensive modifications of carpals and of distal antebrachial joint surfaces, reduction in size of metacarpals and phalanges, and (possibly) increased size of trunk relative to head; less derived than *Hydrodamalis* in smaller body size, dorsoventrally thinner zygomatic-orbital bridge of maxilla, visibility of infra-orbital foramen in ventral view, and retention of functional teeth in the adult.

Morphology

Body size:

Lengths of the skull and limb bones are somewhat less than those of *Dusisiren jordani*

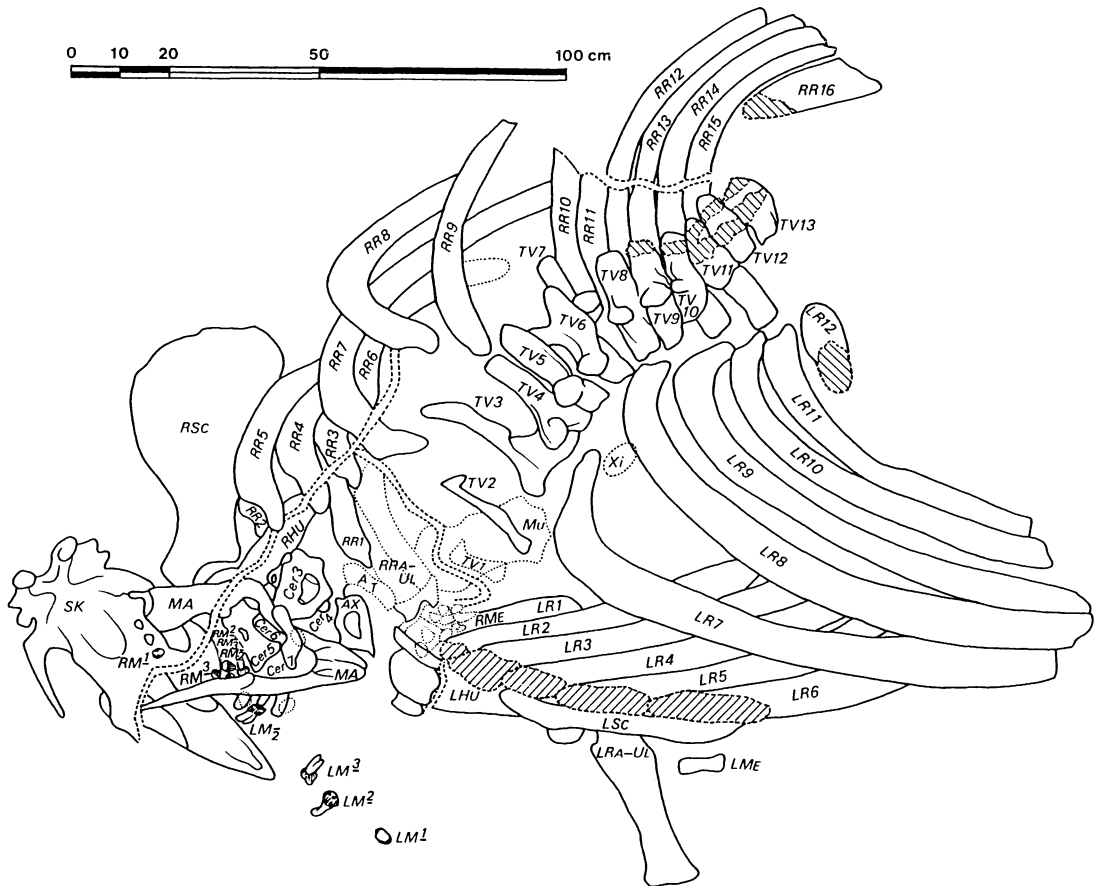
specimens from California (Domning, 1978), though the ribs are larger than those of the latter. Taking into account the dimensions of the incomplete, partly articulated rib cage (Text-fig. 3), the Yamagata specimen probably had an overall length at least equal to that of *D. jordani* (up to 4.3 m or more). It probably weighed between 1 and 2 metric tons.

Skull (Tables 1–3; Text-figs. 4–7; Pls. 53–55.

For other photographs of the skull, mandible, teeth, and limb elements, see Takahashi *et al.*, 1983: figs. III-1 to III-13):

Premaxilla:—Dorsal keel thin forward, widens aft as in *Dusisiren jordani*; sides of forward end concave. Palatal surface not preserved. Nasopalatine canal somewhat flattened dorsoventrally. Masticating surface of rostrum trapezoidal. Incisors absent. Portion of nasal process in contact with jugal and frontal extends about one-half length of mesorostral fossa (*i.e.*, about 9.5 cm). Deflection of rostrum uncertain, 30° or more; judging from the mandibular deflection, it should have been in the neighborhood of 40°.

Nasal:—Sutures not discernible; evidently fused with frontal.



Text-fig. 3. Diagram of holotype skeleton of *Dusisiren dewana* as found in the rock. Paired dashed lines show lines along which block containing skeleton was fragmented. Scale = 1 m. Abbreviations: SK, MA, RM, LM, elements of cranium—skull, mandible, right and left molars; RSC, LSC, RHu, LME, LHu, RRA-UL, LRA-UL, RME, elements of limb—right and left scapulae, humerus, right and left radius-ulna, right and left metacarpals; Cer, AX, AT, TV, elements of vertebral column—cervical, axis, atlas, thoracic vertebrae; Mu, Xi, elements of sternum—manubrium and xiphisternum; RR, LR, right and left ribs.

Table 1. Skull measurements of holotype of *Dusisiren dewana*, in mm. Letters in parentheses denote measurements used by Domning (1978: tab. 2). e = estimated.

Condylbasal length (AB)	511e
Height of jugal below orbit (ab)	52e
Length of premaxillary symphysis (AH)	124+
Rear of occipital condyles to anterior end of interfrontal suture (BI)	269
Zygomatic breadth (CC')	264
Breadth across exoccipitals (cc')	182
Top of supraoccipital to ventral sides of occipital condyles (de)	124
Length of frontals, level of tips of supraorbital processes to frontoparietal suture (F)	177e
Breadth across supraorbital processes (FF')	158e
Breadth across occipital condyles (ff')	127
Breadth of cranium at frontoparietal suture (GG')	72e
Width of foramen magnum (gg')	62
Length of mesorostral fossa (HI)	190e
Height of foramen magnum (hi)	46
Width of mesorostral fossa (JJ')	81
Maximum height of rostrum (KL)	72
Posterior breadth of rostral masticating surface (MM')	64e
Anteroposterior length of zygomatic-orbital bridge of maxilla (n'o')	54e
Length of zygomatic process of squamosal (OP)	136
Anterior tip of zygomatic process to rear edge of squamosal below mastoid foramen (OT)	193
Length of parietals, frontoparietal suture to rear of external occipital protuberance (P)	107e
Length of row of tooth alveoli (p'q')	65e
Anteroposterior length of root of zygomatic process of squamosal (QR)	61
Length of cranial portion of squamosal (ST)	110
Breadth across sigmoid ridges of squamosals (ss')	211
Dorsoventral thickness of zygomatic-orbital bridge (T')	14e
Height of posterior part of cranial portion of squamosal (UV)	96e
Dorsoventral breadth of zygomatic process (WX)	46
Maximum width between pterygoid processes (yy')	60e
Length of jugal (Y'Z')	200e

Ethmoidal region:—Perpendicular plate reaches about 23 mm below roof of narial passage (proportionately slightly farther than in *D. jordani*, UCMP 3794; Domning, 1978: fig. 10f). Second concha of ethmoturbinalia prominent, about 6 mm thick; third concha bulbous, well developed; others not preserved or still enclosed in matrix. Distance between second conchae at level of rear of mesorostral fossa = 37 mm.

Vomer:—Not preserved.

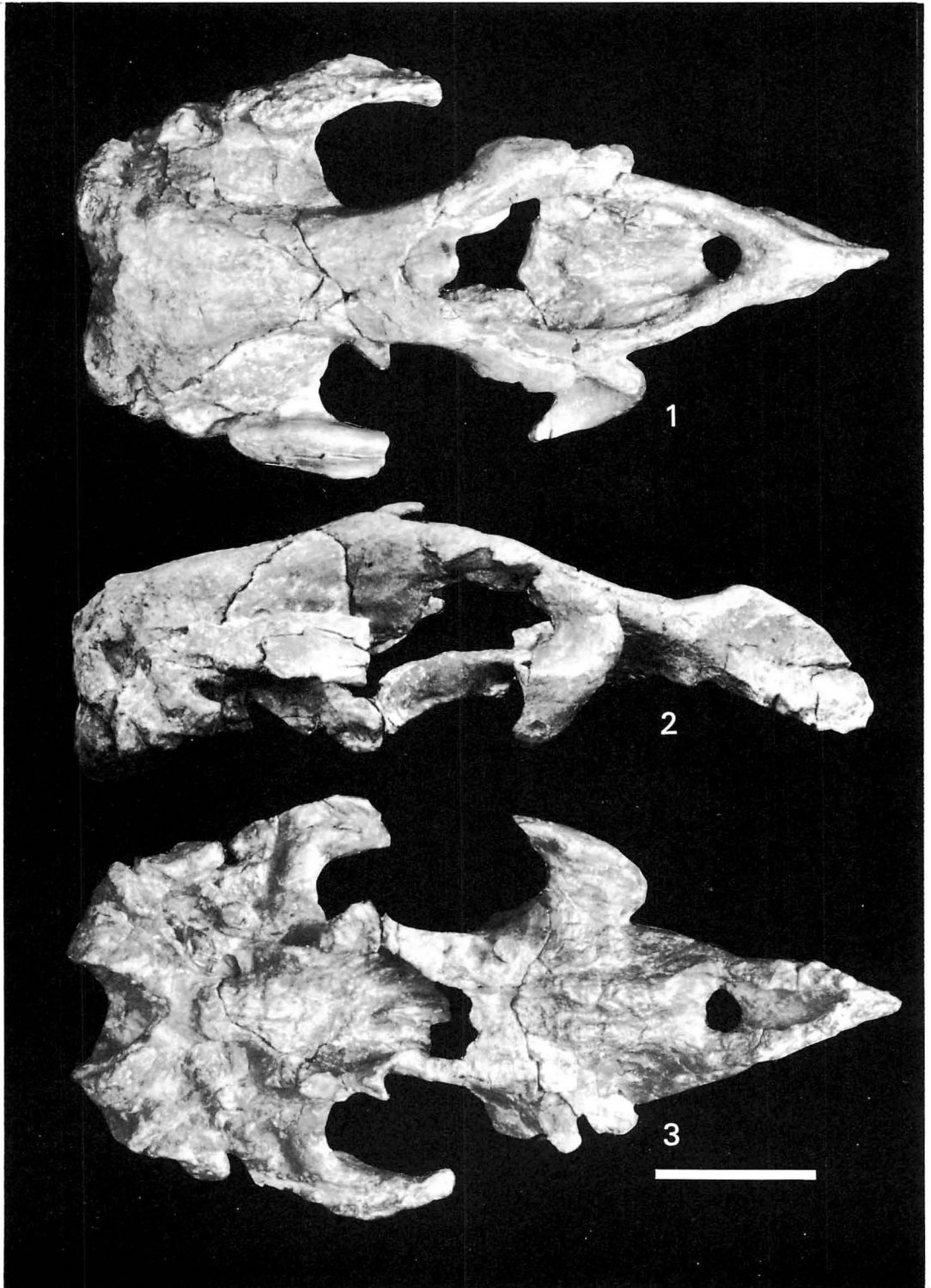
Lacrimonal:—None discernible.

Frontal:—Supraorbital process moderately developed, with distinct posterolateral corner; anterior tip blunt; dorsolateral side slopes very steeply. Internasal process prominent and up-turned, similar to that of one *Dusisiren jordani*

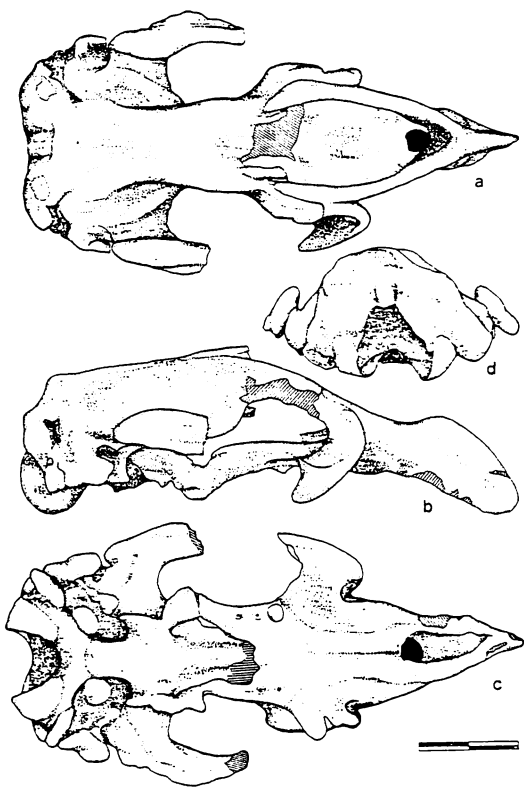
(UCMP 77037). Dorsal surface of frontal slightly and evenly convex; temporal crests slightly overhang lateral sides; cranial vault square in cross section.

Parietal:—Frontoparietal suture indistinct, location uncertain. Temporal crests lyriform, forming thick rounded ridges about 2.5 cm apart with shallow concavity between them on anterior part of parietal roof. Roof flat fore-and-aft, its posterolateral corners indented by squamosals. Endocranial surface not prepared.

Supraoccipital:—Low and wide; height 60 mm, width about 123 mm. Forms angle of 128° with posterior part of parietal roof, resembling *Hydrodamalis gigas* more than it does the earlier species. External occipital protuberance hardly



Figs. 1—3. Holotype of *Dusisiren dewana*, n. sp. Skull: Fig. 1, dorsal view; Fig. 2, lateral view; Fig. 3, ventral view. Scale = 10 cm.



Text-fig. 4. Holotype of *Dusisiren dewana*, n. sp. Skull: a, dorsal view; b, lateral view; c, ventral view; d, posterior view. Scale = 10 cm.

rises above plane of parietals. Median ridge well developed.

Exoccipital:—Supraoccipital-exoccipital sutures indistinct but seem to form angle of about 135° . Exoccipitals do not meet in dorsal midline. Foramen magnum probably had fairly acute dorsal peak, now somewhat distorted. Dorsolateral border of exoccipital about 25 mm thick, rugose, overhangs posterior surface. Paroccipital process does not reach as far ventrally as condyle; forms curved flange as in adult *D. jordani*. Curvature of condyle as in *D. jordani*, forms arc of about 100° . Supracondylar fossa absent, exoccipital surface distinctly convex dorsal to condyle and indented only slightly dorsolateral to condyle.

Basioccipital:—Bears prominent, convex occipitosphenoidal eminence, not divided in midline. Apparently fused with basisphenoid, but a

break extends through approximate position of suture.

Basisphenoid, Presphenoid, Orbitosphenoid, Alisphenoid:—Not seen to differ from those of *D. jordani*.

Pterygoid:—Pterygoid processes broken. Lateral and medial edges of pterygoid fossa appear to intersect dorsally.

Palatine:—Poorly preserved, palatal extent uncertain.

Maxilla:—Dental capsule apparently atrophied. Edges of palatal surface lyriform, palatal gutter narrow anteriorly. Palatal and rostral surfaces probably met in smooth curve. Edges of palatal surface forward of alveoli fairly abrupt and rounded. Zygomatic-orbital bridge elevated high above palatal surface (about 15 mm on left, about 25 mm on right; evidently distorted), about as in *H. cuestasae* (UCMP 86433; Domning, 1978: fig. 8f). Bridge long fore-and-aft, edges fairly sharp; bridge thin dorsoventrally. Anterior opening of infraorbital foramen visible in ventral view; about 21 mm high, about 18 mm wide. Palate about 9 mm thick anterior to molar region.

Squamosal:—Dorsally in contact with squared posterior part of parietal roof. Posterior edge has shallow indentation for mastoid foramen. Sigmoid ridge weak or absent near dorsal end of mastoid foramen, well developed but rounded ventrally (below level of zygomatic root). Cranial portion of squamosal shows distinct bulge dorsal to zygomatic root. Postglenoid process rather low; postarticular fossa fairly deep. Processus retroversus short, not inflected; posterior edge of zygomatic root distinctly notched. Zygomatic process perhaps slightly more sigmoidal in outline than lozenge-shaped, but posterodorsal edge still long, relatively straight, and not noticeably convex laterad. Anterior tip of zygomatic process does not reach level of supraorbital process; anterior part triangular in cross section, lateral edge sharper than medial.

Jugal:—Ventralmost point lies below orbit. Zygomatic process extends back to level of front edge of temporal condyle. Prominent rounded protuberance present on anterodorsal

Table 2. Measurements of mandible, in mm. Letters in parentheses denote measurements used by Domning (1978: tab. 7). e = estimated.

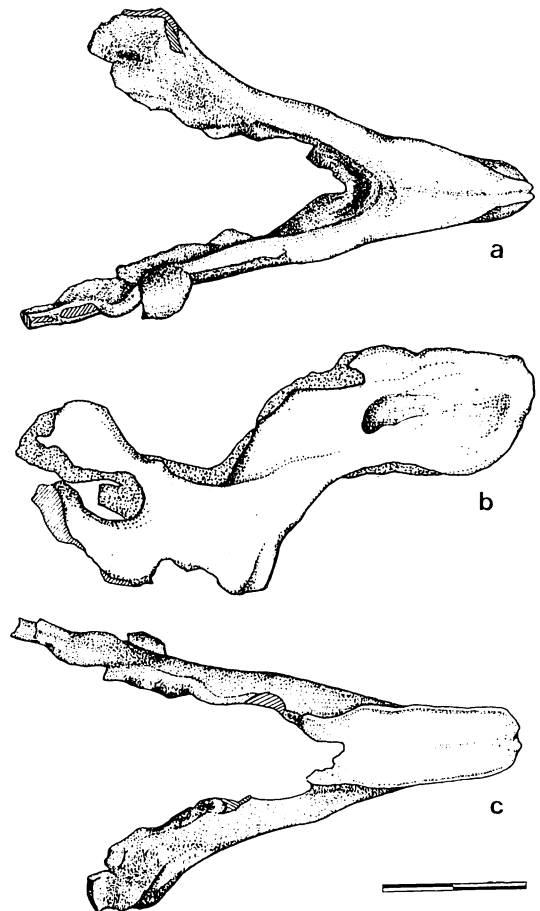
Anterior tip to front of ascending ramus (AG)	235e
Anterior tip to rear of mental foramen (AP)	123
Anterior tip to front of mandibular foramen (AQ)	181
Length of symphysis (AS)	107
Height at deflection point of horizontal ramus (EF)	117e
Deflection point to rear of alveolar row (EU)	124e
Front of ascending ramus to rear of mental foramen (GP)	143e
Minimum dorsoventral breadth of horizontal ramus (MO)	64e
Maximum breadth of masticating surface (RR')	44
Length of alveolar row (TU)	58e
Maximum width between labial edges of left and right alveoli (VV')	90e

margin of orbit.

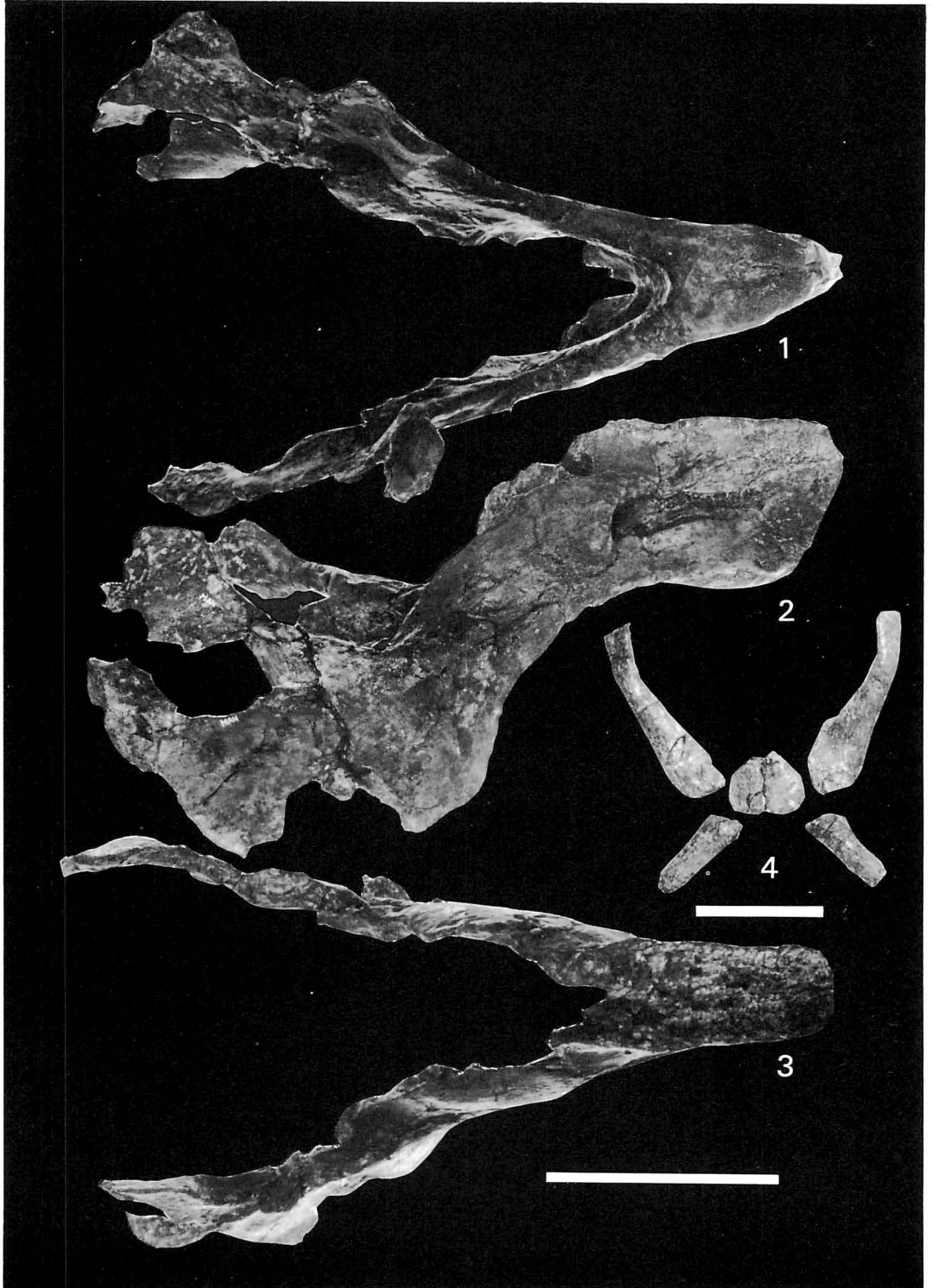
Periotic, Tympanic, Auditory Ossicles:—Not prepared.

Mandible (Table 2; Text-fig. 5; Pl. 54): Ascending rami only partly preserved. Coronoid process very well developed, with backward-pointing dorsal tip. Sharp, prominent vertical ridge on anteromedial side of ascending ramus extends well up into coronoid process, as in *Hydrodamalis*. Region of mandibular foramen, coronoid canal, and tooth alveoli poorly preserved. Bone surface lateral to rear of tooth row slopes steeply, apparently as in young adult or adult *Dusisiren jordani*. Horizontal ramus relatively long and slender as in other hydrodamalines. Dorsal edge forms thin plate between tooth row and anterior masticating surface. Single mental foramen of moderate size lies at about level of anterior deflection, as in *D. jordani*. Deflection of masticating surface = 43° ; deflection abrupt as in *D. jordani*. Masticating surface deeply notched in posterior midline; surface very narrow and rectangular in outline, with lateral edges only slightly overhanging, like *Hydrodamalis gigas* rather than *D. jordani*. Anteroventral edge of symphysis keel-like, thickened with concave sides, but slightly concave in outline, giving symphyseal region distinctly *Hydrodamalis*-like appearance in lateral view. Posteroventral surface of symphysis has distinct bilateral "chin" protuberances separated by shallow groove.

Dentition (Table 3; Text-figs. 6–7; Pl. 55):—



Text-fig. 5. Mandible: a, ventral view; b, lateral view; c, dorsal view. Scale = 10 cm.



Figs. 1—3. Mandible: Fig. 1, ventral view; Fig. 2, lateral view; Fig. 3, dorsal view. Fig. 4, hyoid apparatus. Scales = 10 cm.

Table 3. Dental measurements of holotype of *Dusisiren dewana*, in mm. L = crown length; AW = anterior width; PW = posterior width; w = dimension reduced by wear.

		LEFT	RIGHT
M ¹ :	L	16.1	16.7
	AW	14.8	14.5
	PW	15.6
M ² :	L	18.8	19.0
	AW	19.9	19.2
	PW	18.2	18.2
M ³ :	L	21.4	20.1
	AW	18.0	18.1
	PW	15.9	15.4
M ₂ :	L	17.9w	18.6w
	AW	17.0w	17.9
	PW	18.2	18.0
M ₃ :	L	17.8w	18.5w
	AW	18.0	17.7
	PW	17.2	17.1

No incisors or canines. Deciduous premolars unknown; adult dentition apparently 0.0.0.3. Anterior edge of M¹ approximately level with posterior edge of zygomatic-orbital bridge; empty DP alveoli reach less than halfway forward along bridge. M³ separated by at least 27 mm from presumed position of pterygoid process. All teeth except the right M¹ were loose in the matrix enclosing the skeleton; neither M₁ was located.

M¹: Loose on left but still in position on right, allowing its identification. Heavily worn; all cusps except a tiny posterior cingular cuspule coalesced into a single lake of dentine.

M²: Labial roots coalesced and closely adherent to lingual root. Maximum length of labial root = 25 mm. Anterior interdental wear facet present. Crown moderately worn. Protocone and paracone form continuous dentine lake; no distinct protoconule. Protocone elongated anteroposteriorly or coalesced with anterolingual cingular cusp. Transverse valley constricted lingually. Hypocone-metaconule forms single lake, including posterolingual cingular cusp (not distinct) and extending slightly labiad along low posterior cingular ridge, which had at least one distinct cuspule. Metacone distinct, isolated.

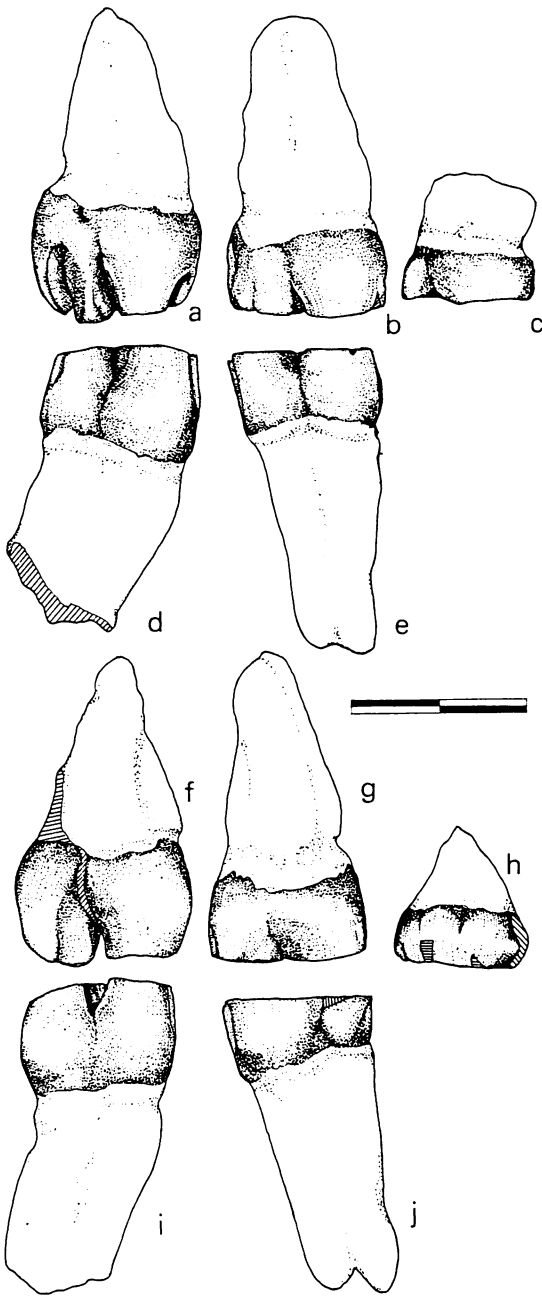
M³: Roots coalesced as on M²; maximum length = 23 mm. Anterior interdental wear facet

present. Crown slightly worn anteriorly, almost unworn posteriorly. Protocone elongate, no distinct anterolingual cusp. Protoconule absent, protoloph formed only by protocone and paracone. Transverse valley deep, narrow. Hypocone-metaconule and posterolingual cingular cusp approximately in line with paracone. Metacone absent. Posterior basin enclosed only by tiny posterolabial cuspule (absent on right).

These teeth differ from those of *D. jordani* in their smaller size and (probably consequent) simplification: reduction of anterior and posterior cingula and loss of the protoconule and, on M³, the metacone.

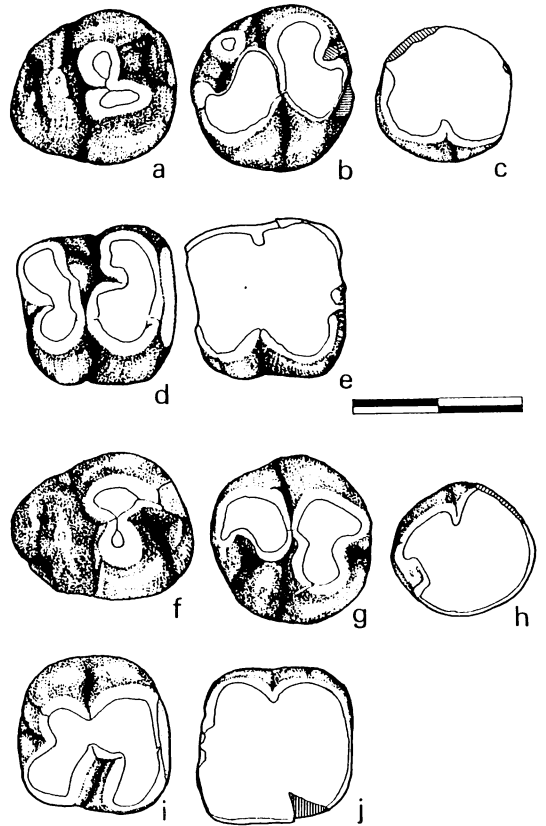
M₂: Has two straight coalesced roots, anteroposteriorly compressed; maximum length of anterior root = 27 mm (posterior root slightly shorter). Very large posterior interdental wear facet present. Crown heavily worn, pattern obliterated.

M₃: Roots coalesced as above; damaged. Very large anterior interdental wear facet present, larger on left tooth. Crown moderately worn; large protoconid and smaller metaconid confluent anteriorly, forming single crescentic lake of dentine. Metaconid with slight suggestion of a posterolabial basal projection. Transverse valley constricted labially. Hypoconid and entoconid also confluent, forming crescentic lake concave



Text-fig. 6. Right teeth, labial views (a–e), and left teeth, lingual views (f–j): a, f, M³; b, g, M²; c, h, M¹; d, i, M₃; e, j, M₂. Scale = 2 cm.

posteriorly; on left M₃ protolophid and hypolophid lakes are confluent labially. Entoconid has blunt rather than sharp posterior edge, but its



Text-fig. 7. Right (a–e) and left (f–j) teeth, occlusal views: a, f, M³; b, g, M²; c, h, M¹; d, i, M₃; e, j, M₂. Scale = 2 cm.

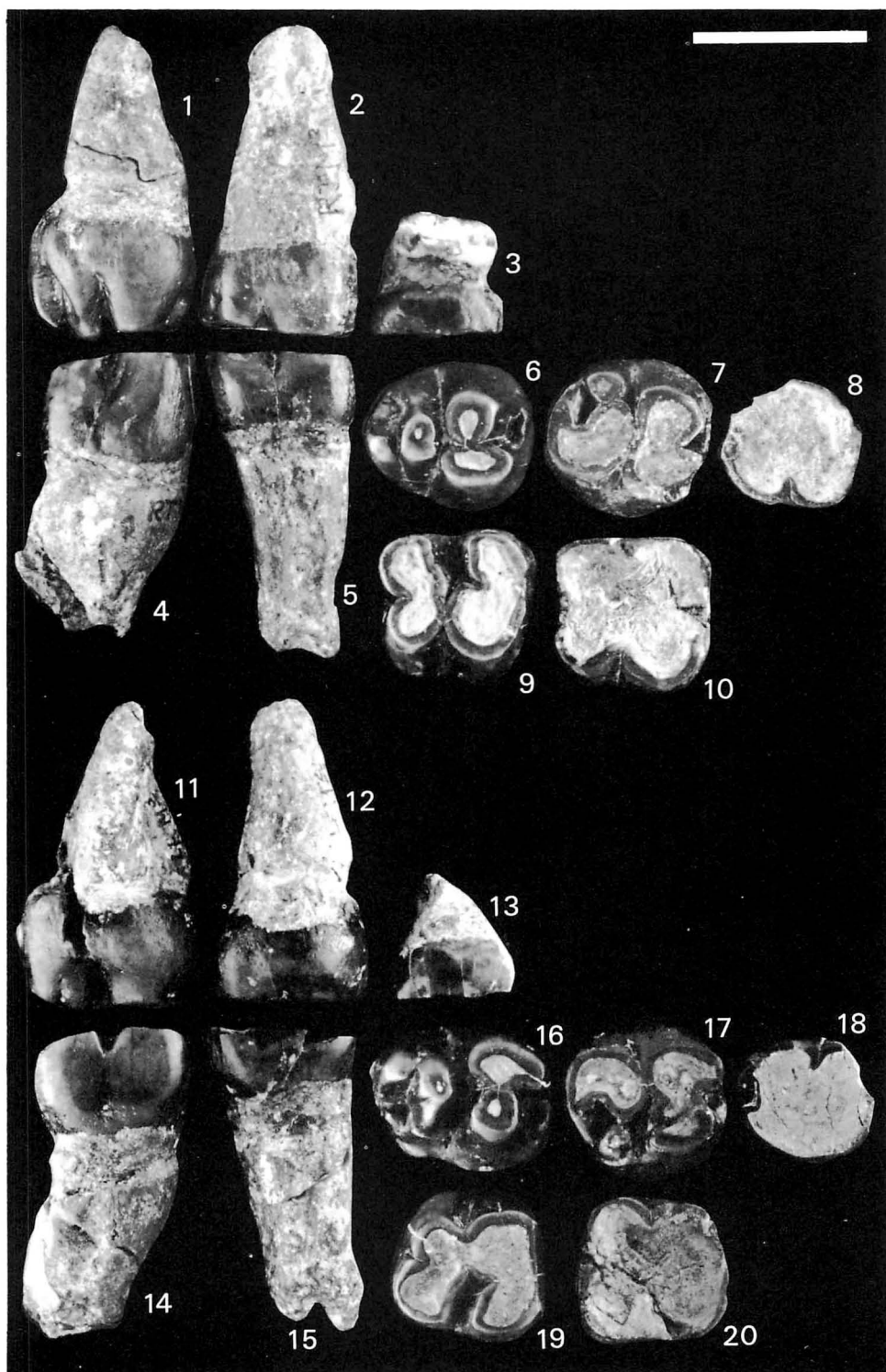
anterolingual corner forms a right angle. Hypoconid elliptical, aligned anterolingual-posterolabially; reaches farther forward than entoconid. Anterior bulge in midline of hypolophid suggests a remnant of a central accessory cusp. No talonid basin or posterior cingular cuspules present.

This tooth, like the upper molars, differs from the M₃ of *D. jordani* in its smaller size, coalesced roots, and simplified pattern, having completely lost the hypoconulid lophule and posterior basin.

Hyoid apparatus (Pl. 54):

Five elements are preserved, which do not differ significantly in size or proportions from those of *Dusisiren jordani* (Domning, 1978: pl. 2d). The tympanohyoids are missing.

Stylohyoid, epihyoid, keratohyoid:—Apparently fused into a single bone on each side. Both left and right elements lack the proximal ends



Figs. 1–20. Teeth: Figs. 1–5, Left M^{1-3} and M_{2-3} , lingual views; Figs. 6–10, same occlusal views; Figs. 11–15, left M^{3-1} and M_{3-2} , occlusal views; Figs. 16–20, same, lingual views. Scale = 2 cm.

Table 4. Measurements of sternum, in mm. e = estimated.

Manubrium	
Length	225+
Maximum breadth (at rib articulations)	164
Breadth of anterior process	119e
Posterior thickness	35
Xiphisternum	
Length	153+
Anterior thickness	37
Maximum breadth posteriorly	87
Posterior rib articulation to attachment of xiphoid cartilage	62e

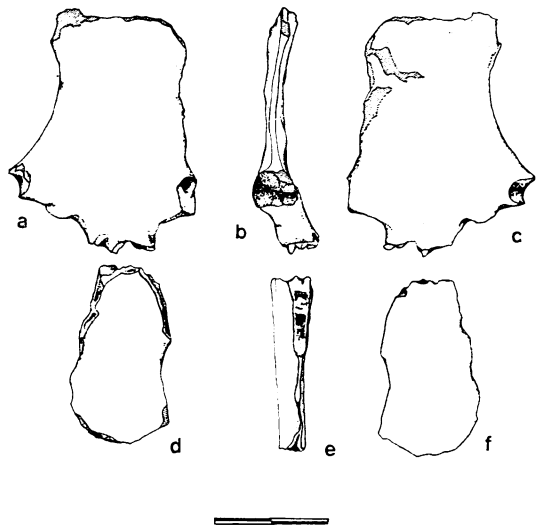
and are about 7.5 cm long. They are narrowest (10 mm) and show a distinct angle at their mid-sections; the distal ends are flattened and expanded (up to 22 mm wide).

Basihyoid:—Roughly triangular, 2.5 cm long and 3 cm wide, with anterior apex and blunt posterior corners.

Thyrohyoid:—4 cm long on one side, 3.5 cm on the other; 1.5 cm wide proximally, tapering distally to some degree.

Postcranial skeleton:

Sternum (Table 4; Text-fig. 8; Pl. 60):—Manubrium and xiphisternum not fused. Anterior process of manubrium broad as in *Hydrodamalis*; about 12 mm thick where anterior edge broken. Ventral surface of anterior process convex downward both fore-and-aft and transversely; ventral keel lacking. Large blunt protuberances for rib articulations project laterad and somewhat ventrad near posterolateral corners of manubrium. Aft these, bone narrows to width of about 6.5 cm and terminates within about 2 cm in straight transverse suture. Ventral surface transversely concave downward at level of rib articulations. Xiphisternum shorter and narrower than manubrium, somewhat spatulate in shape. Anterior part of ventral side convex, with low, smooth median keel that flattens out posteriorly. Anterior part of each lateral edge bears rugose surface about 7 cm long for rib articulation; behind this, lateral edge much thinner. Posterior edge thick and rugose for cartilage attachment. Overall form of sternum intermediate between those of *Dusisiren jordani* and *Hydrodamalis*,



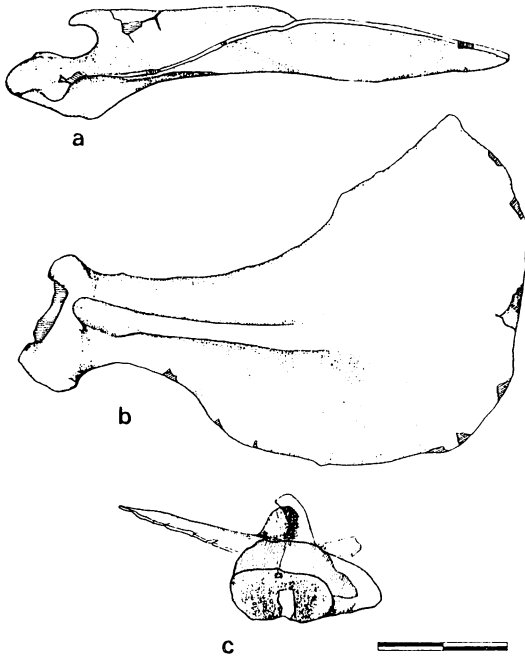
Text-fig. 8. Sternum: a–c, manubrium; d–f, xiphisternum; a, d, dorsal views; b, e, lateral views; c, f, ventral views. Scale = 10 cm.

but more similar to latter in having keel developed on xiphisternum rather than on manubrium.

Scapula (Table 5; Text-fig. 9; Pls. 56–57):—Supraspinous fossa about 9 cm wide, much narrower than in *Dusisiren jordani*; anterior edge convex in outline, but fairly thick and inflected laterad as in *Hydrodamalis cuetae*. Spine well developed, overhanging posteriorly, with robust acromion extending close to distal end, likewise resembling *H. cuetae*. End of acromion flattened somewhat in plane parallel to blade of scapula. Coracoid process blunt, rounded, inflected slightly mediad. Glenoid cavity oval, deeply

Table 5. Measurements of scapulae, in mm. Letters in parentheses denote measurements used by Domning (1978: tab. 17). e = estimated.

	Left	Right
Maximum length, vertebral border to border of glenoid fossa (AB)	...	452e
Mediolateral width of glenoid fossa (BI)	66	65e
Lateral border of glenoid fossa to inside of concave distal end of spine (BJ)	63e	55e
Maximum breadth of blade dorsally (CD)	283e	288
Minimum anteroposterior breadth of neck (EF)	...	73
Maximum anteroposterior breadth of distal end (GH)	112e	116
Summit of spine to medial side of blade, measured parallel to plane tangent to posterior edges of spine and neck (KL)	...	75e
Anteroposterior length of glenoid fossa (MN)	86e	86
Length of teres major origin from teres protuberance to posterior corner of blade (TMO)	115e	102e



Text-fig. 9. Right scapula: a, anterior view; b, lateral view; c, distal view. Scale = 10 cm.

concave.

Humerus (Table 6; Text-fig. 10; Pls. 57–58):—Tubercles large and massive, bicipital groove deep and narrowed by anteromedial flange of greater tubercle. Tubercles diverge at angle of about 75°. Greater tubercle has clear supraspinatus and infraspinatus insertion scars as in *Dusisiren jordani*. Deltoid crest less developed than in *D.*

jordani, more resembling *Hydrodamalis*. Protuberance present on lateral side of neck, possibly for lateral triceps origin. Head nearly circular. Humerus tapers distal to deltoid crest, having dumbbell shape as in *D. jordani*. Pectoralis major insertion not discernible, but depressed area for teres major insertion is well marked distal to lesser tubercle. Axis of trochlea canted about 80° to 85° to shaft. Posterior side of ectepicondyle about even with posterior side of trochlea, but entepicondyle extends about 1 cm farther aft. Anteromedial edge of trochlea prominent; trochlea trapezoidal in outline in distal view, as in *Hydrodamalis* and some *D. jordani* (UCMP 77037). Entepicondyle extends posteromedial a distance less than half width of trochlea. Notch in articular surface for humero-ulnar ligament not visible. Olecranon and coronoid fossae shallow.

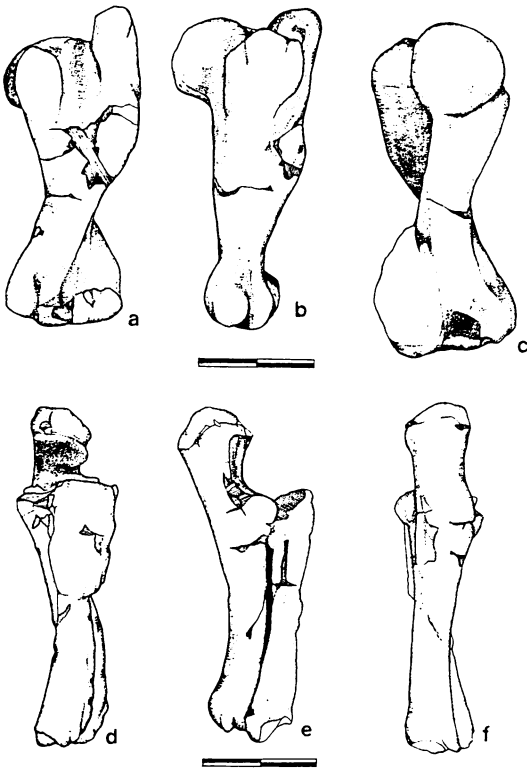
Radius-ulna (Table 7; Text-figs. 10–12; Pls. 57–58):—Fused proximally; distal epiphyses fused to each other but sutures with diaphyses visible. Interosseous space continuous. Much torsion present between radius and ulna, as in *Dusisiren jordani*, but both visibly bowed medially as in *D. jordani*. Distal articular surface much more resembles that of *H. cuestasae*; has subequal convex facets on anterior and medial parts of distal surface, medial facet facing posterodistad and mediad. A separate protuberance, as in



Figs. 1, 2. Scapulae: Fig. 1, left; Fig. 2, right; lateral views. Scale = 10 cm.

Table 6. Measurements of humeri, in mm. Letters in parentheses denote measurements used by Domning (1978: tab. 18). e = estimated.

	Left	Right
Maximum length, greater tubercle to distal end (AB)	296	296
Maximum breadth, greater to lesser tubercle (CD)	133	129
Maximum breadth, ectepicondyle to entepicondyle (EF)	125	119
Maximum thickness, posterior side of head to anterior side of greater tubercle (GH)	129	136
Maximum thickness, posterior to anterior ends of medial rim of trochlea (IJ)	49	...
Mediolateral breadth of head (KL)	78	74
Proximodistal breadth of head (MN)	79	79
Breadth of anterior side of trochlea (OP)	86	90
Length, saddle between head and greater tubercle to saddle of trochlea (QR)	270	...



Text-fig. 10. Left humerus (a—c) and radius-ulna (d—f): a, d, anterior views; b, e, medial views; c, f, posterior views. Scale = 10 cm.

Hydrodamalis, lies lateral to this facet, which however lacks the clearly developed posterolateral extension that forms the L-shape seen in *D. jordani* and *H. cuestasae*. Shape and develop-

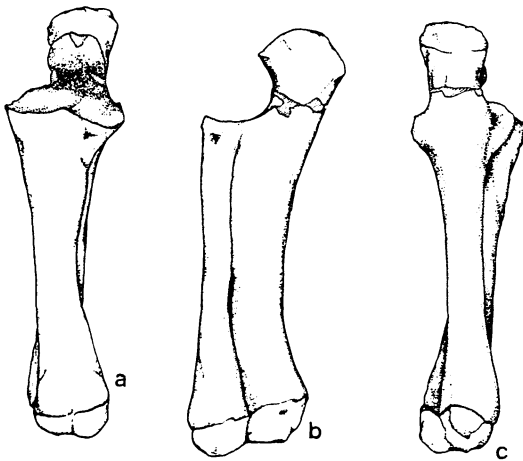
ment of olecranon process resemble those of *H. cuestasae*. Semilunar articular surface notched laterally as in *D. jordani* and *H. cuestasae*. Top edge of semilunar notch slopes laterad. Medial side of olecranon process smooth, convex. Coronoid process has slight concavity continuous with concavity on radius. Sharp ridge on lateral side of distal ulnar shaft lacking. Distal articular facet narrow as in *H. cuestasae* and faces mediolateral, but does not overlap with posteromedial end of radial facet. Groove on lateral side of ulna for extensor digiti quinti tendon distinct but shallow; grooves for other extensor tendons not discernible.

Manus (Text-figs. 13—15):—The almost complete right manus is preserved in articulation with the right radius-ulna; the left fifth metacarpal is also present. The manus consists of four carpals, five metacarpals, and probably seven phalanges (two each on digits II—IV, one on digit V).

Fused scaphoid-lunar-centrale: Of all the carpals, this is the least modified from its condition in *Dusisiren jordani*. Its outline in proximal view is roughly that of a quarter-circle, but with the convex side medial rather than lateral. The concave proximal articular facet is kidney-shaped with the notch in its outline on the posterolateral side, corresponding to the articular surface of the radius. The posterior side of the carpal's outline has a deep indentation; the bone in this

Table 7. Measurements of radius-ulnae, in mm. Letters in parentheses denote measurements used by Domning (1978: tab. 19). e = estimated.

	Left	Right
Total length of ulna (AB)	...	297
Total length of radius, anterior lip of semilunar notch to distal end (CD)	...	253
Height of semilunar notch, anterior tip of olecranon to anterior radial lip of notch (EC)	58	55e
Thickness of olecranon, anterior tip to posterior side (EF)	64e	64e
Distal thickness, anterior side of radius to posterior side of ulna (GH)	...	94
Maximum mediolateral breadth, radial portion of semilunar notch (IJ)	76e	88
Maximum mediolateral breadth, ulnar portion of semilunar notch (KL)	49e	51
Minimum mediolateral breadth of semilunar notch (at its midsection) (MN)	39	41e
Minimum thickness of olecranon, posterior side to semilunar notch (OP)	43	45



Text-fig. 11. Right radius-ulna: a, anterior view; b, medial view; c, posterior view. Scale = 10 cm.

region is rather thin (11 mm) proximodistally, and its articulation with the cuneiform-pisiform is weaker than in *D. jordani*. The distal side has two well-developed facets for the trapezium-trapezoid-magnum, the anterior oval (18 mm wide, 14 mm long) and slightly concave transversely, the posterior larger (22 mm wide, about

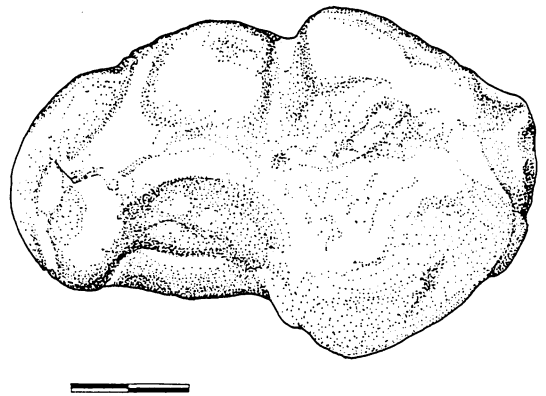
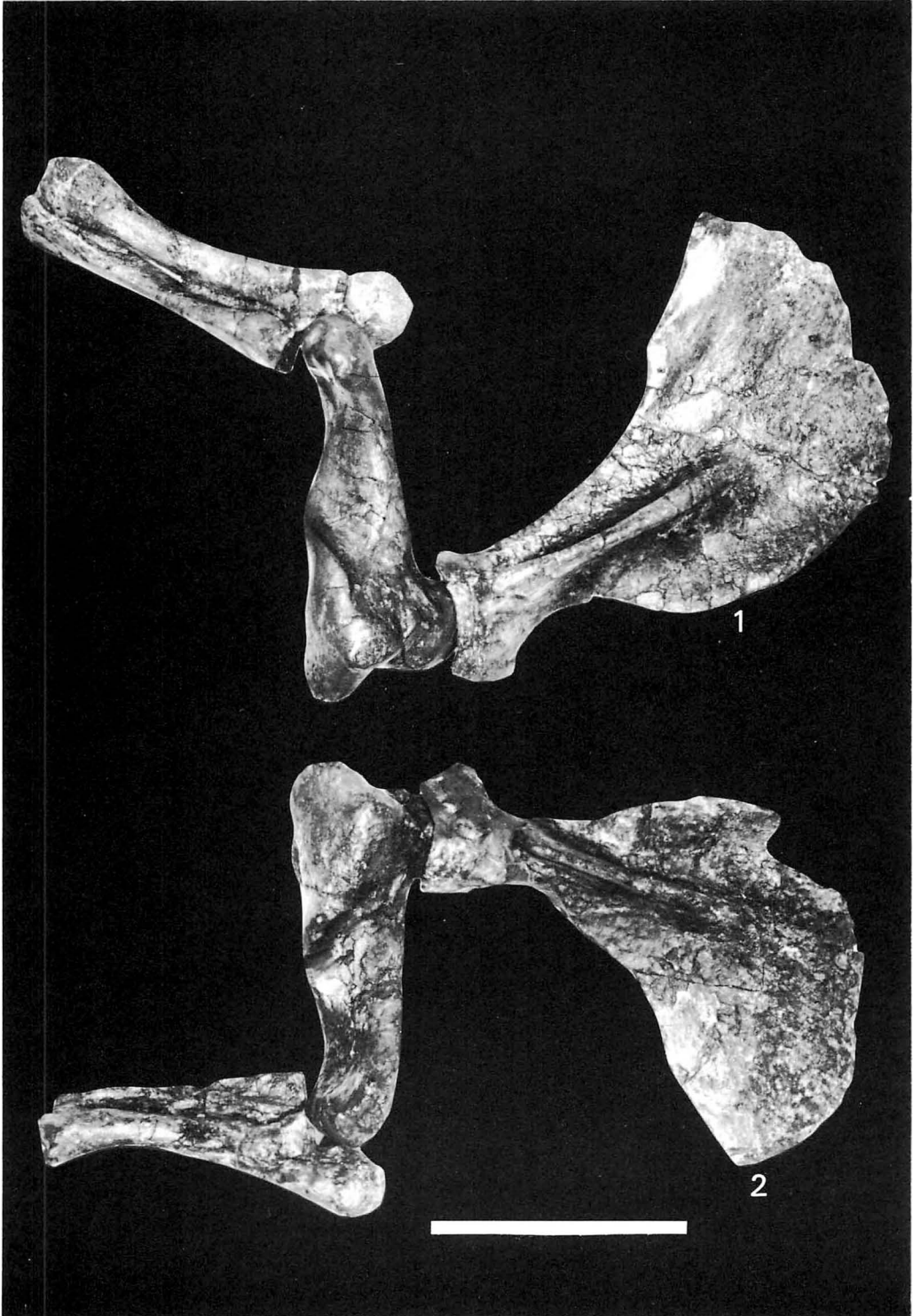


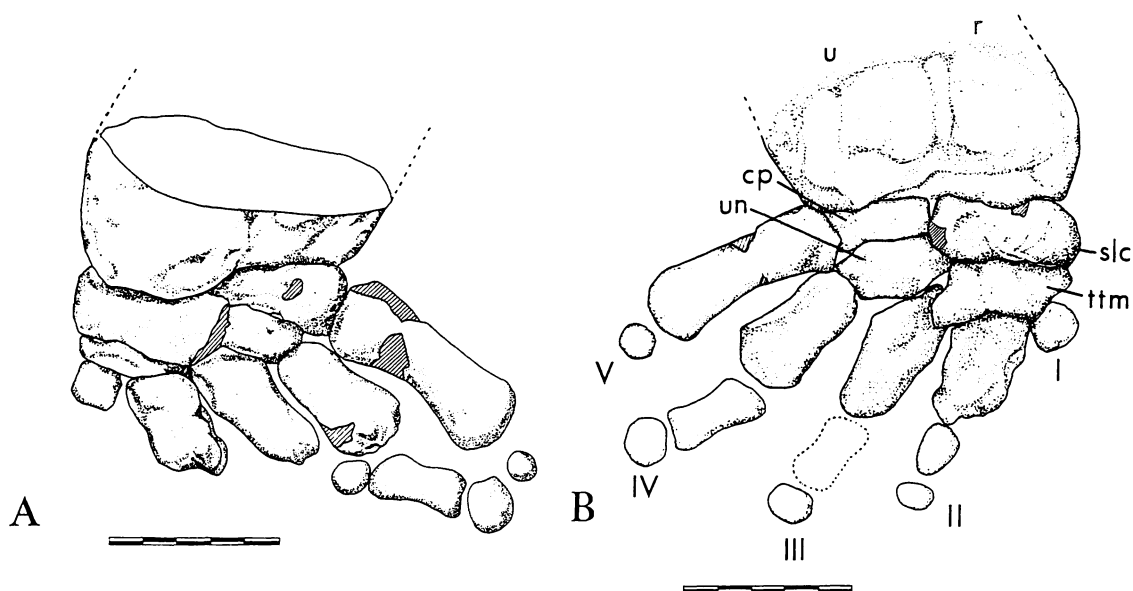
Fig. 12. Right radius-ulna, distal view; lateral side at top. Scale = 2 cm.

17 mm long) and deeply concave; the facets are separated by a groove. The distal extremity of the bone lies medial, rather than lateral, to the posterior facet, and is formed by a distinct protuberance of the bone separated from the facet by a groove. Anteroposterior length of bone = 47 mm, breadth = 47 mm.

Fused cuneiform-pisiform: The anterior (cuneiform) portion is greatly reduced and flattened proximodistally, giving the bone a wedgelike shape tapering anteriorly from the robust metacarpal articulation. This anterior portion, only 11 mm thick, bears a slightly



Figs. 1, 2. Scapulae, humeri, and radius-ulnae in articulation: Fig. 1, right; Fig. 2, left; lateral views. Scale = 20 cm.

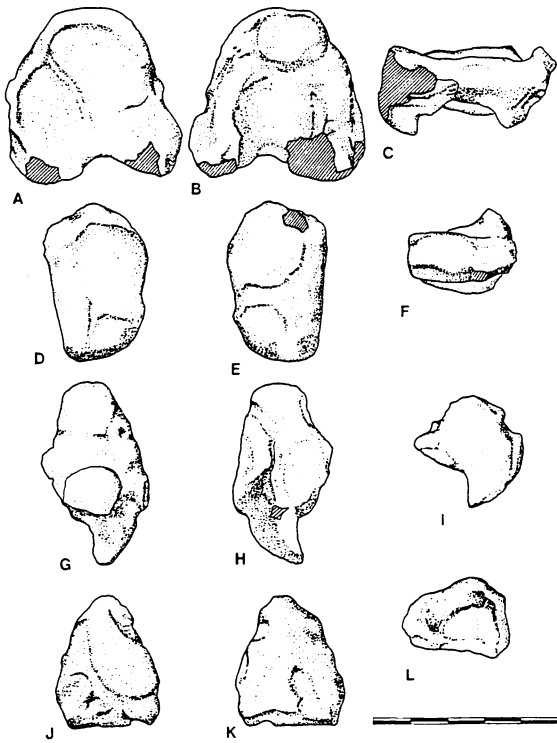


Text-fig. 13. Right manus, medial and lateral views. 13A, figure showing bones articulated as preserved in the rock, together with part of distal end of radius-ulna (continuation of shafts indicated by dashed lines). Scale = 5 cm. 13B, hypothetical restoration in approximate life position, together with part of distal end of radius-ulna (continuation of shafts indicated by dashed lines). Phalanges shown associated with digit II were found in contact with lateral surface of metacarpal III. cp, cuneiform-pisiform; r, radius; slc, scaphoid-lunar-centrale; ttm, trapezium-trapezoid-magnum; u, ulna; un, unciform; I-V, digits I-V. Scale = 5 cm.

saddle-shaped articular facet for the posteromedial-facing surface of the ulna. This facet, triangular but more elongate anteroposteriorly than in *D. jordani*, is about 30 mm long. The anterior end of the bone is 26 mm wide mediolaterally, and convex where it articulates with the scaphoid-lunar-centrale. It is unclear whether distinct facets were developed in the latter joint. The distal facet for the unciform is broad, flat, and oval, 20 mm long and 15 mm wide, and oriented parasagittally (*i.e.*, oblique to the long axis of the cuneiform-pisiform, which is directed posteromedial). Aft of this facet and separated from it by a deep groove is a smaller oval facet, 15 × 9 mm, oriented perpendicular to the former facet; this apparently articulated with the posterior side of the proximal end of metacarpal IV. The pisiform portion of the bone is a robust posteromedial projection with a convex posterodistal articular surface for metacarpal V. This surface is 19 mm wide and trapezoidal in pos-

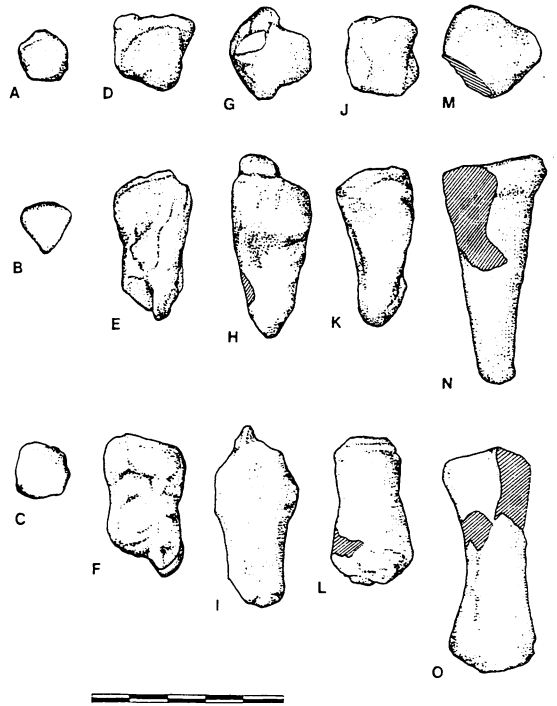
teromedial view, with its smallest proximodistal dimension (about 14 mm) lateral and its largest (23 mm) medial. Maximum overall length of bone = 44 mm.

Fused trapezium-trapezoid-magnum: Much more complex in shape than in *D. jordani*. The quarter-ellipse proximal outline of the latter form is still recognizable, but its posterolateral corner is greatly elongated by a pointed spurlike process directed posterodistal. The two proximal facets correspond in size and shape to the distal facets of the scaphoid-lunar-centrale; the posterior facet is elevated about 7 mm above the plane of the anterior. The after side of this elevation bears a broad, flat facet for the unciform, and lateral and distal to it lies the proximomedial-facing surface of the spurlike process mentioned above. This surface may also have articulated with the unciform. Anteriorly, the trapezium-trapezoid-magnum is only 7 mm thick. Its distal surface bears a flat, triangular anterior facet,



Text-fig. 14. Right carpals; A—C, scaphoid-lunar-centrale; D—F, cuneiform-pisiform; G—I, trapezium-trapezoid-magnum; J—L, unciform; A, D, G, J, proximal views; B, E, H, K, distal views (anterior at top in both); C, I, posterior views; F, L, anterior views. Scale = 5 cm.

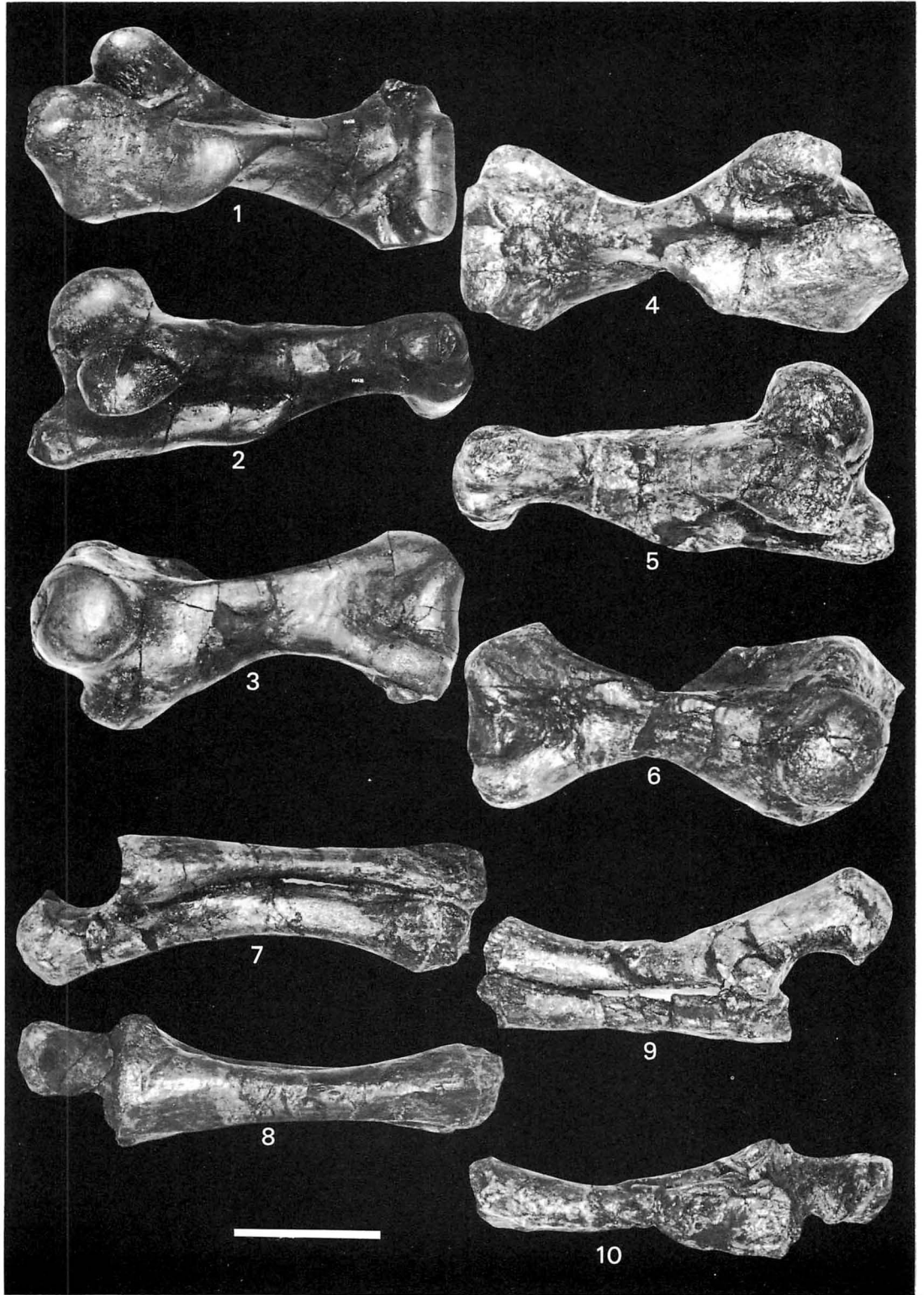
widest (12 mm) anteriorly and about 14 mm long, for metacarpal I, and an irregularly oval or triangular posterior facet, 18 mm long and 12 mm wide, for metacarpal II. The posterior facet is flat forward and slightly concave aft, and forms an angle of about 30° with the anterior facet. Lateral to the posterior facet and separated from it by a groove is a massive flange 7 mm thick, projecting distally about 7 mm below the plane of the facet. From its distalmost extremity, the rounded border of this flange ascends both anteriorly and posteriorly, and at the rear becomes continuous with the posterodistad-projecting spurlike process. This flange articulates with the lateral facet of metacarpal II. A pit lies proximal to the flange's anterior end, and its lateral surface bears an irregular



Text-fig. 15. Right metacarpals; A—C, metacarpal I; D—F, metacarpal II; G—I, metacarpal III; J—L, metacarpal IV; M—O, metacarpal V; A, D, G, J, M, proximal views; B, E, H, K, N, posterior views; C, F, I, L, O, medial views. Scale = 5 cm.

bulge posteriorly, separated by a small vertical groove or fissure from a similar bulge on the spurlike process. Overall length of bone = 48 mm, breadth = 28 mm, maximum proximodistal thickness = 28 mm.

Unciform:—Curiously wedge-shaped, 34 mm long anteroposteriorly, 28 mm wide mediolaterally, and 17 mm thick proximodistally, resembling (and apparently homologous to) the carpal of *Hydrodamalis cuestae* illustrated by Domning (1978: fig. 25). The pointed end, strangely, seems to have been directed anteriorly and proximolaterally, contacting the lateral part of the joint between scaphoid-lunar-centrale and trapezium-trapezoid-magnum. The opposite (posterior), flat end has a trapezoidal surface measuring 24 mm mediolaterally, 16 mm proximodistally at the lateral side, and 12 mm at the



Figs. 1—10. Humeri and radius-ulnae: Right (Figs. 1—3) and left (Figs. 4—6) humeri: Figs. 1, 4, anterior views; Figs. 2, 5, medial views; Figs. 3, 6, posterior views. Right (Figs. 7, 8) and left (Figs. 9, 10) radius-ulnae: Fig. 7, lateral view; Figs. 8, 10, anterior views; Fig. 9, medial view. Scale = 10 cm.

medial side; this surface articulates with metacarpal IV. The proximal surface bears a large flat oval facet laterally for the cuneiform. The distal surface has a semicircular or rectangular posterior area for metacarpal III; each bone's articular surface is divided by a groove into a narrow medial facet and a much broader lateral one. Anterior to this surface and forming an angle of about 50° with it, a smaller, somewhat lozenge-shaped facet articulates with the trapezium-trapezoid-magnum. Lateral to this facet and facing distad rather than anterodistad is a surface related to the spurlike process of the latter bone. Anteromedially and proximally the unciform is related to the distal side of the posteromedial corner of the scaphoid-lunar-centrale; a facet is indistinctly developed here also.

Metacarpal I:—Vestigial; about 14×14 mm proximally, 13 mm long; wedge-shaped, with flat proximal end and chisel-like distal end. Apparently no phalanx articulated with it.

Metacarpal II:—Irregular, squarish bone 36 mm long, diminishing in mediolateral thickness distally. Proximal end trapezoidal, 21×21 mm, with broad, flat medial facet and narrow lateral facet facing proximolaterad, separated by sharp ridge. Anterior surface flattened proximally where it is in contact with metacarpal I. A bulge on medial side of posterior surface near proximal end contacts metacarpal III. A flat oval facet-like area on lateral side of posterior surface does not appear to articulate with anything. Lateral side of shaft concave, medial side more or less flat. Distal end oblique, 21 mm long anteroposteriorly, posterior part extending farther distad and much thicker (about 14 mm), with distinct protuberance on palmar surface. Phalangeal articular surface not well marked.

Metacarpal III:—Anterior side of proximal end has facet for contact with metacarpal II; area on posterior side in contact with metacarpal IV less distinct. Large flat rectangular surface for unciform faces posterad and proximad, sloping steeply and divided as described above. Proximal extremity of bone formed by a styloid process which reaches toward distal extremity of scaphoid-lunar-centrale and may contact it.

Indeed, it seems to form a hook lying anterior to the distal process of the scaphoid-lunar-centrale in such a way that contact between the two would resist straightening of the metacarpal from its posteriorly inclined position; this, however, is not certain. Lateral surface of metacarpal related to spurlike process of trapezium-trapezoid-magnum, but no articular facet is developed. Posterior side of metacarpal broad, slightly concave. Bone tapers distally, end blunt, somewhat compressed mediolaterally, and slightly curved backward, without distinct phalangeal surface. Total length of bone = 48 mm; proximal end 22 mm long anteroposteriorly, 20 mm wide mediolaterally; distal end 17 mm long, 10 mm thick.

Metacarpal IV:—Stubby, 40 mm long, with rectangular proximal end 18 mm long and 20 mm wide; main articular surface irregularly convex. Indistinct surfaces along anterior and posterior edges contact metacarpal III and cuneiform-pisiform, respectively. Lateral side of shaft concave, medial side slightly convex. Bone diminishes in thickness distally to only 12 mm, but broadens to anteroposterior length of 23 mm, with convex outline; lacks distinct distal articular surface.

Metacarpal V:—By far the largest metacarpal, 64 mm long on right side. Proximal end oval (posteromedial corner missing), concave, 26 mm wide, more than 21 mm long. Shaft tapers distally to thickness of about 11 mm, but beyond its narrow midsection it widens to an anteroposterior length of 22 mm. Its midsection is narrower than in *Hydrodamalis cuestae* (UCMP 86433: Domning, 1978: fig. 26), but the bone is otherwise very similar to the metacarpal of the latter, which on this basis is almost certainly metacarpal V rather than II as Domning (1978: p. 90) suggested. Distal end convex in outline, with indistinct articular surface like the other metacarpals. Left metacarpal V similar but damaged proximally. None of the metacarpals shows signs of incomplete epiphyseal fusion.

Phalanges:—Very small compared to metacarpals. Those apparently belonging to digit II were found against the lateral surface of meta-

carpal III; the proximal one measures 15 mm proximodistally, 11 mm anteroposteriorly, 6 mm mediolaterally; the distal one, 8 × 11 × 5 mm. Both are flattened kernels of bone without any distinctive shape. The proximal phalanx of digit III appears to be missing; the distal measures about 11 × 13 × 6 mm. The proximal phalanx of digit IV is the best developed of all, 29 mm in length with expanded proximal and distal ends, measuring 16 × 11 and 15 × 10 mm, respectively. The distal phalanx measures 14 × 16 × 8 mm and has a saddle-shaped medial surface,

convex proximodistally and concave anteroposteriorly. Lying next to it in the matrix was a spheroidal lump of bone about 10 mm in diameter, apparently the sole phalanx of digit V.

Innominate:—Not preserved.

Vertebrae (Tables 8–11; Pl. 59):—All seven cervical vertebrae are present, together with the 13 most anterior thoracics. An articulated series of nine more posterior vertebral centra (posterior thoracics through anterior caudals?) was collected separately in the year before the rest of the skeleton was discovered. The vertebrae resemble

Table 8. Measurements of atlas, in mm.

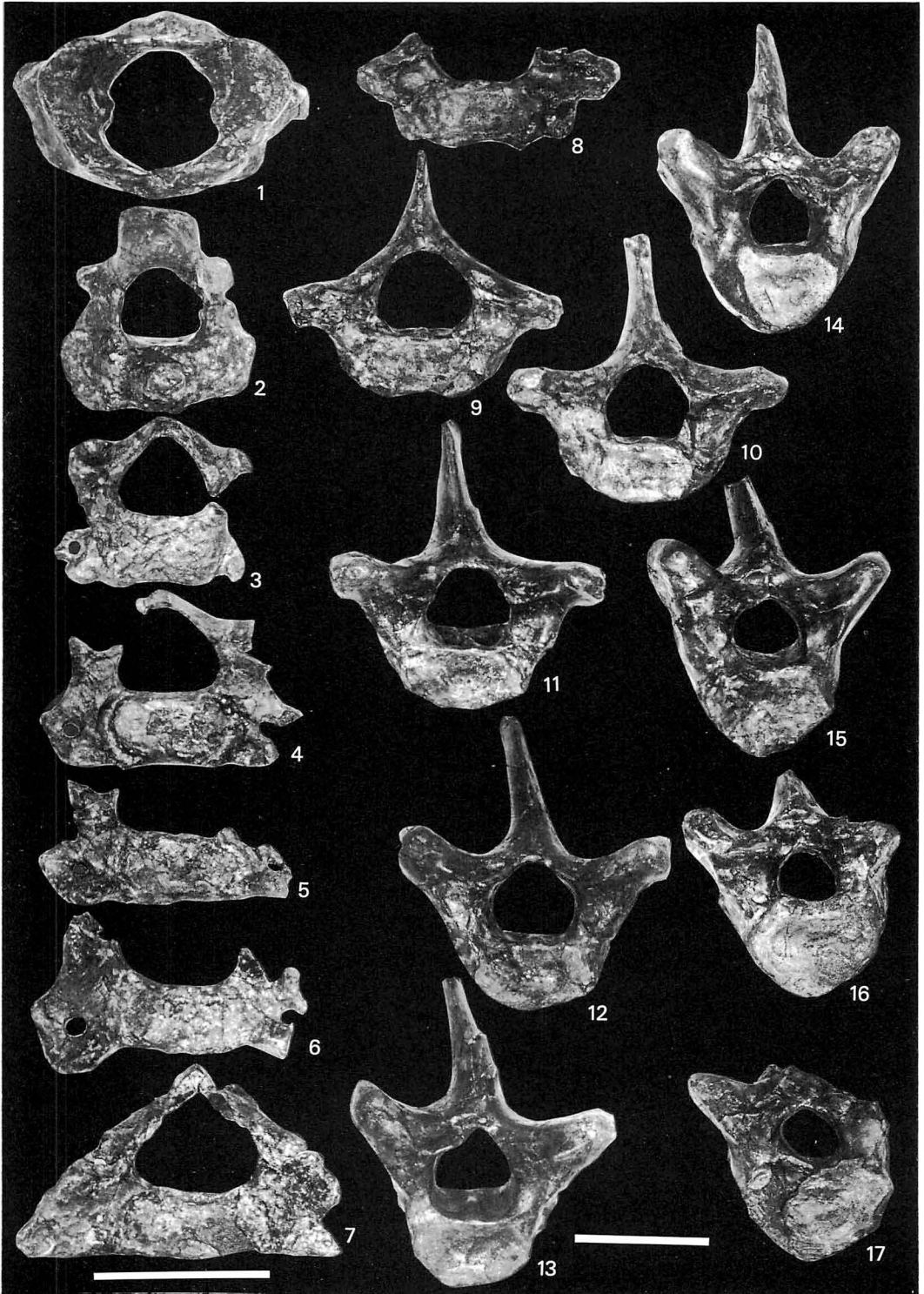
External height	108
Internal height	65
Total breadth	173
Width between processes for transverse ligament	55
Breadth across anterior cotyles	143
Breadth across posterior cotyles	119
Length in dorsal midline	40
Length in ventral midline	39

Table 9. Measurements of axis, in mm. e = estimated.

Total height	119
Length, tip of odontoid process to rear of centrum	68
Breadth across cotyles	114
Breadth of cotyle	40e
Posterior breadth of centrum	73e
Posterior height of centrum	43
Width of neural canal	45
Height of neural canal	42
Length of neural arch in midline	47

Table 10. Measurements of cervical vertebrae, in mm. e = estimated.

	C3	C4	C5	C6	C7
Total height	96	100e	120
Breadth across transverse processes	...	153e
Anterior breadth of centrum	72	71	86	76	84
Posterior breadth of centrum	88	92	92	83	101
Height of centrum in midline	41	42	43	39	41
Thickness of centrum in midline	12	17	18	17	21
Width of neural canal	52	57	51e	68e	73
Height of neural canal	45	46	59
Breadth across prezygapophyses	108e
Breadth across postzygapophyses	...	108e



Figs. 1—17. Vertebrae, anterior views: Figs. 1—7, cervicals; Figs. 8—17, thoracics. Scales = 10 cm.

Table 11. Measurements of thoracic vertebrae of holotype of *Dusisiren dewana*, in mm, e = estimated.

	T1	T2	T3	T4	T5	T6	T7	T8	T9
Total height	...	174e	200	216	216e	216	218
Breadth across transverse processes	...	206e	204	198e	198e	191	174	175e	...
Anterior breadth of centrum	82e	62	...	91	74	97	105
Height of centrum in midline	46	37e	46	47	53	58	72e	68	...
Thickness of centrum in midline	33	38	44	47	47	48	...	55	54
Width of neural canal	79	70	60	62	62	54	44	48	42
Height of neural canal	...	59	54	51	53	50e	47	44	45

those of other hydrodamalines, especially *Hydrodamalis cuetae*. Dorsal arch of atlas appears to lack articular surface for axis. On C3–6, bases of neural arches and bars forming dorsal sides of vertebral arterial canals broader than in *Dusisiren jordani* and more like *Hydrodamalis*. C7 lacks a vertebral arterial canal, as in *H. cuetae*. Dorsal sides of thoracic centra not indented. Arches all solidly fused to centra. None of the first ten thoracics appears to have a neural canal with a slitlike apex. Neural spines only slightly inclined; anterior edges thin, sharp; posterior sides thick. Transverse processes begin to incline dorsolaterad at T5, as in *D. jordani*.

Ribs (Table 12; Pls. 60–62): 12 left and 16 right ribs or fragments thereof from the anterior part of the thorax are preserved. R1 has mod-

erately developed process for m. longus capitis origin on ventral side of neck; distal end flattened anteroposteriorly (60 × 19 mm on right side). Other ribs have robust, ovoid cross-sections throughout most of their lengths. Neck of R2 nearly lacks a ventral process. Ribs 2–5 have slightly swollen distal ends. At least the first four ribs have truncated, rugose distal ends for cartilage attachment. After about R10–11, tubercula draw closer to capitula and become less prominent, and shafts become more mediolaterally compressed. Angles indistinct. Ribs in general intermediate in form between *Dusisiren jordani* and *Hydrodamalis cuetae*, but posterior ribs relatively much larger than in *D. jordani*, indicating a larger body in relation to the head.

Table 12. Measurements of right ribs, in mm, e = estimated.

	Capitulum to distal end in straight line	Tip of capitulum to lateral edge of tuberculum	Maximum midshaft diameter	Minimum midshaft diameter
R1	300	61	43e	30e
R2	388e	73	57	52
R3	469	93	57	43
R4	500	92	54	53
R5	580e	...	60	51
R6	583	103	57	48
R7	655e	111e	68	52
R8	...	82e	63	45
R9	...	96	70	41
R10	...	82	68	35
R11	...	76	69	41
R12	760e	...	70	37
R13	754e	51	63	35
R14	743	49	65	33
R15	756	47	68	29

Discussion

The skull and dentition of *Dusisiren dewana*, n. sp. show such close affinities with those of *D. jordani* that its generic assignment is unquestionable. Almost the only major difference in the cranial region is the reduced size and complexity of the molars, which nonetheless are still fully functional. In sharp contrast with the conservatism of the cranial morphology, however, are the profound and obviously *Hydrodamalis*-like modifications of the postcranial skeleton, particularly the manus.

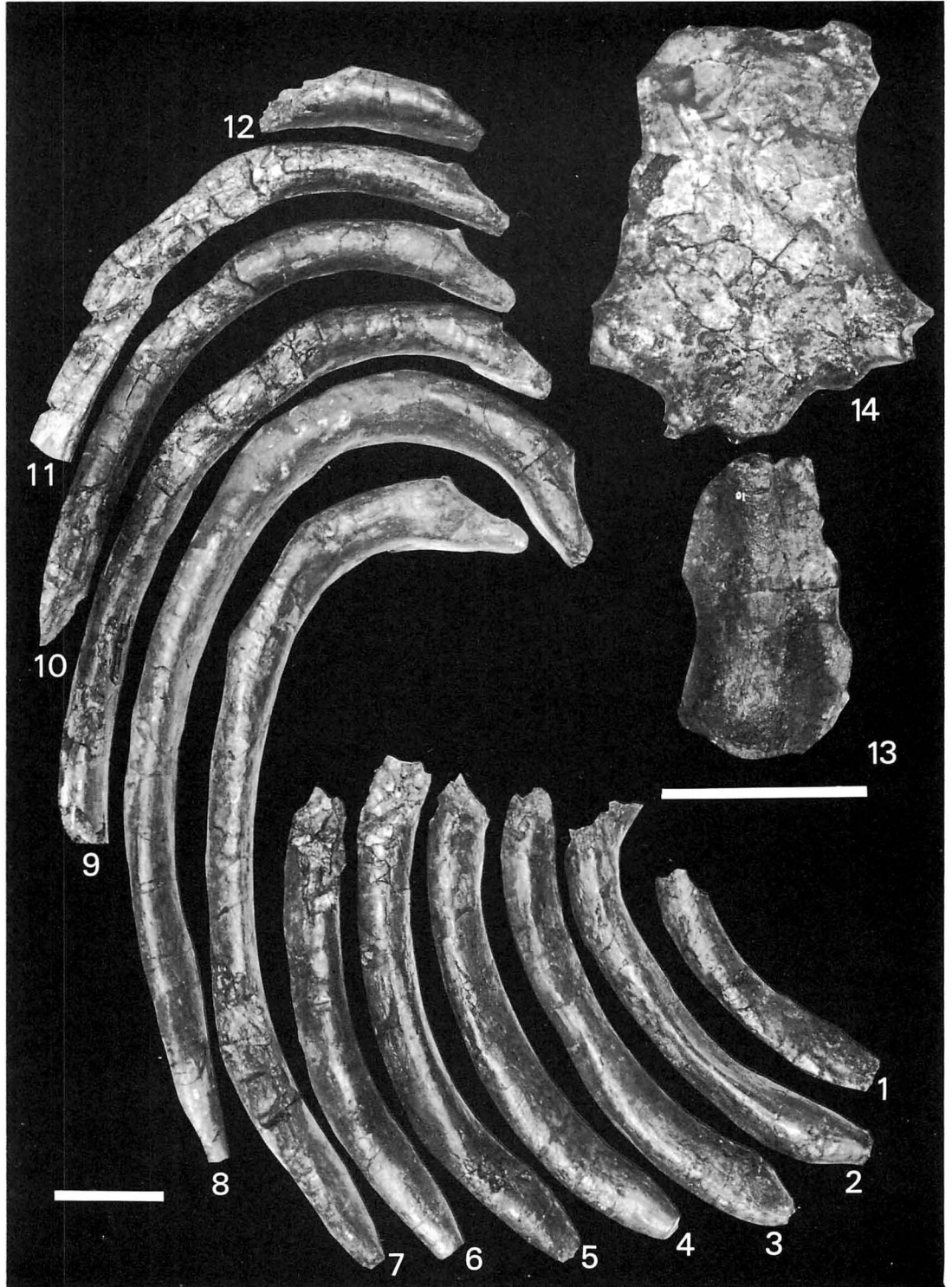
The anatomy of the manus of *Dusisiren dewana* (the first known complete manus of an advanced hydrodamaline) in general bears out the suppositions of Domning (1978: p. 128–129): the phalanges are vestigial (and may well have been lost entirely in *Hydrodamalis*); the after edge of the flipper is the more robust and the anterior digits are the most reduced; the metacarpals were held in a posteriorly inclined and somewhat flexed position; and the carpals are greatly altered in shape. However, there seems to be little if any “built-in pronation” or posterad orientation of the palm; the posterior part of the flipper clearly transmitted most of the force to the substrate.

Compared with *Dusisiren jordani*, the scaphoid-lunar-centrale is little changed, except that (as is clear also from the distal antebrachial joint surfaces) the articular facets and hence the axis of force transmission have shifted medially. The cuneiform is greatly compressed proximodistally, tilting the manus posteriorly around a transverse axis, and apparently bringing digit V into a more strongly “flexed” and “abducted” position. The pronounced lateral flange on the distal surface of the trapezium-trapezoid-magnum is a strong brace resisting extension of metacarpal II and forcing it likewise into a partly flexed position. In the same fashion, the spurlike process of the trapezium-trapezoid-magnum resists extension of metacarpal III. The styloid process of metacarpal III, apparently catching in front of the distal process of the scaphoid-lunar-centrale, seems to lock these bones, together with metacarpal II and

the trapezium-trapezoid-magnum, into a rigid unit when force is applied anteriorly or anterolaterally to the distal end of metacarpal III.

The carpal of *Hydrodamalis cuetae* previously illustrated (Domning, 1978: fig. 25) is now seen to be the unciform, probably the left; but its orientation and relations certainly could not have been guessed prior to the discovery of *Dusisiren dewana*. It appears that fig. 25A represents the medial surface, B the lateral, C the surface in contact with metacarpal IV, D the anterior aspect, E the proximal surface articulating with the cuneiform, and F the facets for the trapezium-trapezoid-magnum (left) and metacarpal III (right). Still the match with the Yamagata specimen is not a perfect one, suggesting that still further changes took place in the carpus before the stage of *Hydrodamalis cuetae* was reached. In particular, the anterior margin seems to have become lengthened proximodistally, and the surface for metacarpal IV reduced to the point of unrecognizability (or nonfunctionality) as an articular surface. Only the discovery of a complete carpus of *Hydrodamalis* will finally show whether this interpretation is correct.

On the whole, the manus of *Dusisiren dewana*, in comparison with those of typical sirenians or other mammals, can only be termed extraordinary. Although reminiscent at first of a severe deformity, or of such highly modified appendages as those of ground sloths or sauro-pods, it is on closer examination seen to be remarkably adapted for transmitting brute force posteriorly or posteromedially to the sea bottom. It dramatically corroborates Steller’s well-known description of *Hydrodamalis gigas*, which some later authors have had difficulty believing: “The ulna and radius terminate bluntly with tarsus and metatarsus [*sic*]. There are no traces of fingers, nor are there any of nails or hoofs . . .” (Steller, 1899, p. 188). It likewise corroborates the other eyewitness descriptions of these peculiar forelimbs and the manner of their use, as well as Domning’s biomechanical interpretations of the forelimb (see Domning, 1978, p. 96–97, 124–129). The structure of the sternum, scapula, humerus, and radius-ulna observed in



Figs. 1—14. Left ribs, manubrium and xiphisternum: Figs. 1—12, left ribs, posterior views; Fig. 13, manubrium; Fig. 14, xiphisternum, ventral views with anterior at the top. Scales = 10 cm.

Dusisiren dewana also bear out these interpretations in that they are modified in the direction of *Hydrodamalis*, and therefore appropriately designed for the exertion of force on the substrate as indicated by the structure of the manus. They confirm that the *Hydrodamalis* type of locomotor apparatus had fully evolved well before the loss of teeth in this lineage. Consequently the loss of teeth and associated modifications of the feeding apparatus must be seen as a (possibly belated) response to the conditions prevailing in a newly entered adaptive zone, the nature of which is suggested by the locomotor adaptations and discussed in detail by Domning (1978).

Occurrences of fossil sirenians in Japan

For a number of years, one rib bone of *Hydrodamalis* sp., described by Shikama and Domning (1970) from the Late Pliocene Sarumaru Formation of Nagano Prefecture, central Japan, gave the only evidence of extinct sea cows having inhabited coastal waters of the Japanese Islands. During the last few years, however, several reports have announced additional discoveries of sirenian fossils in northern Japan (Text-fig. 1).

Our specimen of a Late Miocene sea cow was discovered in 1978 and its identification as a species of *Dusisiren* was confirmed by one of us (Domning) in April of 1979. This discovery was reported at the 86th annual meeting of the Geological Society of Japan (Takahashi, Domning, and Saito, 1979) and in later publications (Takahashi, 1981; Takahashi *et al.*, 1983).

Inuzuka *et al.* (1980) reported an upper molar of "*Dugong*" from the Middle Miocene Bamba-gawa Formation of southern Hokkaido. Since this formation is correlative with the Kunnui Formation of southern Hokkaido which yields planktonic foraminifera indicative of Zones N.8 and N.9, it would be the oldest sirenian-bearing bed in Japan. However, examination of the specimen by one of us (Domning) indicates that the specimen is probably not a sirenian and may instead represent a worm premolar of a des-

mostylian like *Paleoparadoxia*; the latter genus is known to occur at the same locality (Inuzuka, personal communication).

In August 1980, a large skeleton of a sea cow was discovered in the Takikawa Formation, which is exposed in the bed of the Sorachi River, Takikawa City, central Hokkaido. The specimen was later described by Furusawa and Kimura (1982) as possibly representing a new species of *Hydrodamalis*. This specimen was found in direct association with a large pectinid mollusk, *Fortipecten takahashii*. The *Fortipecten*-bearing bed has been correlated with the lower Middle Gilbert Chron (Early Pliocene, ca. 3.7–5.1 Ma) of the geomagnetic reversal sequence (Ujii *et al.*, 1977; Manabe, 1980). A very comprehensive osteological description of the Takikawa specimen and descriptions of associated fossil flora and fauna appeared in a volume published by the Takikawa City Board of Education (1984). From the illustrations and measurements given there, the specimen appears to be an adult *Hydrodamalis cuestae*, with a skull very similar to but smaller than one recently found in the San Diego Formation of California (Domning and Deméré 1984). However, Furusawa (personal communication) feels that it is more derived than *H. cuestae*, so its specific assignment is still in doubt.

In November of 1980, another fossil sirenian was discovered in the Shiotsubo Formation at Takasato Village, Yama County, Fukushima Prefecture. The find consists of a left scapula and an incomplete skull. A short description of the specimen was given by the Aizu Fossil Research Group (1982) and the specimen was assigned to *Dusisiren* sp. cf. *D. jordani*. This locality is situated 83 km south-southwest of the Yamagata sea cow locality, and molluscan fossils associated with the Shiotsubo sea cow appear to indicate that the Yamagata and Shiotsubo sea cows are coeval. The assemblage of fossil mollusks present in the Shiotsubo Formation has long been recognized by Japanese paleontologists as the Yama Fauna (Nomura, 1935). This fauna is considered to characterize offshore environments of the Late Miocene sea, whereas the

contemporary Shiobara Fauna, such as occurs with the Yamagata sea cow, inhabited near-shore environments (Chinzei, 1978). The skull of the Shiotsubo sea cow has not been illustrated or described. The scapula does resemble that of *D. jordani* more closely than *D. dewana* in having a broad suprascapular fossa, but this feature may have been variable in the latter species. In view of the probably equivalent ages of the Shiotsubo and Yamagata fossils, the possibility must be seriously considered that the Shiotsubo sea cow also represents *D. dewana*.

The latest discovery of a fossil sea cow in northern Japan comes from Early or Middle Pleistocene gravel beds exposed in a quarry along the Otoebetsu River, Hiroshima Town, Ishikari District, southwestern Hokkaido. The find consists of broken fragments of skull, left scapula, right humerus, left radius-ulna, and numerous ribs (Kimura *et al.*, 1983). Shinohara (1983) identified these bones as belonging to *Hydrodamalis gigas*.

These publications now provide concrete evidence that sea cows were important elements of coastal marine faunas of the Japanese Islands at least from the Late Miocene onward. At least three species now appear to have occurred in Japan, representing the last three evolutionary stages of the hydrodamaline lineage recorded in western North America: *Dusisiren dewana*, *Hydrodamalis cuestae* (?), and *H. gigas*. Taken at its face value, the Japanese record now indicates that hydrodamaline sirenians first dispersed northward and westward from California in the Late Miocene, after they had evolved the degree of cold-adaptation represented by *Dusisiren dewana* (=“*Dusisiren* Species D”). This is consistent with the suggestion of Domning (1978, p. 110) that this species could tolerate somewhat colder water than *D. jordani*, which so far has not been definitely recorded from the western Pacific.

The Yamagata sea cow's age of 9.0–10.4 Ma is in excellent agreement with the 8–9 Ma date anticipated by Domning (1977) for *Dusisiren* Species D. It is definitely earlier than any well-dated occurrence of *Hydrodamalis*, corroborat-

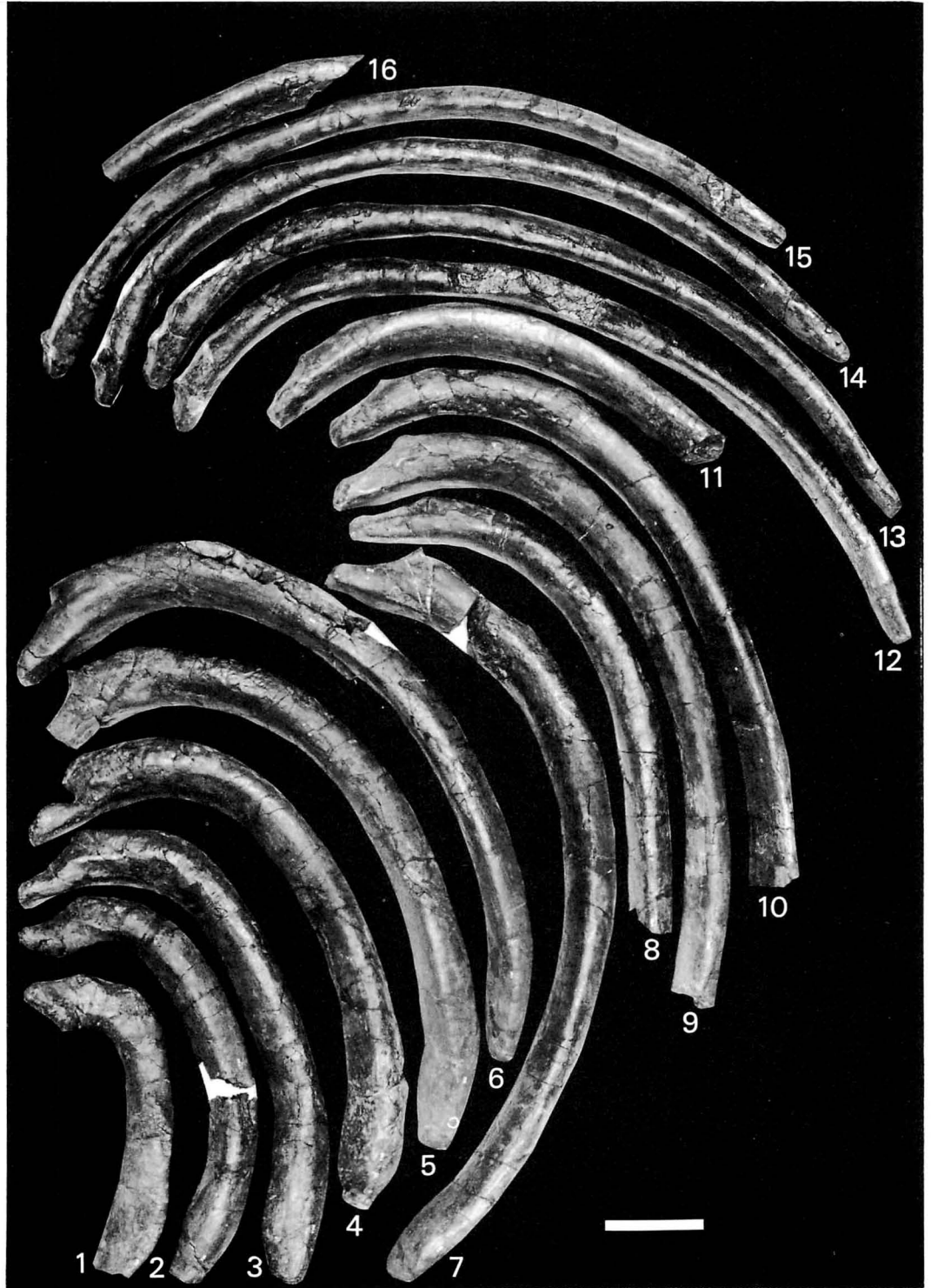
ing Domning's hypothesis of an unbranching phyletic sequence of hydrodamaline chronospecies. The earliest records of *Hydrodamalis* are from the 3.7 to 5.1 million-year-old Takikawa site mentioned above and the lower San Mateo Formation at oceanside, California, correlated with the 4.5 to 8 million-year-old Hemphillian Land Mammal Age (Domning and Deméré, 1984). Thus the known stratigraphic ranges of *Dusisiren* and *Hydrodamalis* are mutually exclusive.

Whether the stratigraphic ranges of *Dusisiren jordani* (estimated at about 10–12 Ma) and *D. dewana* are likewise mutually exclusive cannot be conclusively determined at this time because of the lack of precise radiometric or biostratigraphic control on the localities of *D. jordani* in California. However, no available evidence necessitates a temporal overlap between these species, and for the present the hypothesis of a single hydrodamaline lineage stands unfalsified.

Acknowledgments

Our deepest gratitude is expressed to Masanori Watanabe and Masahiro Saito who, in the summer of 1978 when they were elementary school students, discovered the sea cow specimen in the bed of the Mogami River. Their alertness led to the collection and eventual deposition of the fossil sea cow in the Yamagata Prefectural Museum. A series of posterior vertebrae, which was detached and found lying on the river bed, was collected sometime prior to the discovery of the major portion of the skeleton by Sakae Saito, who kindly donated it to the Museum.

Many people assisted in the excavation of the skeleton from the river bed. It is not possible to acknowledge separately each contribution, but the following organizations and individuals were particularly helpful: the Board of Education of Yamagata Prefecture; the Board of Education of the Township of Ohe; Hogen Takayama of the Cultural Properties Protection Committee (Township of Ohe); Yuei Watanabe, Hiroshi Saito, Matsuji Saito, Takeshi Ohya, Reiichiro Watanabe,



Figs. 1—16. Right ribs, posterior views. Scale = 10 cm.

all of the hamlet of Yoh of Ohe Town; Mamoru Okuyama, Aterazawa Primary School; Shintaro Yoshimi, Murayama Agricultural High School; Masahiro Matsuda, Sagae High School; and Saburo Shirata and Naoji Ohizumi. During the course of preparation of the specimen, assistance was given by: Masaaki Funayama, Tohru Omiya, Yoshiki Kohda (Iwaki City Board of Education), Seiichi Itagaki, Katsunori Kamagami and Shoji Ikeno.

During the course of research on the specimen, the following individuals provided valuable assistance and helpful advice: Richard H. Tedford (American Museum of Natural History, New York), Yoshikazu Hasegawa (Yokohama National University), Teruya Uyeno and Yukimitsu Tomida (National Science Museum, Tokyo), Hiroshi Ozaki (Saito Ho-on Kai Museum, Sendai), Toshiro Kamiya (University of Tsukuba), Norihisa Inuzuka (University of Tokyo), Hitoshi Furusawa (Takikawa City Museum, Takikawa, Hokkaido), Masahiro Suzuki (Yamagata Technical High School), Hohei Uematsu (Yamazoe High School), and Ryoichi Tamiya (Nature Protection Department, Yamagata Prefectural Government).

Grateful thanks are due also to Kyo-on Honda, Raiji Endo and Mikio Suzuki (all Ex-Directors), Gisuke Ohtomo (Current Director), Tomoo Yoshino, Takeo Okuyama, and Kozo Kaneyama, all of the Yamagata Prefectural Museum, for various forms of assistance and constant encouragement.

This research was greatly aided by Fumio Akiba (Japan Petroleum Exploration Company) who established the age of the sea cow through his analysis of associated diatom floras; by Kenshiro Ogasawara (Institute of Geology and Paleontology, Tohoku University) who identified fossil mollusks; and by Hisatake Okada who identified calcareous nannoplankton. Yaeko Ohta, Yoshiko Kurogane and Jennifer Emry drew the figures and Tomonori Ogata aided in photography.

Domning particularly thanks his Yamagata colleagues for their many kindnesses, above all the opportunity to visit Japan and study this

uniquely interesting and important specimen. He was additionally supported by National Science Foundation grant DEB-8020265.

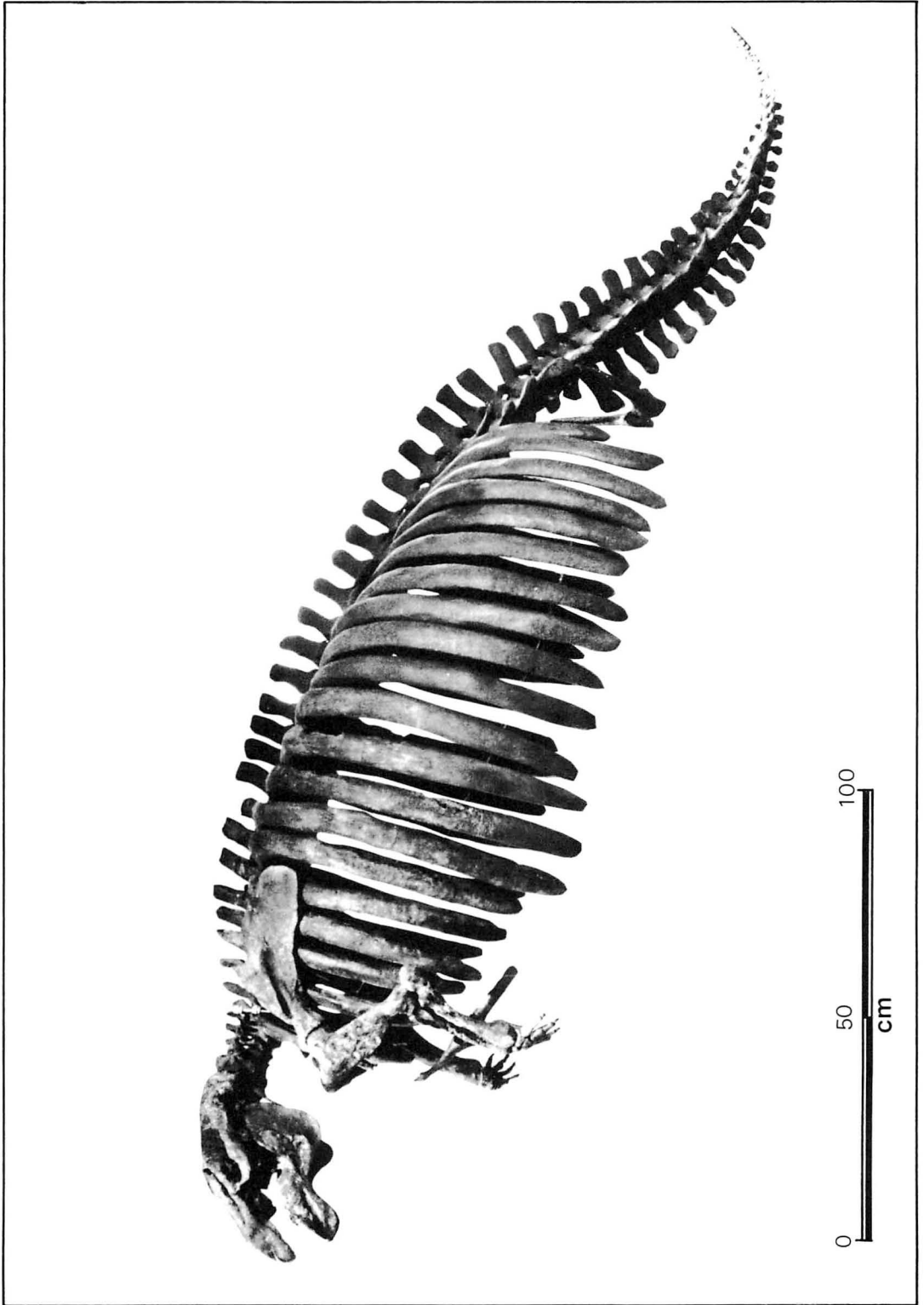
References

- Aizu Fossil Research Group (1982): On a fossil *Sirenia* [*sic*] from the Shiotsubo Formation, Takasato, Yama, Fukushima Prefecture, Northeast Japan. *Earth Sci. (Chikyu Kagaku)*, vol. 36, no. 5, p. 282–284 (in Japanese).
- Akiba, F. (1983a): Fossil diatoms. In: *Research report on the excavation of the Yamagata sea cow*. p. 65–70. Yamagata Pref. Museum, Spec. Publ., Yamagata, Japan (in Japanese).
- , (1983b): Revision of Neogene diatom zonation in the middle-high-latitude North Pacific. *Marine Science (Kaiyokagaku)*, vol. 15, no. 2, p. 717–724.
- , Yanagisawa, Y. and Ishii, T. (1982): Neogene diatom biostratigraphy of the Matsu-shima area and its environs, Miyagi Prefecture, Northeast Japan. *Bull. Geol. Surv. Japan*, vol. 33, no. 5, p. 215–239 (in Japanese with English abstract).
- Barron, J. A. (1981): Late Cenozoic diatom biostratigraphy and paleoceanography of the middle-latitude eastern North Pacific, Deep Sea Drilling Project Leg 63. In: Yeats, R., Haq, B. U., et al., *Scientific Party, Initial Reports of the Deep Sea Drilling Project*, vol. 63, Washington, Govt. Printing Off., p. 507–538.
- and Keller, G. (1983): Paleotemperature oscillations in the Middle and Late Miocene of the northeastern Pacific. *Micropaleontology*, vol. 29, no. 2, p. 150–181.
- Chinzei, K. (1978): Neogene molluscan faunas in the Japanese Islands: An ecologic and zoogeographic synthesis. *Veliger*, vol. 21, no. 2, p. 155–170.
- Domning, D. P. (1977): An ecological model for Late Tertiary sirenian evolution in the North Pacific Ocean. *Syst. Zool.*, vol. 25, no. 4, p. 352–362.
- (1978): Sirenian evolution in the North Pacific Ocean. *Univ. Calif. Publ. Geol. Sci.*, vol. 118, p. 1–176.
- and Deméré, T. A. (1984): New material of

- Hydrodamalis cuestae* (Mammalia: Dugongidae) from the Miocene and Pliocene of San Diego County, California. *Trans. San Diego Nat. Hist. Mus.*, vol. 20, no. 12, p. 169–188.
- Funayama, Y. (1961): The geology and geological structure in the marginal areas of the Yamagata Basin, with special reference to the ore deposits, Yamagata Prefecture, Japan. *Tohoku Univ., Sci. Rep., 3rd Ser. (Mineral. Petrol. & Econ. Geol.)*, vol. 7, no. 2, p. 199–291.
- Furusawa, H. and Kimura, M. (1982): Discovery of new species of Sirenia from the lower Pliocene in Sorachi River, Takikawa City, Hokkaido. *Jour. Geol. Soc. Japan*, vol. 88, no. 10, p. 849–852 (in Japanese).
- Haq, B. U. (1984): Jurassic to Recent nannofossil biochronology: An update. In: Haq, B. U., ed., *Nannofossil biostratigraphy*. p. 358–386. Hutchinson Ross Publ. Co., Stroudsburg, Pa.
- Harms, J. C., Southard, J. B., Spearing, D. R. and Walker, R. G. (1975): Depositional environments as interpreted from primary sedimentary structures and stratification sequences. *Soc. Econ. Pal. Mineral., Short Course*, no. 2, p. 1–161.
- Ichimura, T. (1958): Cross-bedding of the Neogene sediments exposed at the western margin of the Yamagata Basin. *Bull. Yamagata Univ. (Nat. Sci.)*, vol. 4, no. 3, p. 377–385 (in Japanese).
- Inuzuka, N. and Iwamizawa Research Group (1980): First discovery of *Dugong* (Dugonginae) from the Middle Miocene in Kogawa, Kitahiyama-cho, Hokkaido. *Jour. Geol. Soc. Japan*, vol. 86, no. 9, p. 639–641 (in Japanese with English abstract).
- Itoh, O., Suzuki, M., Shibahashi, K., Takahashi, S., Tamiya, R., Yamagata, O. and Yoshida, S., eds. (1979): *Arato. Explanatory text of the geological map of Yamagata Prefecture, scale 1:50,000*. Yamagata Pref. Govt., 25 p., 1 map (in Japanese).
- Kellogg, R. (1925): A new fossil sirenian from Santa Barbara County, California. *Carnegie Inst. Washington Publ.*, no. 348, p. 57–70, pls. 9–11.
- Kimura, M., Tonosaki, T., Akamatsu, M., Kitagawa, Y., Yoshida, M. and Kamei, T. (1983): Occurrences of early-middle Pleistocene mammalian fossils from the Nopporo Hills in the Ishikari Lowland, Hokkaido. *Earth Sci. (Chikyu Kagaku)*, vol. 37, no. 3, p. 162–177 (in Japanese with English abstract).
- Manabe, K. (1980): Magnetostratigraphy of the Yamato Group and the Sendai Group, Northeast Honshu, Japan (II). *Sci. Rep., Fac. Educ. Fukushima Univ.*, no. 30, p. 49–71.
- Maruyama, T. (1984): Miocene diatom biostratigraphy of onshore sequences on the Pacific side of Northeast Japan, with reference to DSDP Hole 438A (Part 1). *Tohoku Univ., Sci. Rep., 2nd Ser. (Geol.)*, vol. 54, no. 2, p. 141–164.
- Nomura, S. (1935): On some Tertiary mollusca from Northeast Honshu, Japan: Pt. 2, Fossil mollusca from the vicinity of Ogino, Yamagata, Fukushima-ken. *Saito Ho-on Kai Mus., Res. Bull.*, no. 5, p. 101–125.
- Ogasawara, K. (1983): Molluscan fossils. In: *Research report on the excavation of the Yamagata sea cow*. p. 61–64. Yamagata Pref. Museum, Spec. Publ., Yamagata, Japan (in Japanese).
- Reading, H. G., ed. (1978): *Sedimentary environments and facies*. 569 p. Blackwell Sci. Publ., Oxford.
- Shikama, T. and Domning, D. P. (1970): Pliocene Sirenia in Japan. *Trans. Proc. Palaeont. Soc. Japan, N.S.*, no. 80, p. 390–396.
- Shinohara, A. (1983): On the fossil sea cow recovered from the Nohoro Hills, Hokkaido. *Geol. Soc. Japan, Abstracts with Programs, 90th Ann. Meet.*, p. 292 (in Japanese).
- Steller, G. W. (1899): The beasts of the sea.

Explanation of Plate 62

Restoration of the skeleton of *Dusisiren dewana*, n. sp. based on the holotype. Posterior half of the skeleton, caudal vertebrae and ribs forming posterior part of thorax, restored with reference to the skeleton of *Dusisiren jordani* (University of California Museum of Paleontology, Berkeley, Specimen no. 77037). Restored specimen, as displayed at the Yamagata Prefectural Museum, measures 3.8 m in overall body length and 3.5 m in thorax circumference.



- In: Jordan, D. S., *The fur seals and fur-seal islands of the North Pacific Ocean*. Part 3, Art. 8, p. 179—218. Washington, Govt. Printing Off.
- Suzuki, U. (1979): Petroleum geology of the Sea of Japan, northern Honshu. *Jour. Japan. Assoc. Petrol. Tech.*, vol. 44, no. 5, p. 291—307 (in Japanese with English abstract).
- Takahashi, S. (1981): Excavation of fossil sea cow. *Yamagata Applied Geol. Assoc. Publ.*, no. 1, p. 1—5 (in Japanese).
- , Domning, D. P. and Saito, T. (1979): On the discovery of a fossil sea cow from Ohe Town, Yamagata Prefecture. *Geol. Soc. Japan, Abstracts with Programs, 86th Ann. Meet.*, p. 228 (in Japanese).
- et al. (1983): *Research report on the excavation of the Yamagata sea cow*. 76 p. Yamagata Pref. Museum, Spec. Publ., Yamagata, Japan (in Japanese).
- Takikawa City Board of Education (1984): *Research Report of the Takikawa Sea Cow*. 206 p. Takikawa City Museum, Hokkaido, Japan (in Japanese with English summary).
- Uyeno, T. (1983): Sharks' teeth. In: *Research report on the excavation of the Yamagata sea cow*. p. 61—64. Yamagata Pref. Museum, Spec. Publ., Yamagata, Japan (in Japanese).
- Ujiiie, H., Saito, T., Kent, D. V., Thompson, P. R., Okada, H., Klein, G. de V., Koizumi, I., Harper, H., E., Jr. and Sato, T. (1977): Biostratigraphy, paleomagnetism and sedimentology of Late Cenozoic sediments in northwestern Hokkaido, Japan. *Bull. Nat. Sci. Mus. (Tokyo), Ser. C (Geol. Pal.)*, vol. 3, no. 2, p. 49—102.
- Zimmermann, E. A. W. (1780): *Geographische Geschichte des Menschen und der vierfüßigen Thiere. Zweiter Band*. 432 p. Weygandschen Buchhandlung, Leipzig.

Aterazawa 左沢, Hashigami 橋上, Hongo 本郷, Jyuhassai 十八才, Kuzusawa 葛沢, Mizusawa 水沢, Mogamigawa 最上川, Ohe 大江, Ohya 大谷, Tsukinuno 月布, Yoh 用.

ステラー大海牛の直系の先祖に位置づけられる山形県上部中新統産哺乳綱海牛目の新種 *Dusisiren dewana*: 1978年8月, 山形県西村山郡大江町を流れる最上川で, 異常湧水のため露出した河床に大型哺乳類の骨格が含まれているのを2名の小学生が発見した。河床の岩層は, 本郷層の橋上砂岩部層で, 初期後期中新世の *Denticulopsis katayamae* Zone (9-10.4 Ma) を指示する珪藻化石を産する。一節の長さ6~8センチ, 直径14~15センチの椎骨が140センチの長さに連なり, 長さ20~90センチの大きく湾曲した肋骨が26本程度数えられた。骨格前部には長さ51センチの頭骨が, 口蓋の上に頭頂を下にした状態で保存され, 長さ41センチの一対の肩甲骨も認められた。

骨格を砂岩からとり出すにつれて, この標本は体前半部の骨格がほぼ完全に揃った, 極めて良く保存された大海牛の化石であることが明らかになった。指・掌骨を含む右前肢は, 絶滅した大海牛類の前肢の構造を示す, 現存する世界唯一の標本である。骨格の特徴により山形の化石は, カリフォルニアから記載された *Dusisiren jordani* に近似するが, 歯の大きさが *jordani* のものの3/4と小さく, しかも咬合面の模様が単純で, 歯が著るしい退化を示す点で大きく異なる。歯の退化は, 大海牛の進化系列のもっとも際立った形質変化で, 大型の歯を備えた先祖型の *Dusisiren* 属から, 歯が退化して失われた *Hydrodamalis* 属への進化系列が北太平洋地域で確立されている。歯の特徴および肩甲骨, 胸骨, 手根骨の性質から, 本骨格は *D. jordani* と *Hydrodamalis cuestae* を結ぶ, これまで未記載の中間型の種であることが判明し, ここに *Dusisiren dewana* (和名: ヤマガタダイカイギュウ) という新種を提唱した。 *H. cuestae* は, ベーリング海で1768年に絶滅したステラー大海牛 (*H. gigas*) の先祖なので, 本新種の設定により, 中期中新世の *D. jordani* にさかのぼる四代の大海牛の進化系列が明らかになった。

高橋静夫・D.P. ドムニング・斎藤常正

810. *FOLLICUCULLUS* (RADIOLARIA) FROM THE UPPER PERMIAN
KUMA FORMATION, KYUSHU, SOUTHWEST JAPAN*

HIROAKI ISHIGA

Department of Geosciences, Faculty of Science, Osaka City University,
Sumiyoshi-ku, Osaka 558

and

TAKAMI MIYAMOTO

Institute of Geology and Mineralogy, Faculty of Science, Hiroshima University,
Naka-ku, Hiroshima 730

Abstract: The Permian radiolarian assemblage characterized by *Follicucullus bipartitus* Caridroit and De Wever and *F. charveti* Caridroit and De Wever occurs from the *Lepidolina kumaensis* Zone of the Kuma Formation, Kyushu, Southwest Japan. This assemblage is different from that of the bedded chert in the Mino-Tamba Belt, concerning the dominant components. However, it is considered to be coeval with the radiolarian assemblage from the upper part of the *Follicucullus scholasticus* Assemblage-zone and/or the *Neobaillella optima* A-zone of the chert facies.

Introduction

Since Ormiston and Babcock (1979) described *Follicucullus* (radiolaria) from the Guadalupian Lamar Limestone in West Texas, the occurrence of *Follicucullus* has been reported from various localities in Japan. *Follicucullus* is now one of the important index fossils of Permian time. Among 10 radiolarian assemblage-zones which have been distinguished in the Japanese Permian (Ishiga *et al.*, 1982b; 1984), the seventh and eighth zones from the base are characterized by *Follicucullus monacanthus* and *F. scholasticus*, respectively. Furthermore, *F. scholasticus* occurs from the ninth and tenth radiolarian assemblage-zones together with some species of *Neobail-*

lella. However, the exact age of these zones has not been determined, because they have been identified mainly in the bedded chert sequences in which biochronologically useful fossils, such as fusulinids and conodonts, are usually absent. It is important to correlate the radiolarian zones with other biozones based on fusulinids and other index fossils.

Recently, Ishiga (1984) reported the occurrence of *Follicucullus* from mudstone of the Permian Maizuru Group and a tentative correlation was made between radiolarian zones and fusulinid zones in the Maizuru Group. Caridroit and De Wever (1984) reported some new species of *Follicucullus* from mudstone in Hyogo Prefecture, Southwest Japan which was supposed to be Late Permian in age. Miyamoto *et al.* (1984) discovered some species of *Follicucullus* from

*Received January 10, 1985; revised manuscript received October 11, 1985.

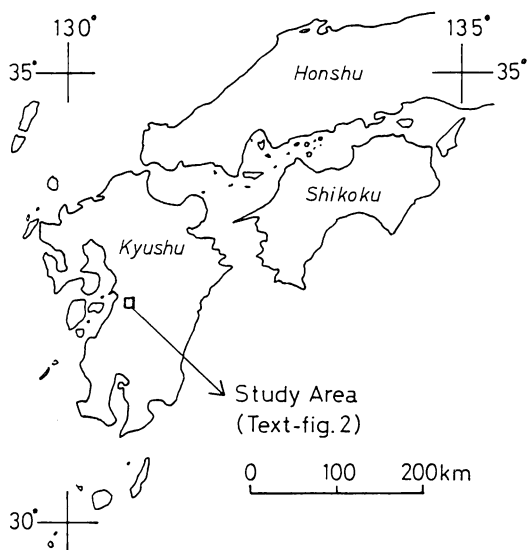
mudstone of the Upper Permian Kuma Formation, Kyushu, which closely resemble the species of *Follicucullus* reported by Caridroit and De Wever (1984). This paper presents the results of the biostratigraphical and paleontological studies of radiolarians from the Kuma Formation and the correlation between radiolarian zones and fusulinid zones in the Upper Permian of Japan. Ishiga is responsible for the chapter on systematic paleontology.

Acknowledgments:—The authors would like to express their appreciation to Professor K. Ichikawa of Osaka City University for his kind comments and critical reading of the manuscript. Special thanks are due to Dr. A. Yao of the same university, for his reading and kind comments on the early version of the manuscript. The authors appreciate the collaboration in the field and laboratory works to Mr. J. Kuwazuru of the Sumiko Consultant Co. Ltd., Mr. T. Nomoto of the INA Shin-Doboku Co. Ltd., Mr. H. Yamada of the Central Systems Co. Ltd. and Dr. R. Tominaga of the Hiroshima University. For instructive advices and suggestions in the various aspects, the authors are much indebted to Professor A. Hase, Assoc. Professor Y. Okimura and Assoc. Professor I. Hara of the Hiroshima University.

Geologic setting

The study area is located at the upper drainages of the Hikawa River, in the vicinity of Kayaba, Izumi-mura, Yatsushiro-gun, Kumamoto Prefecture, Japan (Text-fig. 1). Geotectonically it belongs to the Chichibu Belt of the Outer Zone, Southwest Japan. In the study area, the Kakisako, Kuma and Hashirimizu Formations are distributed from north to south and these three formations are in fault contact with each other (Kanmera, 1952, *etc.*). Along the fault between the Kuma and Hashirimizu Formations, plutonic and metamorphic rocks in addition to Silurian and Carboniferous rocks are distributed.

The "Kakisako Formation" has been recently divided into two formations, namely the Miyama and Kakisako Formations from north to south

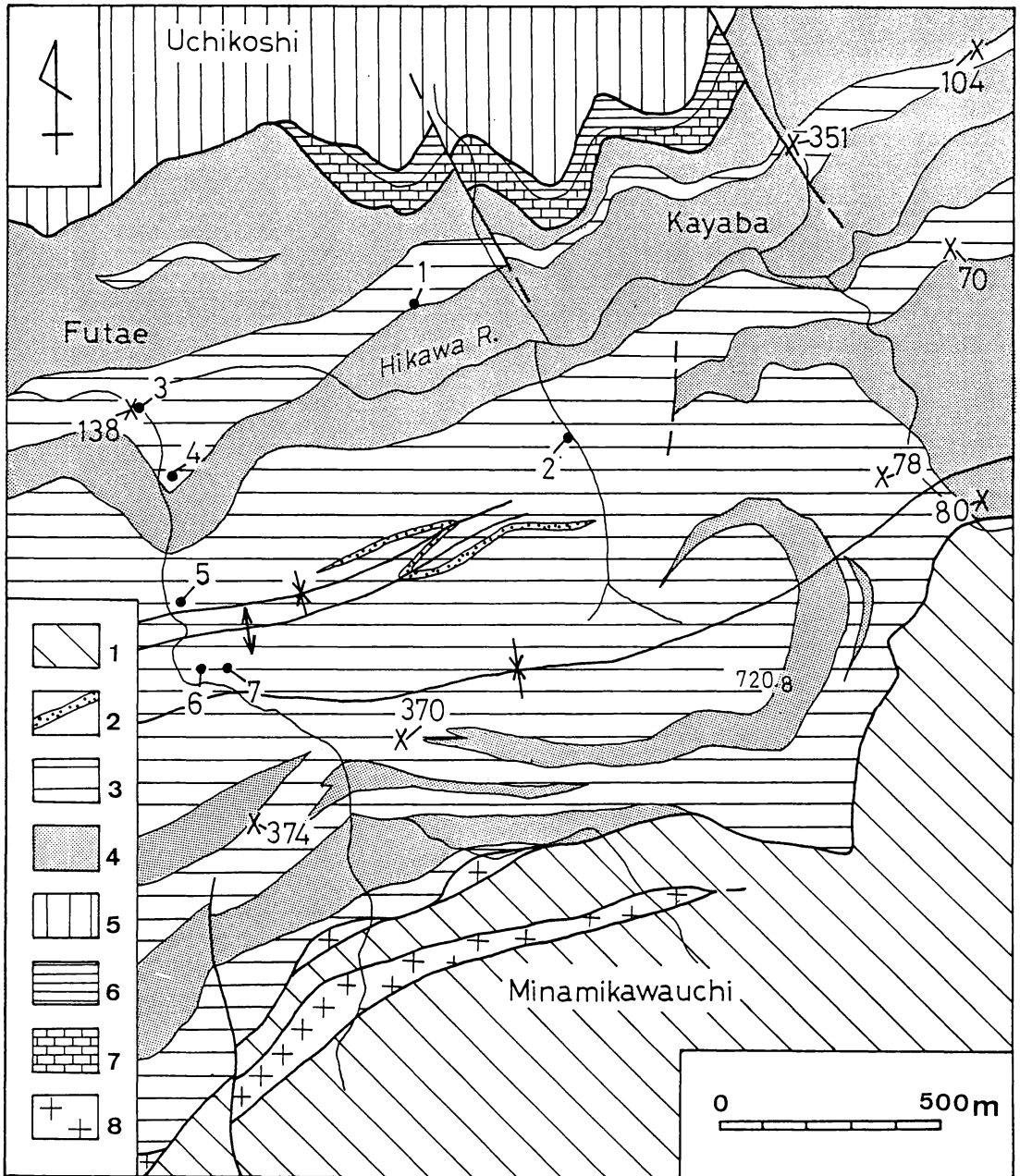


Text-fig. 1. Index map of the study area.

(Miyamoto *et al.*, 1984, 1985). According to them, the Miyama Formation is mainly composed of Late Permian pebbly mudstone including exotic blocks of Permian chert, greenstone and others of various size and shape, while the Kakisako Formation consists of late Early Carboniferous (Viséan) limestone and silty shale.

The Hashirimizu Formation which is distributed along the south of the Kuma Formation mainly consists of black phyllite, slate and sandstone with small lenticular bodies of chert and sandstone. Rarely, greenstones and limestones are included. The age of this formation was regarded as Middle Permian on the basis of occurrence of fusulinids from limestones (Matsumoto and Kanmera, 1964). However, Early Jurassic radiolarians have been recently reported from this formation (Miyamoto *et al.*, 1984).

The Kuma Formation (Kanmera, 1953), about 900 m thick, mainly consists of sandstone, black mudstone and conglomerate and subordinately contains small lenses of limestone. Generally, mudstone is predominant in the lower and upper parts, and sandstone and conglomerate are common in the middle part. Kanmera (1953, 1954) distinguished four horizons of the limestone lenses in the Kuma Formation. The limestone of the lowermost horizon contains *Lepi-*



Text-fig. 2. Geologic map of the study area after Miyamoto *et al.* (1985).

1: Hashirimizu Formation, 2–4: Kuma Formation (2: conglomerate, 3: mudstone, 4: sandstone), 5: Miyama Formation (newly defined by Miyamoto *et al.*, 1984, 1985), 6, 7: Kakisako Formation (6: shale with conglomerate, 7: limestone), 8: mylonitic granite. ●: radiolarian fossil localities. x: fusulinid fossil localities after Kanmera (1953).

dolina multiseptata shiraiwensis, but it does not yield *L. kumaensis* (Kanmera and Nakazawa, 1983). The second and third horizons are characterized by the occurrence of *Leipidolina kumaensis* and have the same specific composition with each other (Kanmera, 1954). From the limestone of the fourth horizon, *Leipidolina* sp., *Pseudodoliolina* sp. and *Schwagerina* sp. have been reported (Kanmera, 1953, 1954). *Codonofusiella* and several smaller foraminifers have been found in limestone about 290 m above the *Leipidolina* limestone in the area 6 km west of the present study area, and this horizon is the uppermost horizon of the limestone lenses in the Kuma Formation (Kanmera and Nakazawa, 1973).

In the study area, sandstone is predominant in the lower part, while mudstone occurs frequently in the upper part of the Kuma Formation. Concerning the fundamental geologic structure of the Kuma Formation, it forms a syncline that trends ENE-WSW with its axis running near the central part of the study area. The strata of the northern wing are folded (Text-fig. 2). The localities of fusulinids reported by Kanmera (1953, 1954) are shown in Text-fig. 2. The generalized columnar section of the Kuma Formation in the

northern wing and the horizons of the occurrences of both fusulinids (in Kanmera, 1953, 1954) and radiolarians are shown in Text-fig. 3. Ku 138, 351 and 104 represent the second horizon, while Ku 70, 80 and 370 belong to the third horizon. Ku 78 represents the fourth horizon. The limestone of the first or the lowermost horizon is distributed outside of the present study area.

Material

Radiolarian fossil localities (1–7) are shown in Text-fig. 2 and their stratigraphic levels are shown in Text-fig. 3.

Loc. 1: Bedded black mudstone was collected by J. Kuwazuru from the small outcrop about 750 m east of Futae. The outcrop (380 m above sea level) is in the small valley which is situated north of the road from Futae to Kayaba.

Loc. 2: Massive black mudstone was collected from the outcrop (380 m above sea level), in the small valley which is situated southwest of Kayaba.

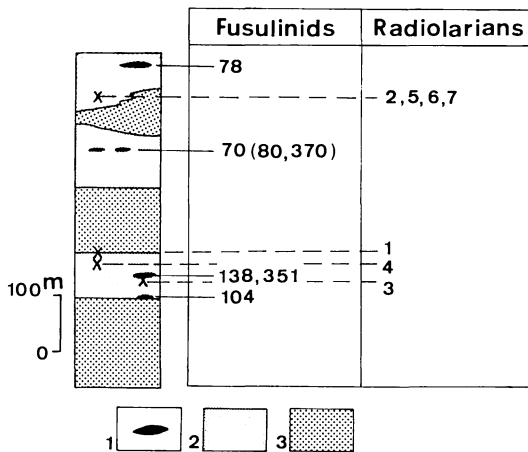
Loc. 3: Silty laminated mudstone was collected about 2 m below the limestone, which is identical with Ku 138 in Kanmera (1953, 1954), at the confluence of two rivers, east of Futae. Black silty laminated mudstone gradually changes upward into calcareous sandstone which in turn changes into limestone and conglomeratic limestone (see Text-fig. 4).

Loc 4: Black laminated silty mudstone from the road-side cutting about 340 m south of Futae.

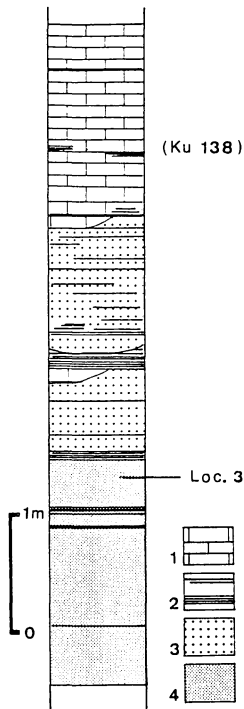
Loc. 5: Black silty mudstone from the road-side cutting about 630 m south of Futae.

Locs. 6, 7: Black silty mudstone from the road-side cutting about 800 m south of Futae.

Samples from the Locs. 2–7 were collected by one of the present authors, T. Miyamoto. The Loc. 3 is situated 2 m below the Ku 138, and stratigraphically Loc. 3 is situated between Ku 138 and Ku 104 both of which correspond to limestone of the second horizon by Kanmera (1953, 1954). The Locs. 1 and 4 are situated between the second and third horizons of fusulinid limestone. Mudstone of these localities



Text-fig. 3. Generalized columnar section of the Kuma Formation for the northern wing of the syncline in the study area. The fusulinid horizons (Kanmera, 1953, 1954) and the radiolarian horizons (this paper) are shown. 1: limestone. 2: mudstone. 3: sandstone.



Text-fig. 4. Detailed columnar section of the Kuma Formation at Loc. 3. Loc. 3 shows the horizon where radiolarian samples were collected, while Ku 138 is the second horizon of the limestone lens by Kanmera (1953, 1954).

1: Limestone and conglomeratic limestone characterized by the occurrence of *Leipidolina kumaensis*. 2: Thin seams of mudstone. 3: Calcareous sandstone. 4: Silty laminated shale.

is from the *Leipidolina kumaensis* Zone. The Locs. 6 and 7 are situated near the axis of the syncline and are regarded as the same horizon as Locs. 2 and 5, considering the folding in the northern wing of the syncline. Mudstone of the Locs. 2, 5, 6 and 7 is situated between the third and uppermost horizons of the limestones. Those are referred to as the upper part of the *L. kumaensis* Zone, since *Leipidolina* has been reported from the limestone of the fourth horizon, Ku 78.

These samples were broken into small fragment pieces and put into a bowl with 5–10% HF solution for 5–10 hours. Subsequently, the residue was gathered by using #200 sieve and radiolarian skeletons were picked up with a fine

brush under stereoscopic microscope.

Type and figured specimens are registered and deposited in the Institute of Geology and Mineralogy, Faculty of Science, Hiroshima University (IGSH R).

Systematic paleontology

Subclass RADIOLARIA Müller, 1858

Superorder POLYCYSTINA Ehrenberg, 1838,
emend. Riedel, 1967

Suborder ALBAILLELLARIA Deflandere, 1953,
emend. Holdsworth, 1969

Family Follicucullidae Ormiston and Babcock,
1979 emend. Kozur, 1981

Genus *Follicucullus* Ormiston and Babcock,
1979

Type species:—*Follicucullus ventricosus* Ormiston and Babcock, 1979, p. 331, pl. 1, figs. 6–14.

Follicucullus bipartitus Caridroit and De Wever,
emend. herein

Pl. 63, Figs. 1–18.

1984 *Follicucullus bipartitus* Caridroit and De Wever, *Géobios*, no. 17, pl. 1, figs. 1–3.

1985 *Follicucullus bipartitus* Caridroit and De Wever; Ishiga, "Earth Sci." (*Chikyu Kagaku*), vol. 39, no. 3, pl. 1, figs. 1–14.

1984 *Follicucullus hamatus* Caridroit and De Wever, *Geobios*, no. 17, pl. 1, figs. 7–14.

Material:—Eight specimens figured in this paper and more than 50 specimens from Loc. 2; 500 m southwest of Kayaba, Izumi-mura, Yatsushiro-gun, Kumamoto Prefecture.

Emended diagnosis:—A species of *Follicucullus* with strongly curving apical cone.

Measurements:—Length of shell excluding flaps: 500–592 μm (av. 536), based on three specimens (Pl. 63, Figs. 1–3).

Length of apical cone: 211–279 μm (av. 232), based on 14 specimens including those illustrated in Pl. 63, Figs. 1–13.

Width of the boundary between apical cone

and pseudothorax: 68–84 μm (av. 75), based on 13 specimens (Pl. 63, Figs. 1–13).

Diameter of curvature of apical cone: 18–106 μm (av. 26), based on 13 specimens (Pl. 63, Figs. 1–13).

Maximum width of pseudoabdomen: 95–126 μm (av. 111), based on 8 specimens (Pl. 63, Figs. 1–3, 14–18).

Description:—Shell tube-shaped gradually tapering distally and curving to ventral side. Circumferential stricture at middle part of shell dividing shell into upper and lower parts. Upper part corresponding to apical cone and lower part to pseudothorax and pseudoabdomen. Shell becoming thin around the stricture and easily broken into two parts. In some specimens (Pl. 63, Figs. 5, 11; IGSH R 15–74, 15–72), middle part of apical cone weakly constricted. Distal part of apical cone curving, radius of curvature variable among individuals as shown in Pl. 63, Figs. 8–13 (IGSH R 15–65, 75, 73, 72, 64, 69). Lower part of apical cone tube-shaped with weakly undulated shell surface, and nearly elliptical in cross section. Pseudothorax long, about half length of shell and pseudoabdomen short. Distinction between pseudothorax and pseudoabdomen obscure. Pseudoabdomen weakly constricted nearby aperture. Aperture elliptical in outline with asymmetrical flaps. Dorsal flap blade-like extending obliquely downward. Ventral flap triangular in outline extending horizontally. Apertural margin nearly horizontal. In some specimens, ventral flap small and spine-like in shape extending obliquely downward (Pl. 63, Figs. 17; IGSH R 15–59).

Remarks:—As indicated by Caridroit and De Wever (1984), shell of this species becomes thin around the stricture at the middle part and is easily broken into two parts from there. Concerning the detached apical cone, the lower margin is characterized by a sharp truncation which occasionally looks like an apertural margin of the pseudoabdomen without complete flaps. Moreover, concerning the dimensions of the specimens from the “Tatsuno Formation”, the length of shell of *Follicucullus hamatus* Caridroit and De Wever is nearly same as that of apical cone of *F.*

bipartitus Caridroit and De Wever. Judging from these observations, *F. hamatus* is regarded to be synonymous with *F. bipartitus*. As described above, specimens of this species from the Kuma Formation show morphological variation, concerning the shape of the apical cone and flaps of apertural margin.

Follicucullus bipartitus resembles *F. scholasticus* morphotype I of Ishiga (1984) in having tube-shaped elongated shell, but it differs from *F. scholasticus* m. I and other species of *Follicucullus* in its strongly curving apical cone.

Concerning the characteristic curving of apical cone, *Neoalbaillella grypus* Ishiga, Kito and Imoto reveals the same lines of morphologic trend (Ishiga *et al.*, 1982a).

Occurrence:—This species occurs at Locs. 2, 3, 4 and 7 of the *Lepidolina kumaensis* Zone of the Kuma Formation.

This species was originally described from the black mudstone of the “Tatsuno Formation” in Hyogo Prefecture (Caridroit and De Wever, 1984). Recently, this species has been reported from bedded chert in the Mino Belt, the upper part of the *Neoalbaillella ornithoformis* Assemblage-zone, and from red bedded siliceous shale and bedded chert of the Katsumi Formation in the northern margin of the Tamba Belt (Ishiga, 1985).

Follicucullus charveti Caridroit and De Wever, 1984, emend. herein

Pl. 63, Figs. 19–22; Pl. 64, Figs. 1–8.

- 1984 *Follicucullus charveti* Caridroit and De Wever, *Géobios*, no. 17, pl. 1, figs. 15–22.
- 1985 *Follicucullus charveti* Caridroit and De Wever; Ishiga, “*Earth Sci.*” (*Chikyu Kagaku*), vol. 39, no. 3, pl. 1, figs. 19–22.
- 1984 *Follicucullus falx* Caridroit and De Wever, *Géobios*, no. 17, pl. 1, figs. 4–6.
- 1984 *Follicucullus orthogonus* Caridroit and De Wever, *Géobios*, no. 17, pl. 1, figs. 23–29.
- cf. 1980 *Follicucullus* sp. cf. *Fo. ventricosus*

- Ormiston and Babcock; Ishiga and Imoto, "Earth Sci." (Chikyu Kagaku), vol. 34, no. 6, pl. 4, figs. 16–19, non 20.
- cf. 1981 *Follicucullus* sp. cf. *Fo. ventricosus* Ormiston and Babcock; Takemura and Nakaseko, *Trans. Proc. Palaeont. Soc. Japan, N.S.*, no. 124, pl. 34, fig. 8.
- cf. 1982 *Follicucullus ventricosus* Ormiston and Babcock; Nishizono *et al.*, *News of Osaka Micropaleont., Spec. Vol.*, no. 5, pl. 2, fig. 4.

Material:—Eight specimens figured in this paper and more than 150 specimens from Loc. 2; 500 m southwest of Kayaba, Izumi-mura, Yatsushiro-gun, Kumamoto Prefecture.

Emended specific diagnosis:—A species of *Follicucullus* which consists of long apical cone, inflated pseudothorax and short pseudoabdomen with long, thick ventral flap and small dorsal flap.

Remarks:—Caridroit and De Wever (1984) described five species of *Follicucullus*. Among them, *Follicucullus charveti*, *F. falx* and *F. orthogonus* are similar to each other concerning the essential features given in the specific diagnosis (see above). They are regarded as varieties within a single species, *F. charveti*. In this paper, the three forms of *F. charveti* are treated as morphotypes, namely, morphotype *charveti*, *m. falx* and *m. orthogonus*.

Follicucullus charveti differs from *F. ventricosus* Ormiston and Babcock in having large ventral flap extending horizontally or obliquely upward. As far as the species which have been described under the genus *Follicucullus* Ormiston and Babcock, *Pseudoalbaillella* Holdsworth and Jones and *Neoalbaillella* Takemura and Nakaseko are concerned, the ventral flap is usually smaller and shorter than the dorsal flap. Therefore, this species is unusual among the species of *Follicucullus* in the relative size of the two flaps.

Occurrence:—These three morphotypes of *Follicucullus charveti* occur together in black mudstone at Loc. 2 of the *Lepidolina kumaensis* Zone of the Kuma Formation. In addition, *m. charveti* occurs from black mudstone at Loc. 7

and *m. orthogonus* from black mudstone at Loc. 4.

This species was originally described from black mudstone of the "Tatsuno Formation" in Hyogo Prefecture (Caridroit and De Wever, 1984). Recently, this species has been reported from red bedded siliceous shale of the Katsumi Formation in the northern margin of the Tamba Belt (Ishiga, 1985).

Follicucullus charveti Caridroit and De Wever, 1984, morphotype *charveti* Ishiga

Pl. 63, Figs. 19–22; Pl. 64, Figs. 1–3, 6, 7

1984 *Follicucullus charveti* Caridroit and De Wever, *Géobios*, no. 17, pl. 1, figs. 15–22.

Material:—Eight specimens figured in this paper and more than 50 specimens from Loc. 2; 500 m southwest of Kayaba, Izumi-mura, Yatsushiro-gun, Kumamoto Prefecture. Standard specimen of this morphotype is the holotype of *Follicucullus charveti* from the "Tatsuno Formation" in Hyogo Prefecture, Southwest Japan.

Measurements:—Based on 7 specimens (Pl. 63, Figs. 19–22, Pl. 64, Figs. 1–3).

Length of apical cone: 153–221 μm (av. 186).

Length of pseudothorax: 64–116 μm (av. 95).

Maximum width of pseudothorax: 116–137 μm (av. 132).

Length of pseudoabdomen: 22–40 μm (av. 35).

Length of ventral flaps: 105–180 μm (av. 150).

Description:—Shell consisting of apical cone, pseudothorax and pseudoabdomen. Apical cone long, about half length of shell, slightly curving to ventral side. Middle part of apical cone weakly constricted. Boundary between apical cone and pseudothorax slightly constricted and shell wall of this part thinner than other part and fragile. Pseudothorax globular in outline and slightly inflated. In small specimens, pseudothorax short and flattened. Pseudoabdomen short, somewhat

curving to ventral side. Large ventral flap extending horizontally or obliquely upward. Ventral flap usually recurving distally. Proximal part of ventral flap blade-like and distal part elliptical in cross section. Basal part of ventral flap keel-shaped as shown in Pl. 64, Fig. 1 (IGSH R 15-14). Boundary between pseudothorax and pseudoabdomen indistinct. Dorsal side of apertural margin slightly slitted. Small and short spine-like dorsal flap extending downward. Aperture obliquely facing to ventral side.

Remarks:—*Follicucullus charveti* m. *charveti* differs from *F. charveti* m. *falx* in having “by-spine” extending vertically downward from the ventral flap. Morphotype *charveti* differs from m. *orthogonus* in strongly curved pseudoabdomen. Among these three morphotypes, morphology of apical cone and pseudothorax is, however, similar to each other.

Specimens of this morphotype from the Kuma Formation show variation in the size of shell as shown in Pl. 63, Figs. 19-22 (IGSH R 15-27, 31, 29, 30) and Pl. 64, Figs. 1-3 (15-14, 28, 10). Shell becomes thin at the boundary between apical cone and pseudothorax, so that the apical cone is liable to be detached from pseudothorax in this morphotype. This tendency is the same as that of *Follicucullus bipartitus*. There have not been observed any internal structure inside of the pseudothorax as shown in Pl. 64, Figs. 6 and 7 (IGSH R 15-26, 12).

Follicucullus charveti Caridroit and De Wever,
1984, morphotype *falx* Ishiga

Pl. 64, Fig. 8.

1984 *Follicucullus falx* Caridroit and De Wever,
Géobios, no. 17, pl. 1, figs. 4-6.

1985 *Follicucullus charveti* Caridroit and De Wever morphotype *falx*; Ishiga, “*Earth Sci.*” (*Chikyu Kagaku*), vol. 39, no. 3, pl. 2, fig. 5.

Material:—One specimen figured in this paper and additional 10 specimens from Loc. 2; 500 m southwest of Kayaba, Izumi-mura, Yatsushiro-gun, Kumamoto Prefecture. Standard specimen

of this morphotype is the holotype of *Follicucullus falx* from the “Tatsuno Formation” in Hyogo Prefecture.

Measurements:—Based on one specimen (Pl. 64, Fig. 8) and other 5 specimens from Loc. 2. The apical cone of the specimens are ill-preserved, so that its measurement is not given.

Length of pseudothorax: 150-230 μm (av. 190).

Maximum width of pseudothorax: 100-140 μm (av. 135).

Length of pseudoabdomen: 20-43 μm (av. 38).

Length of ventral flap: 100-179 μm (av. 138).

Remarks:—As mentioned already, the morphology of shell is the same as that of the morphotype *charveti*, except for the existence of “by-spine” which is extending vertically downward from the ventral flap. Specimens of this morphotype from the Kuma Formation show variation in the shape of “by-spine”. “By-spine” usually shows an inverted triangular outline, but in some specimens it is projected downward like a spine.

Follicucullus charveti Caridroit and De Wever,
1984, morphotype *orthogonus* Ishiga

Pl. 64, Figs. 4, 5.

1984 *Follicucullus orthogonus* Caridroit and De Wever, *Géobios*, no. 17, pl. 1, figs. 23-29.

1985 *Follicucullus charveti* Caridroit and De Wever morphotype *orthogonus*; Ishiga, “*Earth Sci.*” (*Chikyu Kagaku*), vol. 39, no. 3, pl. 2, fig. 12.

Material:—Three specimens figured in this paper and additional 20 specimens from Loc. 2; 500 m southwest of Kayaba, Izumi-mura, Yatsushiro-gun, Kumamoto Prefecture. Standard specimen of this morphotype is the holotype of *Follicucullus orthogonus* from the “Tatsuno Formation” in Hyogo Prefecture.

Measurements:—Based on one specimen (Pl. 64, Fig. 4) and other 4 specimens from Loc. 2.

Length of apical cone: 160–237 μm (av. 180).

Length of pseudothorax: 60–130 μm (av. 100).

Maximum width of pseudothorax: 100–120 μm (av. 112).

Length of pseudoabdomen: 38–55 μm (av. 48).

Length of ventral flap: 100–190 μm (av. 120).

Remarks:—This morphotype differs from *Follicucullus charveti* m. *charveti* and m. *falx* in having strongly curving pseudoabdomen. Apical cone and ventral flap are arranged nearly parallel to each other as shown in Pl. 64, Fig. 4 (IGSH R 15–21). Dorsal flap of this morphotype is longer than that of the other two morphotypes owing to the slit of both sides of the dorsal flap. In accordance with the increase in the curving of the pseudoabdomen, both sides of the dorsal flap are slitted.

Follicucullus scholasticus Ormiston and Babcock, 1979

Pl. 64, Figs. 9–11.

- 1979 *Follicucullus scholasticus* Ormiston and Babcock, *Jour. Paleont.*, vol. 53, no. 2, p. 331, figs. 1–5.
- 1980 *Follicucullus scholasticus* Ormiston and Babcock; Ishiga and Imoto, “*Earth Sci.*” (*Chikyu Kagaku*), vol. 34, no. 6, pl. 4, figs. 4–10.
- 1981 *Follicucullus scholasticus* Ormiston and Babcock; Takemura and Nakaseko, *Trans. Proc. Palaeont. Soc. Japan, N.S.*, no. 124, pl. 34, fig. 6.
- 1982a *Follicucullus scholasticus* Ormiston and Babcock; Ishiga *et al.*, “*Earth Sci.*” (*Chikyu Kagaku*), vol. 36, no. 1, pl. 3, fig. 9.
- 1982b *Follicucullus scholasticus* Ormiston and Babcock; Ishiga *et al.*, *News of Osaka Micropaleont., Spec. Vol.*, no. 5, pl. 2, figs. 8–10.
- 1982 *Follicucullus scholasticus* Ormiston and Babcock; Kojima, *ibid.*, pl. 3, fig. 4.
- 1982 *Follicucullus scholasticus* Ormiston and Babcock; Sato *et al.*, *ibid.*, pl. 1, fig. 5.

1982c *Follicucullus scholasticus* Ormiston and Babcock; Ishiga *et al.*, “*Earth Sci.*” (*Chikyu Kagaku*), vol. 36, no. 5, pl. 4, figs. 13, 14.

1982 *Follicucullus scholasticus* Ormiston and Babcock; Nishizono *et al.*, *News of Osaka Micropaleont., Spec. Vol.*, no. 5, pl. 2, fig. 3.

1983 *Follicucullus scholasticus* Ormiston and Babcock; Wakita, *Bull. Geol. Surv. Japan*, vol. 34, pl. 5, fig. 8.

1983 *Follicucullus scholasticus* Ormiston and Babcock; Suyari *et al.*, *Jour. Sci. Univ. Tokushima*, vol. 16, pl. 3, figs. 1–9.

1984 *Follicucullus scholasticus* Ormiston and Babcock; Ishiga, “*Earth Sci.*” (*Chikyu Kagaku*), vol. 38, no. 6, pl. 1, figs. 1–8.

1985 *Follicucullus scholasticus* Ormiston and Babcock morphotype I; Ishiga, *ibid.*, vol. 39, no. 3, pl. 1, figs. 15–21.

1985 *Follicucullus scholasticus* Ormiston and Babcock morphotype II; Ishiga, *ibid.*, vol. 39, no. 3, pl. 1, figs. 22–28, pl. 2, figs. 1–4.

1982 *Follicucullus ventricosus* Ormiston and Babcock; Sato *et al.*, *News of Osaka Micropaleont., Spec. Vol.*, no. 5, pl. 1, fig. 5.

Specific diagnosis:—A species of *Follicucullus* characterized by conical shell which is weakly differentiated into apical cone, pseudothorax without wing and pseudoabdomen with small apertural flaps.

Measurements:—Based on three specimens (Pl. 64, Figs. 9–11) and other 7 specimens from Loc. 2.

Length of shell excluding flaps (L): 271–301 μm (av. 288).

Length of apical cone 120–143 μm (av. 130).

Width of pseudothorax (W): 75–90 μm (av. 85).

Ratio W/L: 0.25–0.33.

Description:—Shell consisting of apical cone, pseudothorax and pseudoabdomen. Boundary between them obscure, only slightly constricted. Apical cone long, about half length of shell. Shell surface of apical cone weakly undulated. Pseudothorax slightly flattened without pores. Width of pseudothorax (Wt) nearly equal to that of

pseudoabdomen. Ratio Wt/Ls (Ls: length of shell excluding flaps) usually 0.3. Pseudoabdomen short about 1/5 length of shell and weakly curving to ventral side. Apertural margin between dorsal and ventral sides lobated. Dorsal flap tongue-like in proximally, becoming distally blade-like within plane of bilateral symmetry of shell. Both sides of dorsal flap weakly slitted.

Remarks:—Two morphotypes, namely, morphotype I and m. II have been discriminated within *Follicucullus scholasticus* (Ishiga, 1984). Morphotype I is characterized by elongated conical shell without undulation, while morphotype II is characterized by having undulated shell with rather clear differentiation into apical cone, pseudothorax and pseudoabdomen. Concerning the hitherto illustrated specimens of *Follicucullus* listed above, *F. scholasticus* described from West Texas (Ormiston and Babcock, 1979) and from the Sasayama area in the Tamba Belt, Southwest Japan (Ishiga and Imoto, 1980) can be assigned to morphotype I. Moreover, *Follicucullus scholasticus* m. I and m. II have been recently reported from the Katsumi Formation in the northern margin of the Tamba Belt (Ishiga, 1985). Other specimens belong to morphotype II. Specimens of *F. scholasticus* from the Kuma Formation are assigned to morphotype II.

Occurrence:—This species occurs at Locs. 1–7 of the *Lepidolina kumaensis* Zone of the Kuma Formation.

Follicucullus scholasticus was originally described from the Capitanian (Guadalupian) Lamar Limestone of Delaware Basin in West Texas (Ormiston and Babcock, 1979) and has been reported from many localities in the Mino-Tamba and Chichibu Belts, Southwest Japan. Morphotype II of this species was reported from the black mudstone of the Upper formation of the Maizuru Group which corresponds to the *Lepidolina kumaensis* Zone (Ishiga, 1984). *Follicucullus scholasticus* m. II has long range of the occurrence from the upper part of the *Follicucullus monacanthus* Assemblage-zone to the *Neobaillella ornithoformis* A-zone (Ishiga *et al.*, 1982b), while the occurrence of *F. scholasticus* m. I is regarded to be restricted to the *F. scholasticus* A-zone.

Discussion

A. Radiolarian assemblage from the Kuma Formation

Radiolarians obtained from the Kuma Formation are listed in Table 1. Radiolarians from the Locs. 2, 3, 4 and 7 are characterized by the occurrence of *Follicucullus bipartitus* Caridroit and De Wever, *F. charveti* Caridroit and De Wever and *F. scholasticus* morphotype II. *Albaillella triangularis* Ishiga, Kito and Imoto also occurs from the Loc. 2. Radiolarian specimens from the Locs. 1, 5 and 6 are rather ill-preserved,

Table 1. Radiolarians from the Kuma Formation in the study area.

	Localities						
	1	2	3	4	5	6	7
<i>Follicucullus scholasticus</i> m. II	+	+	+	+	+	+	+
<i>F. bipartitus</i> Caridroit and De Wever		+	+	+			+
<i>F. charveti</i> m. <i>charveti</i> Ishiga		+					+
<i>F. charveti</i> m. <i>false</i> Ishiga		+					
<i>F. charveti</i> m. <i>orthogonus</i> Ishiga		+		+			
<i>Pseudoalbaillella</i> sp.				+			
<i>Albaillella triangularis</i> Ishiga, Kito and Imoto		+					
<i>Haplentactinia</i> (?) <i>ichikawai</i> Caridroit and De Wever		+					
<i>Nazarovella gracilis</i> De Wever and Caridroit		+					

although *F. scholasticus* m. II has been identified among them.

As mentioned in the preceding chapter, *Follicucullus bipartitus* has been found in the upper part of the *Neoalbaillella ornithoformis* Assemblage-zone which is the uppermost radiolarian assemblage-zone for the Japanese Permian. Takemura and Nakaseko (1981) reported the co-occurrence of specimens, which resemble *Follicucullus charveti* (pl. 34, fig. 8), with *Neoalbaillella ornithoformis* Takemura and Nakaseko, *N.* sp. B (= *N. optima* Ishiga, Kito and Imoto) and *Albaillellidae* gen. et sp. indet. (= *Albaillella levis* Ishiga, Kito and Imoto). The radiolarian assemblage reported by them is similar to the assemblage in the lower part of the *Neoalbaillella ornithoformis* Assemblage-zone (Ishiga *et al.*, 1982b), considering the association of *N. ornithoformis* and *Albaillella levis*. *Albaillella triangularis* Ishiga, Kito and Imoto occurs from the upper part of the *Follicucullus scholasticus* A-zone to the *Neoalbaillella optima* A-zone, but it has not been reported from the *N. ornithoformis* A-zone. Judging from these stratigraphic distribution of radiolarians, especially the occurrence of *Albaillella triangularis*, it is considered that the mudstone of the Loc. 2 corresponds to the upper part of the *Follicucullus scholasticus* A-zone and/or the *Neoalbaillella optima* A-zone. The radiolarian assemblage of the Locs. 3, 4 and 7 are considered to be nearly the same as that of the Loc. 2.

B. On the radiolarian assemblage characterized by the association of *Follicucullus bipartitus* and *F. charveti*

Recently, the radiolarian assemblage characterized by the association of *Follicucullus*

bipartitus and *F. charveti* has been found in clastic rocks of several places in Southwest Japan. The radiolarian assemblage from black mudstone of the "Tatsuno Formation" in Hyogo Prefecture is characterized by the association of *F. bipartitus*, *F. charveti* and *Albaillella triangularis* (Caridroit and De Wever, 1984), and its specific composition is essentially the same as those from the Locs. 2, 3, 4 and 7 of the Kuma Formation. Moreover, *Haplentactinia*(?) *ichikawai* Caridroit and De Wever and *Nazarovella gracilis* Caridroit and De Wever, originally described from the "Tatsuno Formation", are found also in Loc. 2 (Pl. 64, Figs. 14, 15 and 16). Recently, a radiolarian assemblage, identical with that of the Kuma Formation has been found also from the bedded siliceous shale of the Katsumi Formation in the northern part of the Tamba Belt (Ishiga, 1985). According to him, the radiolarian assemblage from this formation is composed of *Follicucullus bipartitus*, *F. charveti*, *F. scholasticus* m. I, *F. scholasticus* m. II and *Albaillella triangularis* and corresponds to that from the upper part of the *F. scholasticus* Assemblage-zone in the Mino-Tamba Belt. Excepting the occurrence of *F. scholasticus* m. I, the assemblage in the Katsumi Formation is the same as that from the Kuma Formation.

Summarizing the radiolarian assemblage from Locs. 2, 3, 4 and 7 of the Kuma Formation, "Tatsuno Formation" and Katsumi Formation, the assemblage is characterized by the occurrence of *Follicucullus bipartitus* and *F. charveti* and absence of species of *Neoalbaillella*. Noteworthy is that the radiolarian assemblage is different from that of the bedded chert of the *Follicucullus scholasticus* A-zone and *Neoalbaillella optima* A-zone in the Mino-Tamba Belt by Ishiga *et al.*

Explanation of Plate 63

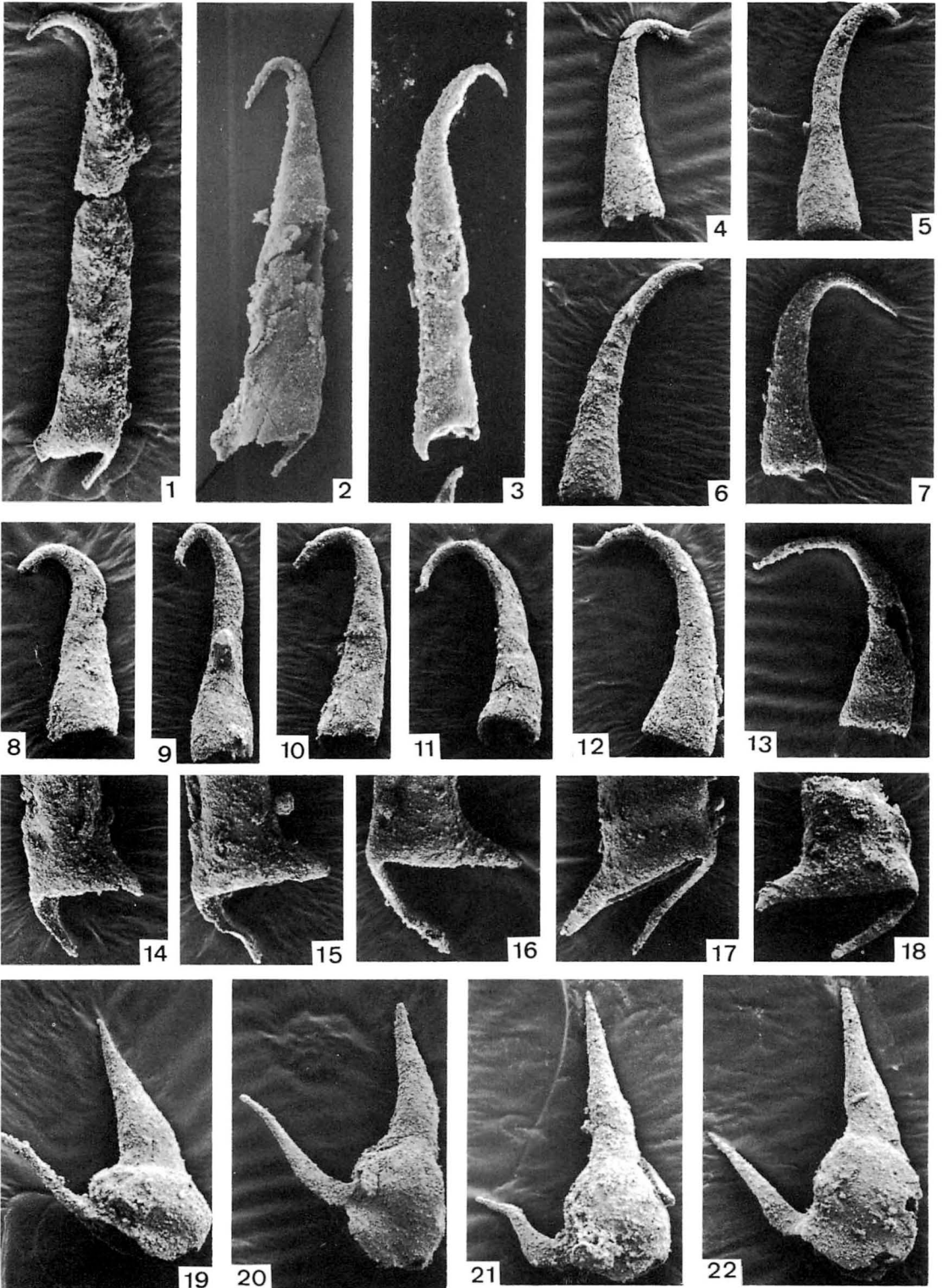
Figs. 1—18. *Follicucullus bipartitus* Caridroit and De Wever

Fig. 1; IGSH R 15—39, 2; 7—6, 3; 9—17, 4; 15—70, 5; 15—74, 6; 15—76, 7; 15—77, 8; 15—65, 9; 15—75, 10; 15—73, 11; 15—72, 12; 15—64, 13; 15—69, 14; 15—57, 15; 15—56, 16; 15—50, 17; 15—59, 18; 15—60.

Figs. 19—22. *Follicucullus charveti* Caridroit and De Wever morphotype *charveti* Ishiga

Fig. 19; IGSH R 15—27, 20; 15—31, 21; 15—29, 22; 15—30.

All from Loc. 2. Scale: Figs. 1—3; ×85. Figs. 4—22; ×133.



(1982b), concerning the dominant components. However, the radiolarian assemblage characterized by *Follicucullus bipartitus* and *F. charveti* is younger than and/or partly contemporaneous with the *F. scholasticus* Assemblage. *Follicucullus bipartitus* and *F. charveti* are regarded to have rather long range of occurrence from the upper part of the *F. scholasticus* A-zone to the *Neobaillella ornithoformis* A-zone.

C. Tentative correlation of some Late Permian radiolarian zones with fusulinid zones

On the basis of the fusulinid fossil evidence from the Kuma Formation, Kanmera and Nakazawa (1973), and Ishii *et al.* (1975) distinguished three fusulinid horizons as follows. The lower horizon is characterized by the occurrence of *Lepidolina multiseptata shiraiwensis* and the middle one is by *Lepidolina kumaensis* and *L. multiseptata*. The middle horizon corresponds to the second and third horizons by Kanmera (1953, 1954), which were referred to in the chapter on geologic setting. The upper horizon is characterized by *Codonofusiella*, and *Lepidolina* is no more represented. This horizon is not identified in the study area.

As mentioned already, the mudstone of Loc. 3 corresponds to the limestone of the second horizon by Kanmera (1953, 1954) and the mudstones of Locs. 2 and 4 are situated between the third and the fourth horizons by Kanmera (1953). The mudstone of Loc. 7 is situated nearly the fourth horizon by Kanmera (1953, 1954). These four localities (2, 3, 4 and 7) correspond to the middle horizon by Kanmera and Nakazawa (1973), and Ishii *et al.* (1975) and they belong to the *Lepidolina kumaensis* Zone.

Recently, *Follicucullus scholasticus* morphotype II has been reported from the mudstone of the Maizuru Group and the *F. scholasticus* Assemblage-zone is considered to correspond to the *Lepidolina kumaensis* Zone (Ishiga, 1984). In conclusion, the *Follicucullus scholasticus* Assemblage and the radiolarian assemblage characterized by *F. bipartitus* and *F. charveti* are found in the *Lepidolina kumaensis* Zone of Japan.

References

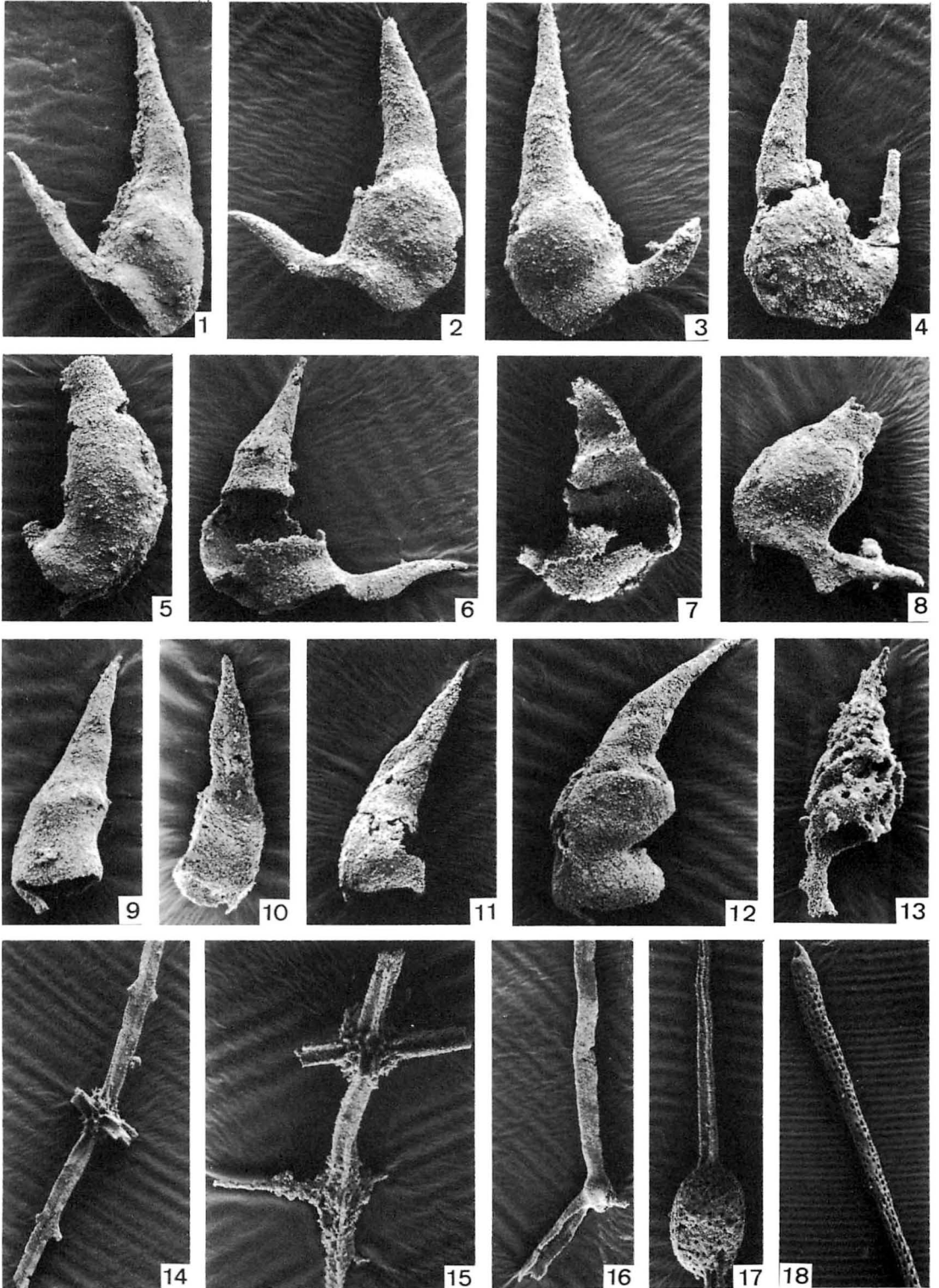
- Caridroit, M. and De Wever, P. (1984): Description de quelques nouvelles especes de Follicucullidae et d'Entactiniidae (radiolaires polycystines) du Permien du Japon. *Géobios*, no. 17, p. 639–644, pls. 1–2.
- Ishiga, H. (1984): *Follicucullus* (Permian radiolaria) from Maizuru Group in Maizuru Belt, Southwest Japan. "Earth Sci." (*Chikyū Kagaku*), vol. 38, no. 6, p. 427–434, pl. 1.
- (1985): Discovery of Permian radiolarians from Katsumi and Oi Formations along south of Maizuru Belt, Southwest Japan and its significance. *Ibid.*, vol. 39, no. 3, p. 175–185, pls. 1–2.
- and Imoto, N. (1980): Some Permian radiolarians in the Tamba District, Southwest Japan. *Ibid.*, vol. 34, no. 6, p. 333–345, pls. 1–5.
- , —, Yoshida, M. and Tanabe, T. (1984): Early Permian radiolarians from the Tamba Belt, Southwest Japan. *Ibid.*, vol. 38, no. 1, p. 44–52, pls. 1, 2.
- , Kito, T. and Imoto, N. (1982a): Late Permian radiolarian assemblages in the Tamba District and an adjacent area, Southwest Japan. *Ibid.*, vol. 36, no. 1, p. 10–22, pls. 1–4.
- , — and — (1982b): Permian radiolarian biostratigraphy. *News of Osaka Micropaleont., Spec. Vol.*, no. 5, p. 17–22, pls. 1, 2.
- , — and — (1982c): Middle Permian radiolarian assemblages in the Tamba District and an adjacent area, Southwest Japan. "Earth Sci." (*Chikyū Kagaku*), vol. 36, no. 5, p. 272–281, pls. 1–4.
- Ishii, K., Okimura, Y. and Nakazawa, K. (1975): On the genus *Colaniella* and its biostratigraphic significance. *Jour. Geosci. Osaka City Univ.*, vol. 19, p. 107–138, pls. 1–4.
- Kanmera, K. (1952): The Upper Carboniferous and the Lower Permian of the Hikawa valley, Kumamoto Pref. Kyushu, Japan. *Jour. Geol. Soc. Japan*, vol. 58, no. 676, p. 17–32 (in Japanese with English abstract).
- (1953): The Kuma Formation with special reference to the Upper Permian in Japan. *Ibid.*, vol. 59, no. 697, p. 449–468 (in Japanese with English abstract).
- (1954): Fusulinids from the Upper Permian

- Kuma Formation, Southern Kyushu, Japan — with special reference to the fusulinid zone in the Upper Permian of Japan —. *Mem. Fac. Sci., Kyushu Univ., Ser. D*, vol. 4, p. 1–38, pls. 1–6.
- and Nakazawa (1973): Permian-Triassic relationship and faunal changes in the Eastern Tethys. In: Logan, A. and Hills, L. V. ed., *The Permian and Triassic Systems and their mutual boundary. Canad. Petrol. Geologists, Mem.*, 2, p. 100–119.
- Kojima, S. (1982): Some Jurassic, Triassic and Permian radiolarians from the eastern part of Takayama City, Central Japan. *News of Osaka Micropaleont., Spec. Vol.*, no. 5, p. 81–91, pls. 1–4 (in Japanese with English abstract).
- Matsumoto, T. and Kanmera, K. (1964): *Geological map of Japan and its explanatory text, Hinagu Sheet (1:50,000)*. Geol. Surv. Japan (in Japanese with English abstract). 147 pp.
- Miyamoto, T., Kuwazuru, J., Nomoto, T., Yamada, H., Tominaga, R. and Hase, A. (1985): Discovery of Late Permian radiolarians from the Kakisako and Kuma Formations in the Futae district, Izumi-mura, Yatsushiro County, Kumamoto Prefecture, Kyushu (Short Report). "*Earth Sci.*" (*Chikyu Kagaku*), vol. 39, no. 1, p. 78–84 (in Japanese).
- , —, Tominaga, R. and Yamada, H. (1984): Discovery of Late Permian radiolarians from mudstones of the Kakisako and Kuma Formations, Kyushu. *Abst. Prog. Ann. Meet. Geol. Soc. Japan*, p. 229 (in Japanese).
- Nishizono, Y., Ohishi, A., Sato, T. and Murata, M. (1982): Radiolarian fauna from the Paleozoic and Mesozoic formations, distributed along the Mid-stream of Kuma River, Kyushu, Japan. *News of Osaka Micropaleont., Spec. Vol.*, no. 5, p. 311–326, pls. 1–3 (in Japanese with English abstract).
- Ormiston, A. and Babcock, L. (1979): *Follicucullus*, new radiolarian genus from the Guadalupian (Permian) Lamar Limestone of the Delaware Basin. *Jour. Paleont.*, vol. 53, no. 2, p. 328–334, pl. 1.
- Sato, T., Nishizono, Y. and Murata, M. (1982): Paleozoic and Mesozoic radiolarian faunas from the Shakumasan Formation. *News of Osaka Micropaleont., Spec. Vol.*, no. 5, p. 301–310, pls. 1–4 (in Japanese with English abstract).
- Suyari, K., Kuwano, Y. and Ishida, K. (1983): Biostratigraphic study of the North Subbelt of the Chichibu Belt in Central Shikoku. *Jour. Sci. Univ. Tokushima*, vol. 16, p. 143–167, pls. 1–7 (in Japanese with English abstract).

Explanation of Plate 64

- Figs. 1–3, 6, 7. *Follicucullus charveti* Caridroit and De Wever morphotype *charveti* Ishiga
Fig. 1; IGSH R 15–14, 2; 15–28, 3; 15–10, 6; 15–26, 7; 15–12.
- Figs. 4, 5. *Follicucullus charveti* Caridroit and De Wever morphotype *orthogonus* Ishiga
Fig. 4; IGSH R 15–21, 5; 15–6.
- Fig. 8. *Follicucullus charveti* Caridroit and De Wever morphotype *falx* Ishiga
Fig. 8; IGSH R 15–38.
- Figs. 9–11. *Follicucullus scholasticus* Ormiston and Babcock morphotype II
Fig. 9; IGSH R 15–45, 10; 15–46, 11; 15–11.
- Fig. 12. *Follicucullus* sp. IGSH R 15–33.
- Fig. 13. *Albaillella triangularis* Ishiga, Kito and Imoto IGSH R 15–47.
- Figs. 14, 15. *Haplentactinia(?) ichikawai* Caridroit and De Wever
Fig. 14; IGSH R 15–82, 15; 15–89.
- Fig. 16. *Nazarovella gracilis* De Wever and Caridroit IGSH R 15–81.
- Figs. 17, 18. Unnamed spumellaria
Fig. 17; IGSH R 15–97, 18; 15–95.

All from Loc. 2. Scales: Figs. 1–12, 15; ×133. Fig. 13; ×225. Figs. 14, 16, 17; ×100. Fig. 18; ×50.



Takemura, A. and Nakaseko, K. (1981): A new Permian radiolarian genus from the Tamba Belt, Southwest Japan. *Trans. Proc., Palaeont. Soc. Japan, N.S.*, no. 124, p. 208—214, pls. 33-34.

Wakita, K. (1983): Allochthonous blocks and submarine slide deposits in the Jurassic formation, southwest of Gujo-hachiman, Gifu Prefecture, central Japan. *Bull. Geol. Surv. Japan*, vol. 34, no. 7, p. 329—342, pls. 4—8 (in Japanese with English abstract).

Hashirimizu 走水, Hikawa 氷川, Izumi-mura 泉村, Kakisako 柿迫, Kayaba 河合場, Kuma 球磨, Miyama 深山.

上部ベルム系球磨層から産出した *Follicucullus* (放射虫) : 熊本県八代郡氷川上流域に分布する上部ベルム系球磨層の *Lepidolina kumaensis* 化石帯より, *Follicucullus bipartitus* Caridroit and De Wever および *F. charveti* Caridroit and De Wever により特徴づけられる放射虫群集を識別した。この群集は美濃-丹波帯の層状チャートから報告されている放射虫群集とは、主な構成種が異なるが、チャート層中で設定されている *F. scholasticus* 群集帯と *Neobaillella optima* 群集帯の放射虫群集の両方に、またはいずれか一方に対比されると考えられる。

石賀裕明・宮本隆実

PROCEEDINGS OF THE PALAEOONTOLOGICAL
SOCIETY OF JAPAN

日本古生物学会1986年年会・総会

日本古生物学会年会・総会が1986年1月31日—
2月2日に東北大学理学部および仙台市戦災復興
記念館で開催された(参会者182名)。

国際学術集全出席報告

第9回オストラコーダ国際シンポジウム(静岡)
..... 池谷仙之・花井哲郎・石崎国熙
第2回国際頭足類シンポジウム(Tübingen, F.R.G.)
.... 小島郁生・蟹江康光・平野弘道・二上政夫

前会長講演

日本における中・新生代有孔虫の研究.. 高柳洋吉

総 会

シンポジウム「古生物の系統分類に関する諸問題」

世話人: 高柳洋吉・森 啓・速水 格
石灰質有孔虫の系統分類: 現状と問題点

..... 野村律夫
放射虫の分類について..... 竹村厚司
腹足類の系統に関する問題点..... 加瀬友喜
へゴ科木生シダ類の進化..... 西田治文
分岐分類学: 系統再構成への道..... 三中信宏
総台討論・総括

特 別 講 演

秩父帯南部の三畳紀テラス二枚貝動物群

..... 田村 実
ウラン系列放射年代測定法の原理と応用例—主と
して波照間島に分布する琉球石灰岩の形成年代
について—..... 大村明雄
最終氷期以降の日本海の環境変遷..... 大場忠道

個 人 講 演

中部ジュラ系毛田層(高知県佐川地域・秩父帯中
帯)に産する材化石..... 綱田幸司・松岡 篤
大阪関西国際空港ボーリングコア中の糞粒化石に
ついて.... 中世古幸次郎・大野照文・山内守明
アケボノ象の産出と大桑層の地質時代
..... 高山俊昭・大塚裕之
福島県梁川層産出の *Paleoparadoxia* .. 長谷川善
和・鈴木敬治・竹谷陽一郎・梁川町教育委員会

中新世白土層群産 *Mastodon* 象類の下顎について

..... 国府田良樹・鈴木 直・長谷川善和
漸新世石城層産骨質歯鳥類

..... 長谷川善和・小野慶一・国府田良樹
Spitsbergen 島 Starostin 岬付近におけるベルム
系の腕足類層序と時代.. 中村耕二・木村 学
関東山地東南部“鳥巢層群”相当層の年代

..... 斎藤 晴・安田 守
KAIKO 計画IIで採集された白亜紀石灰岩内の化

石とその意義..... 小西健二・J. Boulègue・
J. Burgois・石井輝秋・小林和男・中村保夫

中部エゾ層群のイノセラムス化石層序について

..... 浅井明人
ピストン・コアKH-84-3, st. 33(津軽海峡西方域)

の総合研究
その1. 珪藻..... 小泉 格

その2. 放射虫..... 酒井豊三郎
その3. 有孔虫および石灰質ナンノプランクト

ン..... 加藤道雄・高山俊昭
その4. 酸素・炭素同位体比..... 大場忠道

白亜紀デスモセラス亜科アンモナイト数種の殻形
変異と機能形態..... 重田康成・棚部一成

異常巻きアンモナイトの形態解析..... 岡本 隆
二枚貝の殻表にみられる斜彫刻の規則性

..... 速水 格・岡本 隆
イシサンゴ群体の成長速度と“日照時”

..... 今井敏夫・山口真仁・小西健二
“ミクリガイ”の種内変異についての一考察

..... 小坂 淳・小西健二
二枚貝マルスダレガイ科(Veneridae)のhomo-

geneous structure と crossed-lamellar struc-

ture について..... 島本昌憲
現生・化石カガミガイ(*Phacosoma japonicum*;

Bivalvia)の殻の絶対成長
..... 勝田 毅・久米祥子・棚部一成

Dallinacea 超科(腕足動物)の腕骨の形成につい

て—その1—..... 郡司幸夫
Metacrinus rotundus Carpenter (ウミユリ)に

みられる再生枝とその古生物学的意義
..... 大路樹生

珪藻 *Denticulopsis lauta* のバイオメトリー
..... 丸山俊明

北海道蝦夷層群中にみられるアンモナイトの保存

- と産状(2).....前田晴良
内生型二枚貝化石における生息姿勢の保存
.....近藤康生
現生底生有孔虫類の運動について.....北里 洋
アマモ場のオストラコーダ その2—生息場所と
個体群動態の関係.....神谷隆宏
現世潮間帯に分布する底生二枚貝群集の古生態学
的解析.....有村栄一・久米祥子・棚部一成
日本海沿岸地域の第三系珪質鞭毛藻化石層序
.....小林博明
新潟堆積盆地東縁破間川流域の中新世珪藻化石層
序と珪藻化石群集の変遷.....柳沢幸夫
北西太平洋における新生代後期の珪藻示準面と古
海洋.....小泉 格
紅店統(石炭紀上部)の植物化石
.....木村達明・金 鐘憲
豊浦層群西中山層植物群
.....木村達明・内藤源太郎・大花民子
山口県美弥層群産裸子植物(2).....内藤源太郎
高知県横倉山G4層より産するデボン紀コノドン
ト.....二川敏明
岐阜県郡上八幡町安久田層より産出した三疊紀コ
ノドントの混在群集.....猪郷久治
Middle Triassic fused conodonts from
southern Thailand
.....Igo, H., Nagano, N. and Nakinbodee, V.
Molluscan fauna of the Cabatuan Formation
in the Tambac area, north Luzon..Shuto, T.
新潟県上越市西部の鮮新統谷浜層産貝化石
.....天野和孝・菅野三郎・市川敦子
下北半島田名部低地の貝化石群集
.....松島義章・奈良正義
日本の中新世後寒流系軟体動物群に認められる群
集型.....松居誠一郎
日本の中新世後寒流系軟体動物群の歴史の変遷
.....松居誠一郎
日本産中新世介形虫動物群に関する二、三の知見
.....矢島道子
新第三系同時面上の浮遊性有孔虫群の変化
.....茨木雅子
Relationships of globorotaliid taxa in the
Upper Miocene to Pliocene from northeast
Honshu, Japan
..... Oda, M., Bishop, S. and Scott, G. H.
鹿児島湾の底生有孔虫群集—その3・湾口部—
.....大木公彦
琉球層群に含まれる造礁サンゴ群集.....中森 亨
琉球列島石垣島米原沖の無節サンゴ群集I
.....井龍康文・松田伸也
Proolithon onkodes を優占種とするサンゴモ群集
の遷移および分布進度について—石垣島サンゴ
礁の場合—.....松田伸也
日本海底質堆積物中の放散虫群集.....山内守明
南極海の海底堆積物中にみられる放散虫群集
.....西村明子
東アフリカにおける中新世哺乳動物の変遷
.....仲谷英夫
南部北上山地中部ベルム系叶倉層産腕足類
Pseudoleptodus.....田沢純一・高泉幸弘
タイ国北部, Khao Doi Pha Phlung ・
Waagenophyllum について.....枚山哲夫
デボン系福地層から産出した *Spyroceras*
(Orthocerida) について.. 児子修司・西田民雄
Crioceratites (Paracrioceratites) and
Shasticrioceratites from the Japanese Barremian
..... Matsukawa, M. and Obata, I.
北海道の中部チューロニアンから産する
Collignoniceras の特性について.....二上政夫
Taxonomic relationship between
Subprionocyclus bravaisianus and *S. neptuni*,
Turonian collignoniceratid ammonites
..... Tanabe, K. (代読)
アンモナイト属 *Neocrioceratites* について..松本達郎
本邦白亜系カンパニアン—マストリヒチアン階に
産する *Gaudryceratidae* アンモナイトについて
.....松本達郎
後期三疊紀 *Monotis* の形態進化.....安藤寿男
Keijella bisanensis 種群の種分化.....阿部勝己
Cythere 属(介形虫)の種分化
.....塚越 哲・池谷仙之
Systematic and paleobiogeographic studies on
the Japanese Miocene argonautid
“*Nautilus*” *izumoensis*
..Noda, H., Ogasawara, K. and Nomura, R.
本邦後期新生代 *Astartidae* (二枚貝) の分類と
その地史的意義.....小笠原憲四郎
A new species of *Dosinia* from the Pliocene
and Pleistocene formations in Hokkaido,
Japan..... Takagi, T.
Glossaulax didyma (Roeding) の種内変異と
G. vesicalis (Philippi) の起源.....間島隆一
中新統産ニシン科魚類 *Eosardinella hishinaiensis*
の系統類縁関係.....佐藤陽一
北九州芦屋層群産ひげ鯨類マウイクタスの下顎な
どに見られる原始性について.....岡崎美彦
日本の第四紀鹿科 *Sika* 亜属の再検討..大塚裕之
表皮組織による白亜紀初期のベネチテス類の分類
.....木村達明・大久保 敦
北日本の古第三紀 *Populus* 層の再検討..棚井敏雅
兵庫県丹波地方における最終氷期の植生

- 前田保夫
Spiniferites 属 (ダイノフラゲラータ化石) の形態変化による古塩分濃度の解析..... 原田憲一
 底生有孔虫による男鹿半島上部新生界の堆積環境解析..... Jung, Kyu-Kui
 福島県小名浜沖表層堆積物中の底生有孔虫の深度分布..... 海保邦夫・長谷川四郎
 酸素同位体比による現生オウム貝の生息深度の推定..... 甲斐正義・大場忠道
- ポスターセッション**
- コイル状殻の一般的成長モデル..... 岡本 隆
 北海道浦幌町における白亜-第三系の連続層序と古環境変動... 斎藤常正・海保邦夫・山野井 徹
 岩礁地性底生有孔虫類の生態..... 北里 洋・相沢 睦・金崎仁美

1985年度日本古生物学会論文賞は間島隆一君の *Intraspecific variation in three species of Glossaulax* (Gastropoda: Naticidae) from the Late Cenozoic strata in Central and Southwest Japan. *Trans. Proc. Palaeont. Soc. Japan, N. S., No. 138, pp. 111-137, pls. 17-19, 1983* にたいして授与されました。なお推薦文は「化石」に掲載されます。

1985年度日本古生物学会学術賞は山口寿之君の「化石ならびに現生フジツボ類の研究」にたいして授与されました。推薦文は同じく「化石」に掲載されます。

New members approved by the Council Meeting held on January 31, 1985

Ordinary Members

Fujiura, Tsuyoshi; Iwauchi, Akiko; Muramoto, Kouji; Takagi, Yoshiyuki; Yoshida, Hidekazu.

New members approved by the Council Meeting held on June 14, 1985

Ordinary Members

Furukubo, Masako; Goto, Yoshihiro; Hashimoto, Kazuo; Hori, Rie; Iwata, Keiji; Kamishima, Junichi; Kondo, Toshifumi; Kurashige, Yoshimasa; Lee, Yeon Gyu; Mizunuma, Bunji; Nemoto, Naoki; Sato, Hidetoshi; Sato, Touru; Takabatake, Kazuhiro; Tanimoto, Masahiro; Tsukagoshi, Minoru; Uchida, Shigehiro; Ueda, Tetsuro.

Foreign Members

Pa'n, Chang Wu; Wang, Chia Ching.

Withdrawing Members

Hasegawa, Junichi; Shindou, Tetsuya; Watanabe, Akiho; Durham, J. W.; Pak, Soon Heong. Samaniego, R. M.; Schmidt Effing, R.; Stach, Leopold, W.

Patron Members: Sekiyu Kodan; SG Giken Co.

New members approved on January 30, 1986

Ordinary Members

Ando, Jun; Futagawa, Toshiaki; Hayashi, Shunichi; Ishigaki, Shinobu; Ito, Yoshio; Koseki, Osamu; Kotake, Nobuhiro; Miyahashi, Hiroshi; Miyasaka, Yoshihiko; Shigeta, Yasunari; Shirato, Yutaka; Takamura, Kazuko; Tsuru, Toshiyuki; Yamamuro, Masumi; Yoshida, Kouichi.

Withdrawing Members

Hayashi, Shingo; Ichikawa, Wataru; Iguchi, Yutaka; Momoi, Kyoko; Nakagawa, Hiroshi; Oda, Hiroshi; Sogabe, Masatoshi; Suda, Akihiko; Taguchi, Eiji; Yokoyama, Tsuruo; Yoshida, Fumio.

Deceased Members

Ling, Chao Chi; Sugita, Munemitu; Takehara, Heichi.

Fellows

Inoue, Yoko; Iwao, Yushiro; Kase, Tomoki; Nagai, Kouichi; Nishimiya, Katsuhiko; Nishimura, Akiko; Nishimura, Akira; Shibata, Hiroshi.

Palaeontological Society of Japan, Special Papers
List of Available Back Numbers

	A, B (Yen)	C (U.S.\$)
No. 9 (1962): Bibliography of Japanese Palaeontology and Related Sciences, 1951—1960. By F. Takai (ed)	3,600	28
No. 13 (1968): The Echinoid Fauna from Japan and Adjacent Regions. Part 2. By S. Nisiyama	6,800	44
No. 15 (1971): Early Devonian Brachiopods from the Lesser Khingan District of Northeast China. By T. Hamada	3,800	29
No. 16 (1971): Tertiary Molluscan Fauna from the Yakataga District and Adjacent Areas of Southern Alaska. By S. Kanno	5,000	35
No. 17 (1973; reprinted 1980): Revision of Matajiro Yokoyama's Type Mollusca from the Tertiary and Quaternary of the Kanto Area. By K. Oyama	5,500	38
No. 18 (1974): Silurian Trilobites of Japan in Comparison with Asian, Pacific and other Faunas. By T. Kobayashi and T. Hamada	4,500	33
No. 19 (1976): Bivalve Faunas of the Cretaceous Himenoura Group in Kyushu. By M. Tashiro	4,100	31
No. 20 (1977): Devonian Trilobites of Japan in Comparison with Asian, Pacific and other Faunas. By T. Kobayashi and T. Hamada	6,300	42
No. 21 (1977): Mid-Cretaceous Events — Hokkaido Symposium, 1976. By T. Matsumoto (org.)	5,200	36
No. 22 (1978): Bibliography of Palaeontology in Japan, 1961—1975. By K. Kanmera and H. Ujiie (ed.)	6,300	42
No. 23 (1980): Carboniferous Trilobites of Japan in Comparison with Asian, Pacific and other Faunas. By T. Kobayashi and T. Hamada	5,800	39
No. 24 (1981): Permian Conodont Biostratigraphy of Japan. By H. Igo	4,700	34
No. 25 (1982): Multidisciplinary Research in the Upper Cretaceous of the Monobe Area, Shikoku. By T. Matsumoto and M. Tashiro	5,800	39
No. 26 (1984): Permian Trilobites of Japan in Comparison with Asian, Pacific and other faunas. By T. Kobayashi and T. Hamada	5,800	39
No. 27 (1984): Some Ammonites from the Campanian (Upper Cretaceous) of Northern Hokkaido. By T. Matsumoto	6,800	44
No. 28 (1985): Bibliography of Palaeontology in Japan, 1976—1980. By T. Kase and K. Asama	4,100	31

A and B include shipping. C includes bank commission and shipping.

[This new price list is available from August 1, 1986]

PALAEONTOLOGICAL SOCIETY OF JAPAN, SPECIAL PAPERS
ORDER FORM

To: c/o Dr. Juichi YANAGIDA
Editor of Special Papers, Palaeontological Society of Japan,
Department of Geology, Faculty of Science,
Kyushu University 33, FUKUOKA 812, JAPAN

From (in block letters):

Please send me, by surface mail, the following copies (copy) of Special Papers

Cat. No.	Quantity	Short Title	Total Price (yen or U.S.\$)

Payment (Please check one box)

- A International Postal Money Order
(To: Palaeontological Society of Japan,
c/o Department of Geology, Kyushu University 33,
Fukuoka 812, Japan)
- B Postal Transfer Account
(To: No. 5-19014 FUKUOKA)
- C Cheque
(made payable to the Palaeontological Society
of Japan) for U.S. dollars.

Notes. A and B include shipping.
C includes bank commission and shipping. Bank commission
for changing money costs 10 U.S. dollars in Japan.

Date : _____

Signature: _____

行 事 予 定

	開 催 地	開 催 日	講演申込締切日
1986年 135回例会	北九州市自然史博物館 (北九州市中央公民館)	1986年 6月14日・15日	1986年 3月31日
1987年 年会総会	静 岡 大 学	1987年1月30日～2月1日	1986年11月15日

講演申込先：〒113 東京都文京区弥生 2-4-16 日本学会事務センター 日本古生物学会 行事係
(葉書で申し込んでください)

お 知 ら せ

- 135回例会では「秋吉石灰岩層群の石炭紀化石群」の題でシンポジウムが行われます。
(世話人 柳田寿一・太田正道)
- 北九州市での135回例会でもプレプリントを作成いたします。
行事係 (東京大学・理・地質, 速水 格)

日本古生物学会報告・紀事・編集出版規約の変更について

同規約のⅡ投稿, ⅡB執筆制限-1で「原著論文では挿図, 表などを含めて24印刷頁」とあるのを「20印刷頁」とする変更が1986年度総会で承認されました。これは1986年4月30日発行の本号から適用されます。

著者負担超過料金値上げについてお願い

上記編集出版規約の変更に関連して, 著者負担超過料金を1印刷頁あたり10000円(現行6000円)とNo. 141から改訂させて頂きます。なお現行の図版1枚20000円は据え置きです。この値上げは従来からの印刷代の値上りに対処し, 実費に近い金額を著者に負担していただくものです。またなるべく多くの論文を投稿後できるだけ早く印刷するための止む負えぬ措置ですので, 既に投稿中の方々をも含めて, 宜しくご了承下さるようお願い致します。
編集係 猪郷久義・会計係 木村達明

お こと わ り

本誌第3論文, Takahashi et al.; A new ancestor of Steller's sea cow from the Upper Miocene of Yamagata Prefecture, Northeastern Japan は図版が制限枚数を大きく超過しておりますが, これは著者からの申しでにたいして, 常務委員会ならびに編集委員会で慎重に協議検討の結果, その研究対象が大型の哺乳類化石であること, ならびに記載図示は日本の古生物学上きわめて重要な貢献であると判断し, 特例として受理したものです。
編集係 猪郷久義

○文部省科学研究費補助金(研究成果刊行費)による。

1986年 4月25日 印 刷 1986年 4月30日 発 行 ISSN 0031-0204 日本古生物学会報告・紀事 新 篇 141号 2,500円	発 行 者 日 本 古 生 物 学 会 文京区弥生 2-4-16 日本学会事務センター内 (振替口座東京 84780番) (電 話 03-817-5801) 編 集 者 猪 郷 久 義 ・ 浜 田 隆 士 編 集 幹 事 野 田 浩 司 印 刷 者 東 京 都 練 馬 区 豊 玉 北 2ノ13 学術図書印刷株式会社 富 田 潔 (電 話 03-991-3754)
--	---

Transactions and Proceedings of the Palaeontological
Society of Japan

New Series No. 141

April 30, 1986

CONTENTS

TRANSACTIONS

807. OHOTSUKA, Yasuo: Early internal shell microstructure of some Mesozoic Ammonoidea: Implication for higher taxonomy 275
808. KOIKE, Hiroko: Microstructure of growth increments in the shell of *Mercenaria mercenaria* (Linne) 289
809. TAKAHASHI, Shizuo, DOMNING, Daryl P. and SAITO, Tsunemasa: A new ancestor of Steller's sea cow from the Upper Miocene of Yamagata Prefecture, Northeastern Japan 296
810. ISHIGA, Hiroaki and MIYAMOTO, Takami: *Follicucullus* (Radiolaria) from the Upper Permian Kuma Formation, Kyushu, Southwest Japan 322
- PROCEEDINGS 337